USE OF CALCIUM-ALGINATE AS A COAGULANT FOR LOW TURBIDITY WATERS

A THESIS SUBMITTED TO
THE GRADUATE SCHOOL OF NATURAL AND APPLIED SCIENCES
OF
MIDDLE EAST TECHNICAL UNIVERSITY

BY

AVNİ METE YÜKSEL

IN PARTIAL FULFILLMENT OF THE REQUIREMENTS
FOR
THE DEGREE OF MASTER OF SCIENCE
IN
ENVIRONMENTAL ENGINEERING

DECEMBER 2007

Approval of the thesis:

USE OF CALCIUM-ALGINATE AS A COAGULANT FOR LOW TURBIDITY WATERS

submitted by **AVNİ METE YÜKSEL** in partial fulfillment of the requirements for the degree of **Master of Science in Environmental Engineering Department, Middle East Technical University** by,

Prof. Dr. Canan Özgen _____
Dean, Graduate School of **Natural and Applied Sciences**

Prof. Dr. Göksel N. Demirer _____
Head of Department, **Environmental Engineering**

Prof. Dr. F. Dilek Sanin _____
Supervisor, **Environmental Engineering Dept., METU**

Examining Committee Members:

Prof. Dr. Celal F. Gökçay _____
Environmental Engineering Dept., METU

Prof. Dr. F. Dilek Sanin _____
Environmental Engineering Dept., METU

Assoc. Prof. Dr. Ayşegül Aksoy _____
Environmental Engineering Dept., METU

Assoc. Prof. Dr. İpek İmamoğlu _____
Environmental Engineering Dept., METU

Assist. Prof. Dr. Ayşegül Latifoğlu _____
Environmental Engineering Dept., HÜ

Date: _____

I hereby declare that all information in this document has been obtained and presented in accordance with academic rules and ethical conduct. I also declare that, as required by these rules and conduct, I have fully cited and referenced all material and results that are not original to this work.

Name, Last Name:

Signature:

ABSTRACT

USE OF CALCIUM-ALGINATE AS A COAGULANT FOR LOW TURBIDITY WATERS

YÜKSEL, Avni Mete
M.Sc., Environmental Engineering Department
Supervisor: Prof. Dr. F. Dilek Sanin

December 2007, 143 Pages

This study aims to investigate the possibility of using calcium-alginate as a coagulant in low turbidity waters. Jar tests were initially performed with synthetically prepared turbid waters to investigate the effect of alginate and calcium concentrations, alginate's molecular weight, rapid mixing time and speed (schedule), initial pH and alkalinity of synthetic water on turbidity removal efficiency of calcium-alginate system step by step. Alum as a coagulant was then used in jar tests conducted with synthetic water to compare with calcium-alginate in terms of its turbidity removal efficiency and produced sludge properties. Finally, raw water acquired from water treatment plant was tested for treatability by using calcium-alginate based on previously determined optimum parameters via jar tests.

Experiments of calcium-alginate system with synthetic water showed that calcium was a key parameter in coagulation and high molecular weight alginate performed better in turbidity removal. Significant improvements in turbidity removal were observed when mixing schedules were

rearranged; especially in case of increasing rapid mixing time following calcium dosing. Calcium-alginate system neither was notably affected by pH or alkalinity nor did significantly change the pH or alkalinity of the medium. Alum worked well in turbidity removal with additional adjustments of pH and alkalinity, however; alum produced higher quantities of sludge than calcium-alginate system. “Raw water“ experiments with calcium-alginate did not result in desired level of turbidity removals due to the excessively different characteristics of this water compared to the synthetically prepared turbid water.

Keywords: Calcium Alginate, Coagulation, Flocculation, Mixing Speed, Mixing Time, Molecular Weight of Alginate, Turbidity

ÖZ

KALSİYUM ALGİNATIN DÜŞÜK BULANIKLIKTAKİ SULARDA KOAGÜLAN OLARAK KULLANIMI

YÜKSEL, Avni Mete
Yüksek Lisans, Çevre Mühendisliği Bölümü
Tez Danışmanı: Prof. Dr. F. Dilek Sanin

Aralık 2007, 143 Sayfa

Bu çalışma kalsiyum-alginatın düşük bulanıklıktaki sularda koagülan olarak kullanımı olasılığını araştırmayı amaçlamaktadır. İlk aşamada, sırasıyla kalsiyum ve alginatın konsantrasyonlarının, alginatın molekül ağırlığının, hızlı karıştırma süresi ve hızının (süreç), sentetik suyun başlangıç pH ve alkalinitesinin, kalsiyum-alginat sisteminin bulanıklık giderim verimi üzerine olan etkilerini araştırmak için jar test çalışmaları sentetik olarak hazırlanmış bulanık sularda yürütülmüştür. Sentetik suyla yapılan jar test deneylerin devamında alum koagülan olarak kullanılmış ve kalsiyum-alginat ile bulanıklık giderim verimleri ve üretilen çamurun özellikleri karşılaştırılmıştır. Son bölümde, önceden belirlenmiş optimum parametrelere dayanarak, arıtma tesisinden alınan ham suyun jar test çalışmaları vasıtasıyla kalsiyum-alginat kullanarak arıtılabilirliği test edilmiştir.

Kalsiyum-alginat sisteminin sonuçları: kalsiyumun kilit bir parametre olduğunu ve yüksek molekül ağırlığına sahip alginatın bulanıklık gideriminde daha etkili olduğu göstermiştir. Özellikle kalsiyum

dozlamasını takip eden hızlı karıştırma süresinin arttırılması durumunda olduğu gibi; hızlı karıştırma sürecinin yeniden düzenlenmesiyle sistemde önemli gelişmeler kaydedilmiştir. Kalsiyum-alginat sistemi, ortamın pH ve alkalinitesinden etkilenmemekte ve ortamın pH ve alkalinitesinde de önemli bir değişikliğe yol açmamaktadır. Alum, bulanıklık giderimde fazladan pH ve alkalinite ayarlamasıyla olumlu sonuçlar vermiş, ancak kalsiyum-alginat sistemine oranla daha fazla çamur üretimine sebep olmuştur. Ham suyun, sentetik olarak hazırlanmış bulanık suya kıyasla oldukça farklı karakterizasyonundan dolayı; kalsiyum-alginat kullanılarak yapılan “ham su” deneyleri istenilen seviyelerde bulanıklık giderimi sağlamamıştır.

Anahtar Kelimeler: Kalsiyum Alginat, Koagülasyon, Flokülasyon, Karıştıma Hızı, Karıştırma Süresi, Alginatın Molekül Ağrılığı, Bulanıklık

To My Family,

ACKNOWLEDGEMENTS

I would like to express my sincere thanks to my supervisor, Prof. Dr. F. Dilek Sanin, for her guidance and support through out the research period and especially for her patience during the preparation of this thesis.

I would like thank to Prof. Dr. Celal F. Gökçay, Assoc. Prof. Dr. Ayşegül Aksoy, Assoc. Prof. Dr İpek İmamoğlu and Assist. Prof. Dr. Ayşegül Latifoğlu for their comments and suggestions.

I would also like to thank to my friends Özge Yılmaz, Gülçin Özsoy, Recep Tuğrul Özdemir, Onur Güven Apul, Volkan Çağın, Kadir Gedik, Murat Varol, Fadime Kara, and Çiğdem Kıvılcımdan Moral.

I am also grateful to my dear friend and laboratory coworker Cavit Burak Bural for his support, guidance and friendship whenever I was in trouble.

Finally, I thank to my family, for their endless support in all part of my life.

TABLE OF CONTENTS

LIST OF TABLES

LIST OF FIGURES

CHAPTER 1

INTRODUCTION

1.1 General

As water flows in streams, detents in lakes, and filters through layers of soil and rock in the ground, it dissolves or absorbs the substances contacting with it. Some of these substances are harmless and even gives water a pleasing taste. On the contrary contamination might also occur during deposition or transportation of water. Point sources like discharges from factories or wastewater treatment plants, non point sources usually covering fluxes of contaminants over a specific area related with chemical usage in agriculture are the main sources for water contamination. Besides these sources, the ecosystems may also contribute to some organic species due to decomposition of plant and animal remains called natural organic matter. These organic impurities may result in aesthetics of the color, taste and odor; also cause some problems during water treatment like production of potential health hazard disinfection by products, the fouling of membranes and ion-exchange resins, deterioration of water quality in distribution systems because of bacterial growth (Bolto et al., 2004)

In addition to organic impurities, inorganic impurities may be present in water. Especially, colloidal particles are the main portion in this class. They usually come from erosion of natural rock and soil during the water movement. Since colloidal particles have a negligible settling velocity, they remain suspended in water causing turbidity. Turbid waters have cloudy appearances due to interception of light by colloidal particles. That reduction in light penetration may impact the aquatic life within the

water and so reduce water quality in an indirect way. Also, existence of colloidal particle may favor pathogeneses growth by supplying them a suitable medium. For this reason, authorities set a limit value to turbidity. United States, European Union and Turkish authorities have all set a maximum allowable turbidity limit as 1 NTU for drinking waters.

Turbidity removal is achieved by a series of conventional methods: Coagulation, flocculation, sedimentation (or flotation) and filtration. In the coagulation process, metal salts or polymers, namely coagulants, are dosed in to the raw water and kept in rapid mixing unit for complete distribution of coagulants in water. Carrying a charge opposite of suspended particles make coagulants destabilize colloidal particles in a short time. Once the particles are destabilized, they begin to agglomerate by colliding with each other forming flocs. This step is called flocculation and a slower mixing intensity than that of coagulation is applied both to induce particle agglomeration and to prevent particles from breaking again, in a rather longer periods of time. Once the flocs reach a critical mass, they are able to settle down by gravity. To achieve that, sedimentation tanks are used in which treated water pass at a slower rate letting flocs settle down in that period of time and clear water is removed by surface weirs placed generally around the top of tank. However, sedimentation may sometimes be inefficient for complete particle removal, so to ensure complete removal of particles from water, water is filtered through granular, slow sand or membrane filters.

It is important that processes be optimized and controlled to achieve consistent and reliable performance. Chemical coagulation is the most important step in determining the removal efficiency of treatment processes. It also directly affects the removal efficiency of granular media filtration units and has indirect impacts on the efficiency of the disinfection process. To do that, the turbid water samples are firstly

treated in laboratory via Jar Test. Jar Test can be thought like a simulation of water treatment plant as batch reactor. In Jar Test, proper coagulant/ coagulant aid and their optimum concentrations for turbidity removal efficiencies of particular water can be determined.

It is known that coagulants and coagulant aids, mainly synthetic polymers, posses some health hazard potential. For this reason, researches intent to find an alternative coagulants or coagulant aids which are non toxic for humans and environment. Several natural polymers also called biopolymers, extracted from living species, seem to be an alternative to conventional coagulants (Salehizahed and Shojaosadati, 2001).

One of these biopolymers is alginate which has a specific ability to form gel with reaction of calcium ions. This property of alginate inspired the research of using with calcium alginate as a coagulant to remove turbidity from water. Calcium-alginate was tested for its coagulation ability on synthetically prepared and natural raw waters. It was found that calcium-alginate could be used to remove turbidity for high and medium turbidity waters. Whereas; for waters of low turbidity and samples taken from the inlet of water treatment plant, turbidity removal efficiency of calcium-alginate was not good enough. It is investigated with the purpose of improving its effectiveness as a coagulant in this work.

1.2 Aim and Scope of the Study

The aim of the study is to improve calcium alginate's coagulant properties for water treatment and to develop the parameters that will enable the use of calcium-alginate as a coagulant in low turbidity waters (10 NTU) so that the applicable turbidity standards (1 NTU) are met or approached.

Within this context, the studies were conducted on turbid water samples prepared either in the laboratory or taken from Ivedik Water Treatment Plant (IWTP) inlet by running different jar tests. Calcium chloride and alginate were used as coagulant. The main experimental variables were alginate concentration, alginate molecular weight, calcium concentration, rapid and slow mixing times and mixing intensity.

Final turbidity of the water samples were measured after each treatment. In addition, unsteady state electrokinetic measurements were conducted to understand the coagulation mechanism. Depending on the experiments, other parameters like final pH, residual calcium concentration or residual alkalinity were also measured. Similar jar tests were conducted with alum alone or in combination with alginate to compare the turbidity removal efficiency of alum with calcium alginate or to evaluate usability of alginate as a coagulant aid. In addition to these, properties of sludge produced at different conditions or by different coagulants (alum or calcium alginate) were investigated in terms of its solids concentrations and dewaterability.

CHAPTER 2

LITERATURE RESEARCH

2.1 Colloid Stability

The particles in a colloidal dispersion are sufficiently large for definite surfaces of separation to exist between the particles and the medium in which they are dispersed. Therefore, simple colloid systems consist of two phases. The phases are distinguished by the terms dispersed phase, forming the particles, and dispersion medium in which the particles are distributed. One of the groups defined in colloidal systems is colloidal dispersion, which are thermodynamically unstable owing to their high surface free energy and are irreversible systems meaning that they are not easily reconstituted after phase separation (Shaw, 1979).

It was observed that solid colloidal particles in an aqueous dispersion move in an electrical field since particles carry an electrical charge, namely surface charge. This phenomenon was explained by electrical double layer theory. The theory suggests that a plane of charge exist on the particle surface. Ions of opposite charge (counterions) are attracted towards the surface and ions of like charge (coions) are repelled away from the surface. Attraction of counterions and repulsion of coions creates several layers around the particle surface. The first layer around the surface is called fixed layer or Stern layer in which counterions are adsorbed and hold on the surface. Outside of the Stern Layer is diffuse layer. Diffuse layer consists of a mixture of counterions and coions. Counterions in the diffuse layer are still attracted by particle surface charge and repelled by the counterions in the Stern plane as well as nearby counterions. Similarly, coions concentration increases gradually

in diffuse layer while approaching from the particle surface to bulk solution due to decreasing of repulsive forces exerted by particle surface and reaches equilibrium in bulk solution. The thickness of diffuse layer is impacted by the solution's ionic strength. A higher level of ionic strength of solution reduces the thickness of diffuse layer by contributing more counterions in neutralization of particle as shown in Figure 2.1 (Reynolds, 1982; Ravina, 1993).

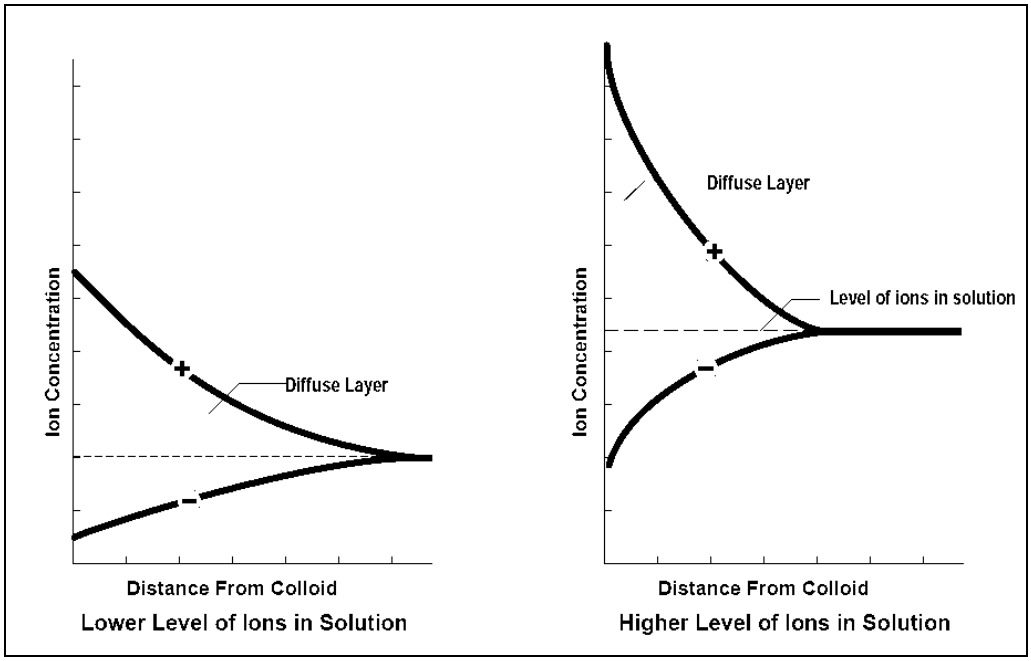

Figure 2.1 Effect of Ion Concentration on Diffuse Layer Thickness (Ravina, 1993)

The surface charges might originate from three principal ways. First, the charge could arise from chemical reactions at the surface. Many solid surfaces contain functional groups which are easily ionizable, e.g. -OH, -COOH or $-OPO_3H_2$. The charge of particles with such surfaces becomes dependent on the degree of ionization and accordingly on the pH of the surrounding liquid. For such a situation, as pH of liquid increases from

acidic to basic values, the surface charges turns from positive to negative values. Moreover, surface charges can also originate by process in which solutes become co-ordinatevely bound to solid surfaces. Secondly, lattice imperfections at the solid surface can cause surface charge. Clays are examples of such atomic substitutions. This type of origination is also dependent on pH as well. Lastly, adsorption of one type of ion on a surface might establish surface charges. Adsorption of ion on a surface can arise from London-van der Waal's forces or from hydrogen bonding (Stumm and Morgan, 1962; Bratby, 1980).

For the colloidal particles occurring in natural waters nearly always carry a negative surface charge over the usual range of natural water pH (pH 5-9). This might be due to being the water pH above isoelectric point at which surface carries no net electrical charge. That is usually the case for particles of biological origin. Even for mineral particles possessing high isoelectric point adsorption of natural organic matter usually gives a negative surface charge (Hunter and Liss, 1982; Duan and Gregory, 2002).

2.2 Colloid-Colloid Interactions

Colloid-Colloid interactions were investigated in conjunction with electrical double layer theory. DLVO (Derjaguin–Landau–Verwey–Overbeek) theory is the main one describing the relation between repulsive and attractive forces around the colloidal particle. Attractive forces are the van der Waal's forces originating due to chemical structure of the atoms or molecules. On the other hand, repulsive forces arise due to surface charge of the colloidal particle as afore mentioned and colloidal particles are repelled by other same charged particles that inhibit agglomeration and stabilize colloidal suspension (Maximova and Dahl, 2006). Briefly, the theory assumes that the effect of two forces is

additive, and the results can be displayed in the form of a potential energy diagram like in Figure 2.2. The main points of interest in the Figure 2.2 are the height of the energy barrier and the low potential well (energy trap) at very small distances. So, DLVO theory suggests that a large energy barrier must first be overcame, and then it is energetically favorable for particles to come into close contact. Once the energy barrier is overcome, the net interaction energy is all attractive so that particles can be easily agglomerated (Thomas et al., 1998).

Destabilization of colloidal particles could be achieved along DLVO lines, either by adding relatively large amounts of salts or smaller quantities of cations that interact specifically with negative colloids and neutralize the charge (Duan and Gregory, 2002).

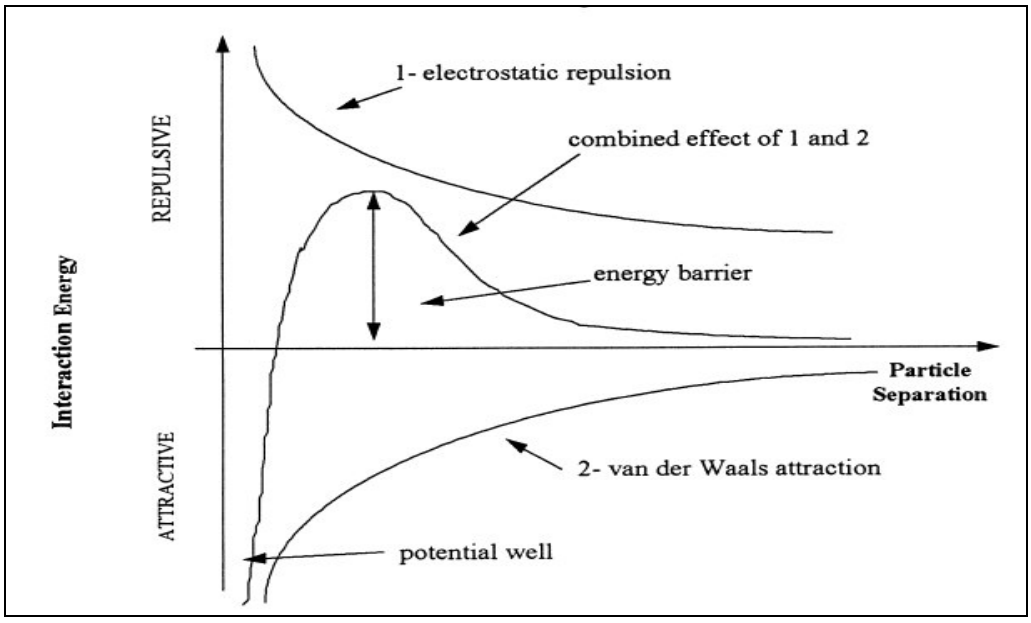

Figure 2.2 Forces acting on particle surface according to DLVO theory (Thomas et al., 1998)

2.3 Coagulation Mechanisms

When a coagulant is introduced into the solution, it quickly interacts with colloidal particles and yields particle agglomeration by several coagulation mechanisms. There are number of different mechanisms involved in a coagulation process, including double layer compression, adsorption and charge neutralization, inter-particle bridging, and sweep coagulation (Menezes et al., 1996; Ahmad et al., 2006). Also, combination of these mechanisms can take place in coagulation processes (Gregory, 1985). Within this context the way of how coagulants interact with colloids will be discussed in a detailed manner.

2.3.1 Double Layer Compression

The interactions of some coagulant species with a colloidal particle are purely electrostatic; namely, coions are repelled and counterions are attracted and other interactions are insignificant. Coagulants acting in this limited manner are sometimes called indifferent electrolytes. Destabilization by counterions is accomplished by compressing the diffuse layer surrounding the colloidal particles. High concentrations of electrolyte in the solution result in correspondingly high concentration of counterions in the diffuse layer. The thickness of diffuse layer necessary to maintain electroneutrality is decreased and consequently the thickness of diffuse layer is reduced. As a result of this, the range of the repulsive interaction between similar colloidal particles decreases, and energy barrier can disappear (Weber, 1972). However, achieving agglomeration of colloidal particles just with double layer compression is found impractical in water treatment processes instead of making use of other destabilization mechanisms (Duan and Gregory, 2002).

The effect of counterions on diffuse layer was investigated and proved by Schulze-Hardy rule. Briefly, the rule indicates the destabilization power of

an electrolyte is primarily arising from the valence of its counterion. The destabilization power of an ion can be determined by measuring experimentally the critical coagulation concentration (CCC) of an electrolyte, i.e. the minimum concentration required to rapidly coagulate a given colloid. The formula is defined as;

$CCC=constant/z^6$,
Where;
z: the charge on the counter ion

For z=1, 2 and 3 the ratio of the CCC's are thus $1/1^6$ (1), $1/2^6$ (0.016) and $1/3^6$ (0.0014) (Verrall et al., 1998). Namely, to reduce diffuse layer by the same amount, while 1 mol/L of ions having valence of one is required, 0.016 mol/L is required for ions of valence two.

2.3.2 Adsorption and Charge Neutralization

Adsorption and charge neutralization mechanism has ultimately similar effects like electrical double layer compression. However; unlike double layer compression, in this mechanism, counterions or oppositely charged polymers are adsorbed by the surface resulting in reduction of the extent of double layer repulsive interaction between other colloidal particles (Bratby, 1980).

It is worth to discuss herein briefly how hydrolyzing metal salts (e.g. alum) interact with colloidal particles, because adsorption and charge neutralization with these coagulants bring about in different ways depending on coagulant concentration. Following the addition of hydrolyzing metal coagulant into the water, it quickly dissociates and forms monomeric and polynuclear hydrolysis products. If solubility limit of

hydrolyzing coagulant is exceeded, it forms amorphous hydroxide precipitates in the solution (Ching et al., 1994).

Precipitation-Charge Neutralization model was developed to predict stability of suspension on the basis of electrokinetic characteristics of colloidal materials prior to and following coagulation. The model assumes two different mechanisms how hydrolyzing metal coagulants interact with colloidal particles: First, initial adsorption or precipitation on the surface (surface precipitation) of positively charged metal hydroxide and then serving as a nucleation site for further precipitation. Second, precipitation occurs in solution followed by rapid deposition onto colloidal surfaces (Dentel, 1988)

2.3.3 Sweep Flocculation

It was recognized that optimum removal of particles from water is achieved under condition of rapid and extensive hydroxide precipitation (Wu et al., 2007). When a metal salt is added with a concentration sufficiently high to cause rapid precipitation of metal hydroxide, colloidal particles can be enmeshed in this precipitate as it is formed. In other words, colloidal particles themselves can serve as nuclei for the formation of the nuclei, so that the rate of precipitation increases with increasing concentration of colloids (Weber, 1972). This process is known as sweep flocculation since particles are swept out of water by a hydroxide precipitate. Usually, sweep flocculation term is used in the coagulation studies conducted with hydrolyzing metal salts, in addition to that, some other metal hydroxide yield sweep flocculation under proper pH values like $CaCO_{3(s)}$ and $Mg(OH)_2$ (Semerjian and Ayoub, 2001).

2.3.4 Adsorption and Interparticle Bridging

In last decades, the polymeric substances started to be used as coagulant or coagulant aids. The major mechanisms of coagulation by polymers are surface charge neutralization and bridging. In polymer bridging, the high molecular mass polymer chains are adsorbed onto the particle surface and form bridges between adjacent particles. Adsorption occurs by electrostatic forces, van der Waal's forces, hydrogen bonding and chemical bonding. When very long polymer molecules are adsorbed on the surface of particles, they tend to form loops that extend some distance from the surface into the aqueous phase and their ends may dangle. These loops and ends may come in contact with and attached to another particle forming a bridge between the two particles. In order for effective bridging to occur, there must be sufficient chain length, which extends far enough from the particle surface to attach to other particles (LaMer and Healy, 1963, Singh et al., 2003).

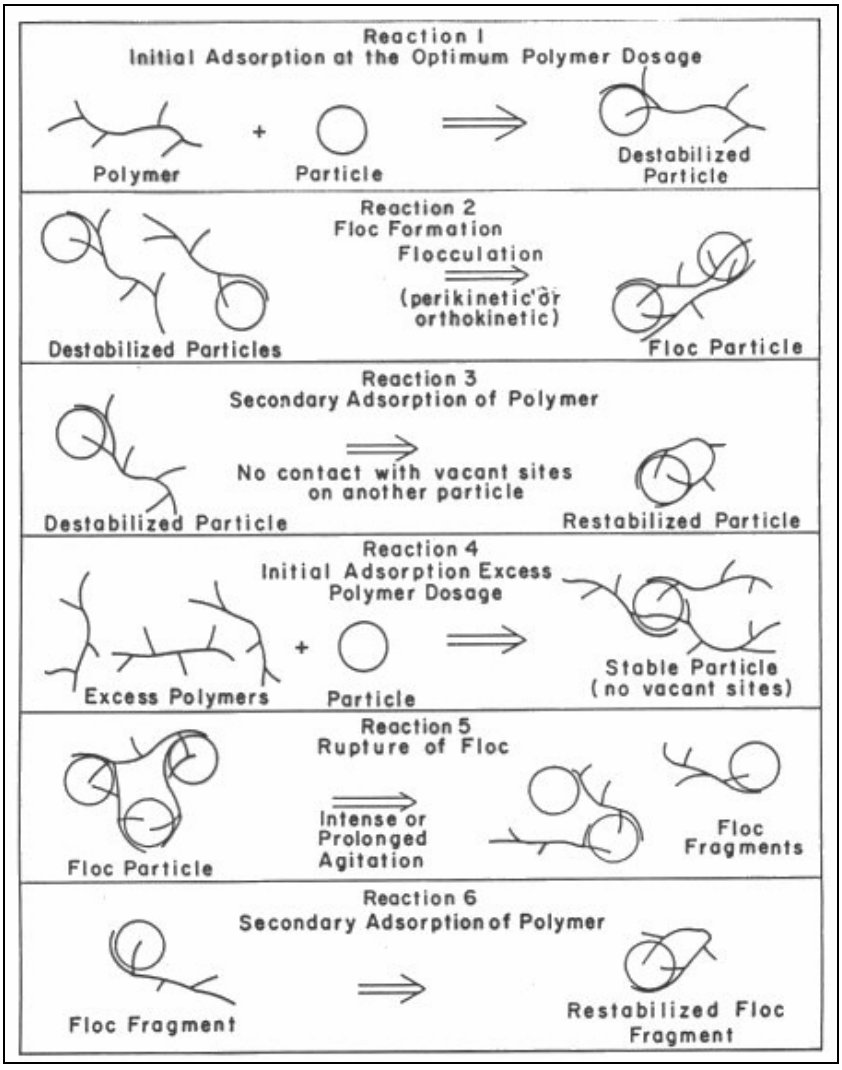

Figure 2.3 Schematic representation of the bridging model for the destabilization of colloidal particles (Weber, 1972)

In Figure 2.3 some possible scenarios related to bridging mechanism is postulated. The first two reactions depict the destabilization of particles and forming bridge with other destabilized particles. In case of no interaction with another particle, polymer adsorbed particle restabilized ultimately by extended segments of polymer itself, like in reaction 3. Also addition of excess amount of polymer may cover the particles' surfaces and hinder bridging due to no vacant sites availability on the particle (Reaction 4). Reactions 5 and 6 represents the situation in which

extended agitation cause breaking of polymer surface bonds and afterward restabilization of colloid by folding back of extended segments on the surface of the particle. (LaMer and Healy, 1963; Weber, 1972)

2.4 Electrokinetic Measurements

Electrokinetic measurements are useful tools in understanding colloidal particle's surface charges and so their stabilities. By knowing about surface charge values, it would be investigated how colloidal materials behave in nature, their stability degrees and responses to different physicochemical situations. To measure electrokinetic properties of particles, different methods or apparatus were developed; some of these are electrophoresis measurements, zeta potential and streaming current.

2.4.1 Electrophoresis and Zeta Potential Measurements

Electrophoresis refers to the movement of a charged particle in a fluid induced by an applied electrical force. When a direct current electric filed is applied across a suspension containing particles with a net double layer charge, the particles will migrate to the positive or negative pole depending on whether the particles carry a net negative or positive charge respectively. Counterions surrounding the colloid will migrate in the reverse direction of particles. Viscous forces acting on the particles tend to resist this movement. When equilibrium is reached between these two opposing forces, the particles move with constant velocity. The velocity is dependent on factors like strength of electric field or voltage gradient, zeta potential, the dielectric constant and viscosity of medium. While particles are moving towards the pole of opposite charge, their velocity is measured and expressed in unit field strength as their electrophoretic mobility (Bratby, 1980; Zetasizer, 2004). However; there is interference in the electrophoretic measurement originating from

interaction between cell in which liquid is placed and the medium called as electroosmosis effect. The apparatus is needed to be calibrated in a way excluding electroosmosis effect, i.e. the movement of a liquid relative to a stationary charged surface under the influence of an electric field. The movement of liquid adjacent to cell wall must be compensated for by reverse flow in close systems. The true electrophoresis measurement can be done at point where electroosmosis flow is zero or the point where flows in different directions cancel each other called as stationary layer. The schematically representation of stationary layer is illustrated in Figure 2.4. (Zetasizer, 2004; Malvern, 2007)

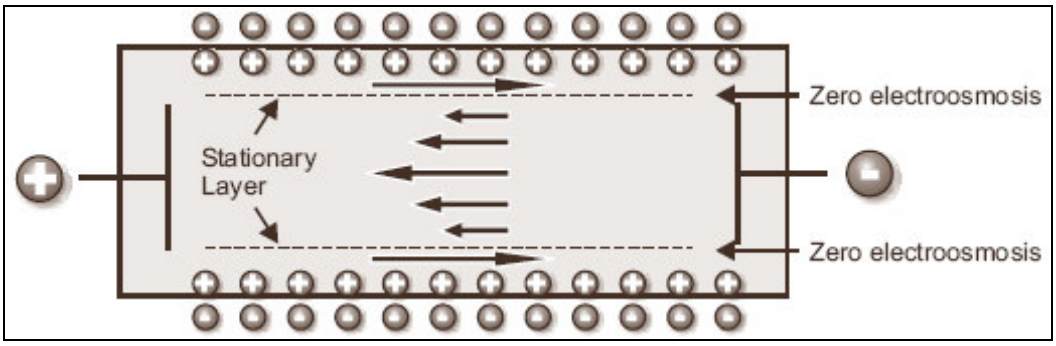

Figure 2.4 Representations of fluid motions and stationary level in case of electroosmosis effect (Zetasizer, 2004)

Another method in measuring surface charges is zeta potential. Within the diffuse layer there is an imaginary boundary inside which the ions and particles form a stable entity. When a particle moves (e.g. due to gravity), ions within the boundary move with it, but any ions beyond the boundary do not travel with the particle. The boundary is called slipping plane or shear plane, the charge on which refers to zeta potential (Figure 2.5) (Reynolds, 1982; Zetasizer, 2004).

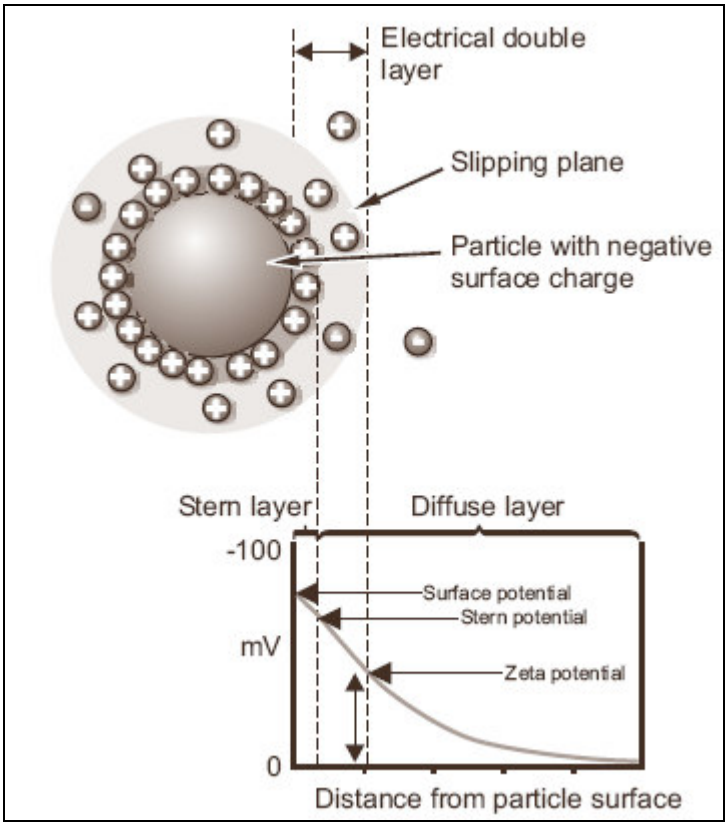

Figure 2.5 Distribution of ions around a negatively charged particle and location of zeta potential (Zetasizer, 2004)

Measurements are performed in a similar way like in electrophoretic mobility measurements. Even though both methods are based on same technique; it is usually expressed surface charges in zeta potential units rather than electrophoretic mobility, because zeta potential unit is easier to interpret and globally accepted than electrophoretic mobility. Henry's equation is used to convert electrophoretic mobility to zeta potential (Csempesz, 2000). This equation involves the parameter of dielectric constant, viscosity, and Henry's function. Henry's function takes usually a constant value in measurements of aqueous media and moderate electrolyte concentration referred as Smoluchowski approximation. However; approximation is valid for the particles larger than about 0.2

microns dispersed in electrolytes containing more than 10^{-3} molar salt (Zetasizer, 2004, Hou, 2007).

Though zeta potential measurements are easy way to express surface charges, in some cases it become useless in applications. The limitations of zeta potential measurements are listed below (McFadyen, 2004; Edney, 2005).

- It can only be determined for particles that are either large enough to be detected and tracked or low enough to distinguish particle from solution through a microscope.
- It is not very accurate near zero, which unfortunately is the point of greatest interest, because of the difficulty in tracking the particle motion.
- It requires a lab technician to operate the apparatus and to observe the particles through a microscope. It is labor intensive and cannot be used online.

Even with newcoming technologies, some of the problems related with measurement were resolved. The apparatus is still incapable of online monitoring and automation systems.

2.4.2 Streaming Current

The streaming current measurement is one of the methods used in surface charge measurements. On the contrary to zeta potential or electrophoresis measurement, in streaming current measurements, particles are stationary and fluid is moving. That is achieved by a reciprocating piston located in a dead-end cylinder forming an annulus structure. If a colloidal suspension is placed inside the annulus and the piston is started to reciprocate, electrically charged colloids in a fluid

sample are momentarily attached to the piston and cylinder surfaces due to van der Waal's forces. The charged layer attached to piston travels with piston velocity while that attached to cylinder walls remains stationary. Since relative velocity of the fluid in the annulus has much greater velocity than that of the piston, counterions beyond the shear plane are transported causing a measurable current. The current is measured by the electrodes placed on the opposite end of flow path, and amplified and processed by device (Chemtrac, 1999). The output of the device is called streaming current and can be related to zeta potential by using formula consisting of apparatus and solution specific parameters: (Elickler et al., 1992).

$$SC = K_{amp}\left(\frac{8\pi fs\varepsilon\zeta}{1+\frac{1+\lambda^2}{1-\lambda^2}\ln\lambda}\right)$$

Where;

SC: Streaming current detector reading (relative units)

K_{amp}: Streaming current amplification factor [A^{-1}]

f: Frequency of piston motion [cycles/sec]

s: Piston stroke [m]

ε: Solution dielectric constant

ζ: Zeta potential [v]

λ: Ratio of piston radius to housing inner radius

However; it is rather preferred using streaming current value instead of converting to zeta potential value, because results obtained from same streaming current meter can be compared with each other and also streaming current meters can be standardized with special solution with known charge characteristics (Abu-Orf and Dentel, 1997, 1998).

Advantage of streaming current devices over zeta potential devices is their online monitoring availability (Dentel et al., 2000). One of their online application areas is wastewater treatment plant's sludge dewatering units. With online streaming current measurements of conditioned sludge and filtrate, one can be able to optimize sludge dewaterability efficiency by relating streaming current with capillary suction time (CST), solid recovery and polymer concentration (Abu-Orf et al., 2003).

A study was performed with streaming current device for automatic monitoring of polymer dosage in three different sludge dewatering facilities, they were using rotating bowl centrifuges, belt filter press or a combination of rotating drums and belt filters. The study aimed optimization of polymer concentration to avoid excess polymer usage and condense its chemical costs and environmental adverse effects subsequently. Results at all three treatment plant indicated that a liquid stream (filtrate or centrate) streaming current in the neutral range occurred at the optimum polymer concentration concerning improvements in the parameters of solid measurements and recoveries and by minima in filtrate turbidity, filtrate viscosity, conditioned solids filterability an capillary suction time (in some cases). Nonetheless, it was reported that several clogging problems were encountered during the measurement, but the problem was resolved by manual flushing (Abu-Orf and Dentel, 1997).

In a similar fashion, streaming current devices can be used in water treatment plants. In the water treatment plant dose arrangement is carried out via jar test. However; it has some disadvantages like the necessity to perform manual intervention and the limitation to feedback control. Automatic coagulant control is ensured mainly by streaming current detectors. Since the net charge on the particles changes

following coagulant addition, allowing streaming current device to track the charge changes on the particles enables the automated system work close to optimum coagulation conditions (Bernazeau et al., 1992; Valentin et al., 1999), for the streaming current values around neutral it was observed optimum coagulation efficiency is achieved (Adgar et al., 2004; Xia et al., 2004).

2.5 Parameters Influencing Coagulation-Flocculation Efficiency

Coagulation and flocculation systems are complex processes so that many parameters affect the system efficiency. In brief, efficiency is influenced by properties of raw water (e.g. pH or alkalinity), impurities type and amount present in water, characteristic of coagulant and coagulant aids, applied mixing intensity and duration or a combination of all of these and other parameters which is not listed here.

2.5.1 Mixing Intensity and Mixing Duration

Coagulation-flocculation process consists of two different mixing regimes. The first mixing regime is called rapid mixing usually aiming a complete dispersion of coagulant through the water and causing particles destabilization. Following rapid mixing, slow mixing takes place aiming to agglomerate destabilized particles by colliding them with each other.

Mixing intensity is calculated with the formula below and it is usually defined as velocity gradient. In another words, velocity gradient is the power imparted from impeller to water (McConnachie and Liu, 1999).

$$G = \sqrt{\frac{P}{\mu * V}}$$

Where; P is the power dissipated in the tank [W], V is the volume of tank [m^3], μ is the dynamic viscosity of the fluid [$N*s/m^2$] and G is the velocity gradient. Power dissipated in tank is further calculated with another formula;

$$P = N_p * \rho * N^3 * D^5$$

Where; N_p is the power number, a dimensionless number related to geometry of impeller, ρ is the density of the fluid [kg/m^3], N is the rotation frequency of the impeller [s^{-1}], D is the impeller diameter [m] (Coufort et al., 2007).

The power dissipated (P) can also be calculated experimentally. It is achieved in a way that the power delivered from the impeller to the fluid is correlated to shaft revolution number by measuring the torque exerted from the fluid on the container wall. The mechanism to measure the torque works is set up like in Figure 2.6; the container is placed on a frictionless rotating circular plate and one end of a thread is attached to the outside surface of the container and the other end of that to a weight placed on a precision balance. When the stirrer is switch on, the container rotates until the torque equal to the tension exerted by the weight. The tension, T [N], in the thread is the difference between weighing values before the agitation and during the agitation. By multiplying the torque with the arm of thread, r [m] (length from stirrer shaft to container wall) yields torque. Finally, power imparted to the fluid is calculated by multiply shaft angular velocity [s^{-1}] and the torque value. In case of knowing power dissipated, viscosity and volume of fluid, one can calculate velocity gradient. The critical point in this experiment is mounting a frictionless circular plate to eliminate the static friction and fluctuation. It is achieve with a thin layer of lubricating oil flowing radially

and continually under low pressure between two specular granite surfaces. (Grisafi, 1994; Rossini, 1999)

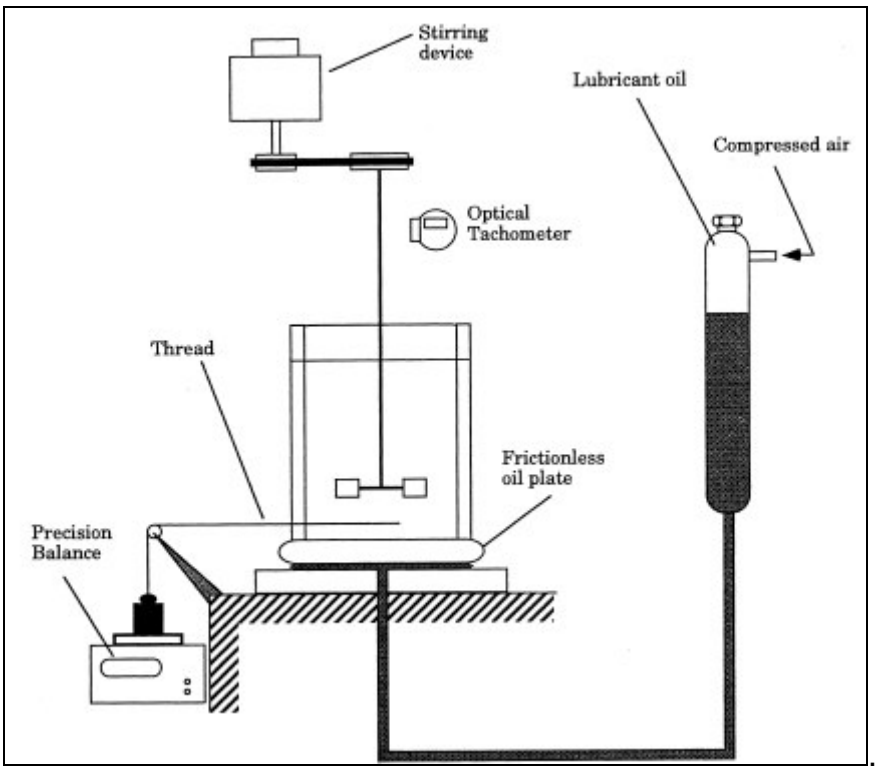

Figure 2.6 Experimental setup to measure velocity gradient (Rossini, 1999)

The velocity gradient calculation formulas are useful in design of coagulation and flocculation units in determining power requirement, diameter of impeller or adjusting impeller rotation speed. The determination of velocity gradient for rapid mixing is based on design criteria suggesting a velocity gradient changing from 1000 to 700 s^{-1} depending on detention time changing from 20 seconds to 2.5 minutes (Reynolds, 1982). For slow mixing, the velocity gradient must fall within limits such that it should allow neither less than a value to inhibit particle interaction nor more than a value to cause flocs breakage. A typical

value varying between 200 and 50 s^{-} is suggested by authorities (Tchobanoglus et al., 2003).

Rapid mixing intensity and duration is important in coagulation-flocculation processes. The effect of mixing intensity and duration was studied that on removing turbidity of a synthetic water (prepared by kaolin) with an initial turbidity of 900 FTU by using conventional coagulants, i.e. alum and ferric chloride. First, an initial rapid mixing time of 60 s was fixed and velocity gradient varied over the range of 100 and 420 s^{-1}. The residual turbidity values showed that increasing velocity gradient to some extent, 360 s^{-} and 200 s^{-} for ferric chloride and alum respectively, increased turbidity removal efficiency and further increment of that resulted in again an increase in residual turbidities because of floc breakage. After determination of optimum velocity gradient, effect of mixing time was investigated up to 180 seconds while keeping velocity gradients at previously determined optimum values. Two optimum mixing durations were observed around 10 and 60 seconds, in this part of the experiment. Ten seconds of rapid mixing duration was explained by peculiar structure of hydroxide flocs which present four aggregation levels: primary particles, microflocs, flocs and floc aggregates and the bonds between these structures are elastic and progressively weaker and weaker. Since aluminum hydroxide precipitates takes about 7 seconds for their formation, with 10 seconds of rapid mix large floc aggregates break in flocs during flocculation but maintain good resistance to erosion (Amirtharajah and Mills, 1982; Jaussens, 1992). Another optimum point occurred around 60 seconds was explained as of homogenous particle size distribution obtained after rapid mixing which provides the optimum sweep-floc able to wrap primary particles. Further increases in rapid mixing duration gave rises in residual turbidity values due to microflocs breakage into primary particles and resulted in a slow

down of floc growth during flocculation (Françoise, 1988; Rossini et al., 1999).

Having the flocs with a density close to that of water, the settling of flocs in agitated tank is negligible compared to velocity of the agitated liquid. For this reason the flocs follow the fluid motion and collisions are induced by local velocity gradient within the fluid during flocculation. The successive collision of the particles causes their agglomeration. If the velocity gradient is higher, the exerted hydrodynamic stresses overcome the aggregate strength resulted in floc breakage, in hydrodynamic aspect (Bouyer et al., 2005).

The floc's fragmentation is investigated by fractal aggregation theory provided a means of expressing the degree to which primary particles fill the space within the nominal volume occupied by an aggregate (Gardner, 1999). The theory is based on determination of fractal dimension, D_f, i.e. relationship between the increase in radius and the corresponding increase in mass contained within the circle or in other geometrical terms, and relation of it with hydrodynamic and physicochemical conditions (Chakraborti et al., 2003). Fractal dimensions can be two or three dimensional depending on the method used in the measurement. Measurements are performed either by image analysis or light scattering methods yielding a two or three dimensional analysis of aggregates, respectively. Fractal dimensions is expressed as follows,

$$A \alpha r^{D_f} \; or \; M \alpha r^{D_f}$$

where; A and M are the sum of areas or masses of all primary particles within a circle of radius r respectively. D_f has a value between 1 and 2 or 3 according to two or three dimensional space, respectively. The higher

D_f the aggregates have the more compact the aggregates are. During coagulation and flocculation, characteristics of the particles change as they interact with coagulant and with each other. As fine primary particles combine to form flocs, they form irregular structure incorporating increasing amount of interstitial water. Conversely; when flocs break by applied shear, they break off from their weakest points in the floc structure. This produces fragments that are stronger and more compact but smaller than their parent floc. Thus flocculation increases the average floc size, but decreases its average compactness; on the contrary, fragmentation decreases the average floc size and increases the average floc compactness (Thomas, 1964; Tambo, 1991).

Floc sizes are highly related to velocity gradient or applied shear rate on the particles. Studies dealing with interrelation of mixing time and floc size revealed that the floc size increases and after a time approaches a steady state, as slow mixing time increases. Steady state situation is defined as the equilibrium between breakage and agglomeration of flocs. Generally the time required for steady state situation is around 30 or 40 minutes (Spicer et al., 1998; Glover et al., 2000). On the other side, high velocity gradient produces smaller flocs but relatively more compact flocs than that of slow one. The effect of velocity gradient on floc structure is extensively studied and found that D_f value changes between 2.5 and 1.50 for aggregates, usually produced by alum or alum-polymer, and tends to increase while velocity gradient is increased (Jullien and Meakin, 1989; Torres et al., 1991; Oles, 1992; Kusters et al., 1996; Spicer, 1997).

Fractal dimensions of flocs formed via sweep flocculation is the highest and that formed via bridging flocculation is the lowest. Enmeshment of particles in the precipitation of amorphous hydroxide produces more compact flocs in sweep flocculation mechanism. On the contrary,

polymers connecting the particle form the floc structure in a loose and irregular shape yielding lowest fractal dimensions (Li et al., 2006).

Flocs are subject to breakage in case of higher shear stress exertion than its floc strength, as previously mentioned. After breaking floc under high shear stress, and then reducing shear stress to original value allows regrowth of flocs. Comparing regrowth floc size with original one, it is able decide whether suspension exhibits reversible or irreversible floc dynamics. For the flocs produced by indifferent electrolyte (i.e. NaCl), the system exhibit a reversible behavior. Because floc fragmentation and regrowth does not affect the van der Wall's forces binding forces between primary particles (Kusters, 1991).for the flocs produced by alum, however, system responses an irreversible behavior. Once the floc broken, they are not able to regrow into their original size but attain a new steady state floc size. Also, the higher shear rates to break flocs applied the smaller particle sizes in new steady state situation obtained. If this break up and reaggration steps are repeated twice, it produces floc with same size as previous broke down and regrowth flocs indicating that floc breakage is reversible. The reason why second break up and reaggregation of flocs shows a reversible dynamic system lies within history of hydrodynamics condition experienced by the flocs (Bouyer et al., 2005).

Investigation of floc structure under different coagulation mechanisms gives a better insight in understanding how these mechanisms works. Varying the velocity gradient and measuring particle size with respect to that shows floc strength. For the flocs showing a steep decrease in size while velocity gradient increasing, these are classified stronger than the other showing a sharp decrease. Among three different coagulation mechanisms, charge neutralization, bridging and sweep flocculation, flocs formed via bridging flocculation is the strongest followed by sweep

flocculation and as weakest charge neutralization. Flocs formed by charge neutralization have the weakest strength among the others, because there are not enough physical bonds. In addition to these, increasing shear rate also increases floc strength at the same order independent from mechanism involved (Li et al., 2006).

2.5.2 Polymer Properties

A polymer is a chain of small subunits or monomers. Many polymers contain only one kind of monomer; nevertheless some contain two or three different types of subunits. The total number of subunits in synthetic polymer can be varied, producing material at different molecular weight. Polymer chains may be linear or branched to varying degrees. The polymer can be called polyelectrolyte depending on its ionizable group. The classification is done according to ionizable group; cationic, anionic or ampholytic (containing both positive and negative charge). If polymer does not have an ionizable group it is called non-ionic (Weber, 1972).

The ability of a polymer to act as a flocculent depends on its ability to bond to the surface of the colloidal particles making them quite specific for destabilization of the colloids. Some other important parameters which affect the performance of a particular polymer are its molecular weight, degree of branching and charge density. Moreover, solution characteristics can be important.

Anionic polyelectrolyte posses a negative charge, so for this reason cations must be present in the medium for an efficient flocculation. Because initially cations must destabilize the particles with negative surface then anionic polymers can be used to combine particles together to occur successive particle-particle bridging. In a detailed manner,

cations form complexes with certain ionogenic groups on the polymer on the particle surface. This complex formation occurs at the particle/solution interface where the concentration of cations is high due to attraction of negative surface charge. Thereby, cations enhance the adsorption of the anionic polyelectrolyte on the negatively charged colloid. In addition to that cations hinder the repulsion between particle-particle and polymer-polymer (Black et al., 1965; Sommerauer et al., 1968; Levin and Friesen, 1987; Levy et al., 1992). The functional groups of anionic polymers are usually carboxyl, sulfonic and hydroxyl groups (Davis et al., 2003). Interaction of non-ionic polymer with particles is achieved via hydrogen bonding. A molecular weight higher than 10^6 g/mol is suggested for proper bridging flocculation (Besra et al., 2006). Coagulation with cationic polyelectrolytes happens in two distinct steps. Either they can be adsorbed by negatively charged particles using positively charged functional groups, thereby suppressing charge repulsion or by formation of the charge patches by adsorption of polymers onto the particles ,let some part of particle posses opposite charge to that of surface charge, and further attraction through opposite charges (Gregory, 1973; Ghosh, 1985; Sableviciene et al., 2005).

The polymer used for flocculation can be classified into two types in terms of their molecular structure, linear or branched. Branched polymer is usually obtained by grafting polymers on the other polymer segments. It was expressed that grafted polymers improves flocculation efficiencies. For instance, PAM-grafted amylopectin is better at flocculating a kaolin suspension than analogous grafts of PAM onto starch or amylose, as these water-soluble polysaccharides are less branched and of lower MW than amylopectin (Bolto and Gregory, 2007). The reason for better flocculating power of the graft copolymers than the linear polymers is as follows; essentially polymer bridging occurs because segments of a polymer chain adsorb on different particles, thus linking the particles

together. In order for effective bridging to occur, there must be sufficient chain length, which extends far enough from the particle surface to attach to other particles. In cases of linear polymers, the polymer segments attach to the surface in trains, project into the solution as tails or form part of loops, which link trains together. This way they can form bridges between the colloidal particles to form flocs as in Figure 2.7. Whereas, the dangling grafted chains can easily bind the colloidal particles through bridging to form flocs for graft copolymers. This type of intense bridging is not possible in cases of the linear polymers. A simple illustration of that mechanism is demonstrated in Figure 2.8 (Singh et al., 2003; Tian et al., 2006).

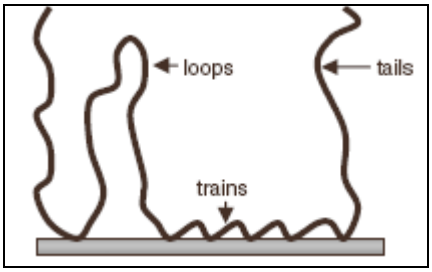

Figure 2.7 Typical adsorption of a linear polymer on particle surface (Tian et al., 2006)

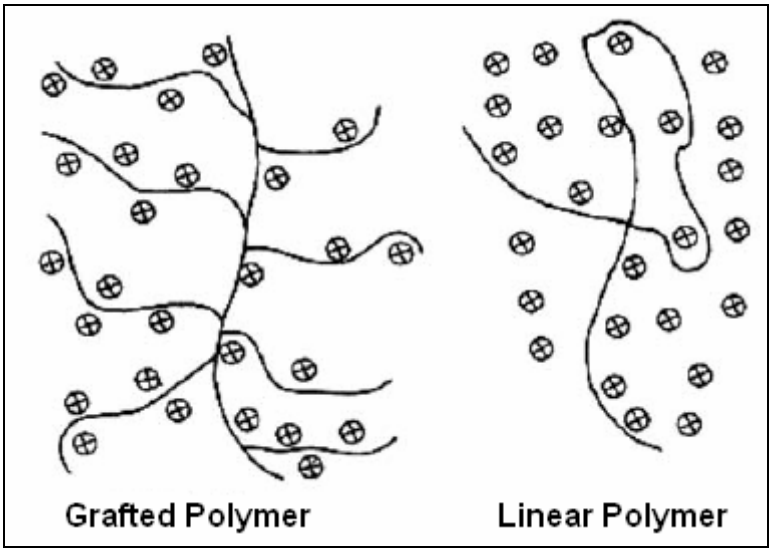

Figure 2.8 Schematically representation of the efficiencies of grafted polymer and linear polymer on particle bridging (Singh et al., 2003)

Position of functional groups in polymer structure is also affecting the flocculation efficiency. In a comparison study of the effect on flocculation of carboxyl group's positioning on different parts of the acidic polysaccharides indicated that the main parameter for a better flocculation was the accessibility of acidic sites to interactions with clay particles. Indeed, the ionic interaction was more efficient when acidic part are located in polymer's side chains, well exposed toward the outside rather then located on the backbones. Also short side chains prevent favorable exposure of acidic sites resulting in low flocculation efficiency (Labille et al., 2005).

The effect of charge density or percentage hydrolysis of polyelectrolytes is of influence the configuration in solution. For a given molecular weight, increasing charge density has the effect of increasing the viscosity of the polyelectrolyte solution (Katchalsky, 1953). Since the viscosity increases with the length of molecule, the implication is that with increasing charge

density, polyelectrolyte chains are increasingly stretched by increasing electrostatic repulsion between charged units. At low charge densities polyelectrolyte assumes a tightly coiled almost spherical configuration due to the predominance of Brownian movement. For the medium charge densities polyelectrolytes configuration resembles to flexing coil. For high charge densities configuration is of fully extended filamentous rod. Also, it is accepted that for a fixed charge density, the longer the polyelectrolyte chain, the higher the viscosity (Bratby, 1980). In conclusion, the higher the molecular weight of polyelectrolyte, the higher is the viscosity. An empirical relation is developed by Mark–Houwink as below (Huang et al., 2000).

$$IV = k(MW)^a$$

Where; IV is the intrinsic viscosity (dL/g), MW the molecular weight and k and a are the Mark–Houwink constants,

In many studies it was found that optimum flocculation occurs at polyelectrolyte dosages around that needed to just neutralize the particle charge, or to give a zeta potential close to zero (Kleimann et al., 2005). It was also indicated that polyelectrolytes of high charge density are more effective, because they deliver more charge to the particle surface for a given dosage (Bolto and Gregory, 2007). In a study on sewage floc strength showed that the optimum charge for producing strong flocs with ultrahigh molecular weight cationic polyelectrolytes was between 0.18 and 1.42 mequiv./g. It was proposed that at charge densities below this range, the polyelectrolyte adsorption is low and the subsequent floc strength is weaker, while at higher charge densities electrostatic patch flocculation occurs. This form of flocculation is inherently weaker than polymer bridging because there are fewer polymer chains adsorbed on more than one particle (Gray and Ritchie, 2006).

The molecular weight effect on flocculation differs depending on solutions flocculated. While higher molecular weight of anionic polyelectrolytes yields a better performance in turbidity removal from natural stone suspension, higher molecular weight of cationic polyelectrolyte causes a decrease in dye removal process efficiency due to a reduced availability of functional groups and a less flexible structure. However, it should be noted that pH of the medium directly effects conformation of molecular structure and become predominant parameter over molecular weight. (Bayraktar, 1996; Ersoy, 2005; Guibal and Roussy, 2007).

Polymer concentration and adsorption on particles subsequently effects efficiency of flocculation. It was proposed that the optimum dosage corresponds to ‘‘half surface coverage’’. The idea is based on defining covered (θ) and uncovered (1-θ) surface fraction and the product of covered and uncovered surface fractions should be maximum, expressing in mathematical terms that is θ(1-θ). This term has a maximum value when θ is 0.5, in line with the half surface coverage idea. However, for adsorbed polymers, it is difficult to define ‘‘surface coverage’’ precisely and so quantitative predictions based on this concept are of limited value. It is generally found that optimum bridging flocculation occurs at well below saturation (monolayer) coverage of the particle surfaces by adsorbed polymer. Under these conditions, practically all the polymer is adsorbed and it follows that the optimum dosage should be directly proportional to the total particle surface area and hence to the particle concentration (La Mer, 1966; Bolto and Gregory, 2007). Another method for determination the required concentration of polymer for half surface coverage was calculated by adsorption isotherms which are done by measuring equilibrium polymer concentration in bulk solution and calculating adsorbed amount of polymer per total mass of suspended particles. The data acquired from

adsorption isotherm was analyzed and assessed further by Langmuir monolayer adsorption equation to determine the amount of monolayer absorbance density. The equitation is as follows:

$$\frac{C_e}{A_s} = \frac{C_e}{C_m} + \frac{K}{C_m}$$

Where; C_e is the equilibrium concentration [mg/L], A_s is the amount of polymer adsorbed polymer [mg/g], C_m is the monolayer adsorption density [mg/g] and K is a constant. The reciprocal of the slope of C_e/A_s vs. C_e represents the monolayer adsorption. Relying on these equation, calculated corresponding monolayer coverage tended to increase from 0.079 mg/g for anionic polymer to 1.500 mg/g for cationic polymer at a constant pH of 6.4 for a negatively charged particles. Once the monolayer coverage value was determined, it was shown that around half of that value shows the best flocculation efficiencies (Besra et al., 2004).

2.5.3 pH

pH has a combination of different effects on the coagulation and flocculation by changing surface charges, dissolution properties of coagulants, polymer adsorption amounts and polymer's structural properties.

The first dramatic effect of pH is on the particle charges. For this reason usually surface charges of particles reported with pH of the medium in which measurement was done. For negatively charged particles a decrease in pH results in an increase in surface charge from negative to positive. Vice versa is also valid for positively charged particles. (Walaszek and Ay, 2005; Ersoy, 2005). The pH value at which the

particles carry no net surface charge is called isoelectric point and one can come to a conclusion whether the particle carry a negative or positive charge by comparing pH of the solution and isoelectric point as long as the solution properties is the same with that of the isoelectric point measurements, except pH. For the negatively charged particles, the pH values lower than isoelectric point carry positive charges and vice versa those for positively charged ones. Also adsorption of polymers is highly affected by pH changes. For the anionic polymer, adsorption is higher at the acidic ranges and becomes lower in the basic ranges and opposite of it is valid for cationic polymers and it seems that non-ionic polymer adsorption is nearly independent of pH. Degree of relative charge differences between surface and polymer plays an important role in adsorption amount of polymers (Besra et al., 2004).

Secondly, the solubility and hydrolyzed products of metal coagulants and polymers is affected from pH of the solution. Once hydrolyzing metal salts is added to solution, it hydrolyzes into different species depending on their equilibrium constants. At the end of coagulation/flocculation process pH should be checked to keep soluble products of metal salts in a minimum level to avoid adverse health effects and some esthetical problems arising from those species (Ching et al., 1994).

The conformation of polymers on particle surface is also affected from solution pH. Depending on pH and polymer type (cationic or anionic), polymers react with hydrogen or hydroxide ions. For instance, in the acidic ranges, anionic polymer tends reacts with hydrogen ions and forms a more coiled structure and for basic ranges polymers form an expanded structure due to repulsion of negative hydroxide ions. A stretched polymer structure can easily extend from particle surface to other particle surface rather than in a coiled form that affects flocculation efficiency ultimately. The schematic illustration of the conformational

state of adsorbed polymers at different pH is illustrated in Figure 2.9 schematically (Singh et al., 2003; Besra et al., 2004).

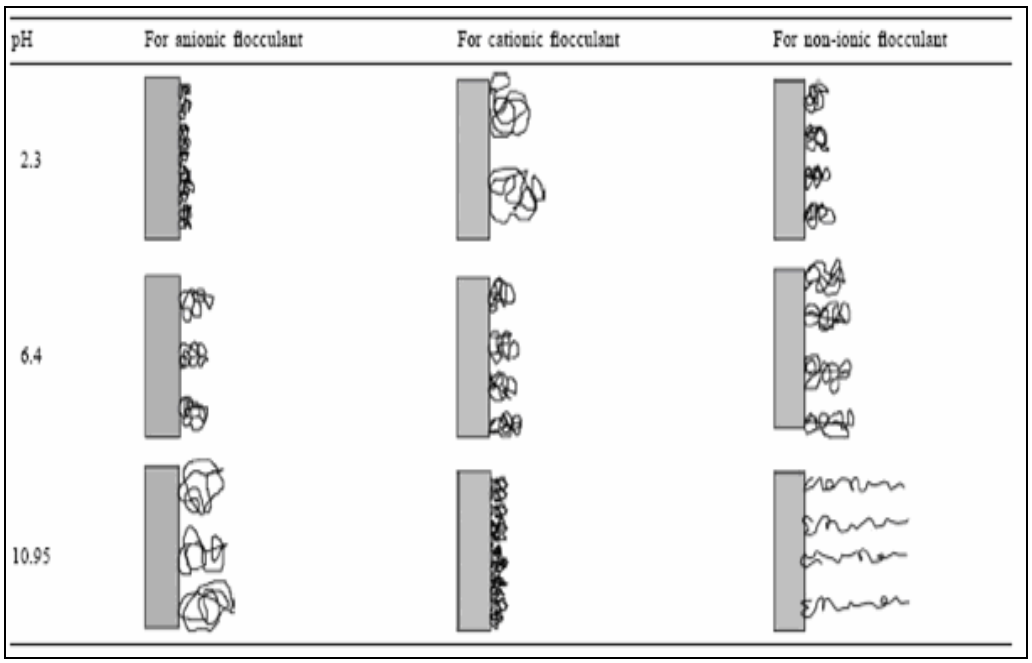

Figure 2.9 Conformation of different types of flocculants on particle surfaces under different pH values (Besra et al., 2004)

2.6 Hydrolyzing Metal Salts in Coagulation

Hydrolyzing metal salts, based on aluminum and iron are widely used as coagulants in water treatment. Usually these coagulants are sold in the form of aluminum sulfate, namely alum, ferric chloride and ferric sulfate. Aluminum sulfate has been used for water purification since ancient times and plays a vital role in the removal of many impurities from polluted water like colloidal particles and dissolved natural organic matters (Cohen and Hannah, 1971).

Dissolving the sulfate or chloride products of this metal salts in water produce not only trivalent $Al^{+3}$and Fe^{+3} ions but also a range of

monomeric and polynuclear hydrolysis products present depending on pH. Many hydrolysis products are cationic and these can interact strongly with negative colloids, resulting in destabilization and flocculation, under the correct conditions of dosage and pH.

Al^{+3} and Fe^{+3} ions present in water at hydrated form consisting of six water molecules. Owing to the high charge on the metal ion, water molecules are polarized and this can lead to a loss of one or more protons, depending on the solution pH. The degree of proton lost gives a lower positive charge; monomeric hydrolyzed form, their equilibrium formulas and hydrolyzing constants (K_1, K_2, K_3, and K_4) are given below (Duan and Gregory, 2003):

$$[M(H_2O)_6]^{+3} \leftrightarrow [M(OH)\ (H_2O)_5]^{+2} + H^+ \qquad K_1$$
$$[M(OH)(H_2O)_5]^{+2} \leftrightarrow [M(OH)_2(H_2O)_4]^{+} + H^+ \qquad K_2$$
$$[M(OH)_2(H_2O)_4]^{+} \leftrightarrow [M(OH)_3(H_2O)_3]_{(s)} + H^+ \qquad K_3$$
$$[M(OH)_3(H_2O)_3]_{(s)} \leftrightarrow [M(OH)_4(H_2O)_2]^{-} + H^+ \qquad K_4$$
$$[M(OH)_3(H_2O)_3]_{(s)} \leftrightarrow [M\ (H_2O)_3]^{+3} + 3OH^- \qquad K_{sp}$$

M, here represent Al or Fe and K_{sp} represents solubility product. As well as simple hydrolysis product, there are many possible polynuclear forms like $Al_2(OH)_2{}^{+4}$ and $Al_3(OH)_4{}^{+5}$ and there are equivalent species for Fe (Richens, 1997). Since the equilibrium expressions include the hydrogen or hydroxide ion, pH become an important parameter reflecting portions of the monomeric species. Concentration of monomeric hydrolysis products in equilibrium with amorphous hydroxide precipitate of iron and aluminum as a function of pH is shown in Figure 2.10 below.

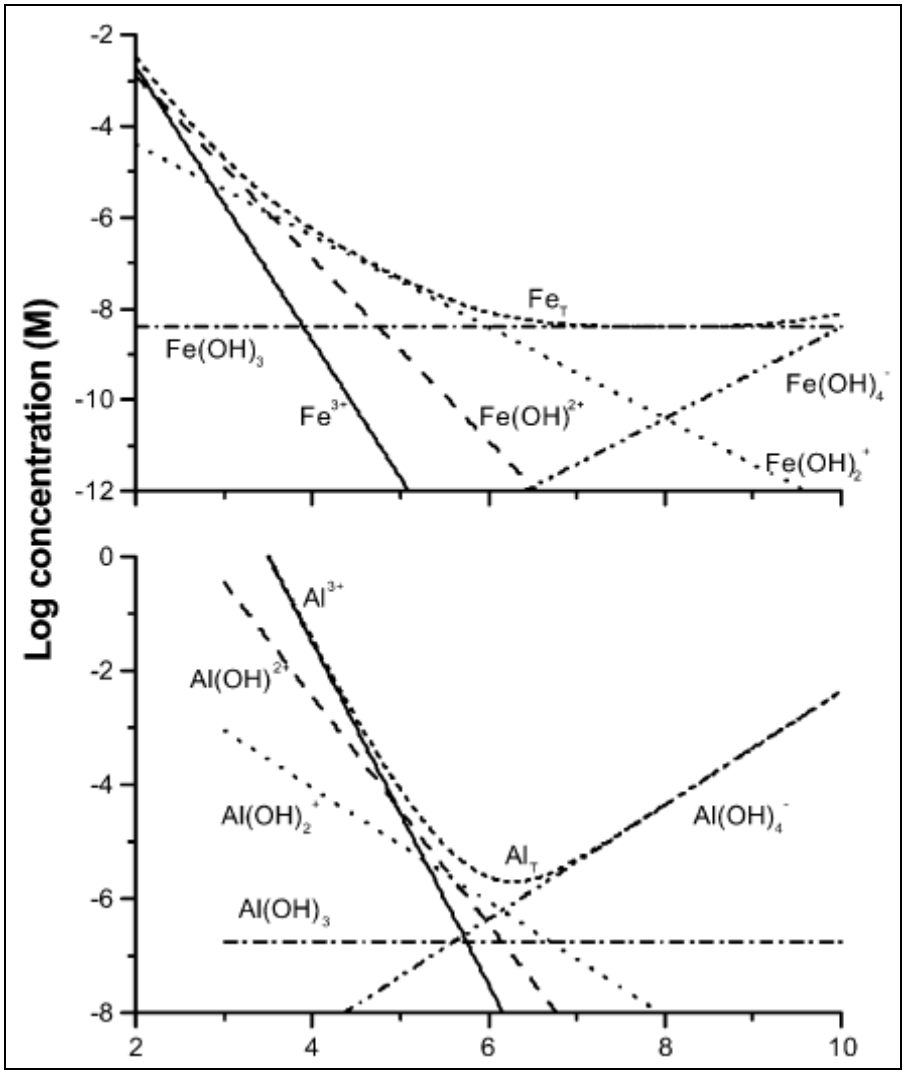

Figure 2.10 Concentration of monomeric hydrolysis products of Fe(III) and Al(III) in equilibrium with amorphous hydroxides (Duan and Gregory, 2003)

As it can be seen from Figure 2.10, hydrolysis products of iron spread into wide range of pH, whereas, that of aluminum squeezes in a narrow range. That makes ferric species attain significant relative concentrations in solution at appropriate pH values and offer application in a wide pH range. Additionally, Al has minimum solubility at certain pH around 6, Fe corresponds a higher pH region in terms of minimum solubility (Duan and Gregory, 2003).

As mentioned before, aluminum and iron have limited solubility in water. In case of solubility limit exceeded, amorphous precipitate occurs and it may change the destabilization mechanism of coagulation. Two modes of destabilization mechanism are present when hydrolyzing metal salts are used. Firstly, adsorption of cationic species onto particle surface and destabilize them. Secondly, particles can be enmeshed in a growing precipitate if the solubility limit exceeded. A typical Al concentration in the order of 1-2 µM would be sufficient for adsorption and charge neutralization and higher amount of Al is required for sweep floc mechanism 70-90 µM (Ching et al., 1994). Since Al or Fe goes through hydrolysis, they quickly depress solution pH following their addition to water. To control pH value, a buffer or alkalinity must be supplied to water. The stoichiometric equation of alum and alkalinity is like: (Tchobanoglus et al., 2003);

$$3Ca(HCO_3)_2 + Al_2(SO_4)_3{*}18H_2O \rightarrow 2Al(OH)_3 + 3CaSO_4 + 6CO_2 + 18H_2O$$

2.7 Biopolymers Used in Coagulation-Flocculation

Currently metal salts (especially alum) are used alone as coagulant or in combination with synthetic polymers that act as coagulant aids. However, recent studies indicate residual aluminum causes Alzheimer's disease and other related problems. In addition to that, synthetic polymers used to increase coagulation efficiency have some negative impact on human health due to the presence of residual monomers from manufacturing process and reaction by products of these with chemicals used in water treatment. For these reasons, natural organic polymers, which are non-toxic and biodegradable, was studied for their flocculating ability to replace inorganic coagulants in recent years (Huang, et al.,

2000; Salehizahed and Shojaosadati, 2001; Ozacar and Sengil, 2003). Examples of these studies are provided below.

The natural coagulants extracted from Prosopis Juliflora and Cactus Latifaria were evaluated by jar test experiment with synthetic water prepared using kaolin. The coagulants performed well to meet the required turbidity standards both in high and low turbidity waters. The optimum coagulant dose was found to be lower than that for aluminum sulphate. For both biopolymers non-polar sites are thought to be responsible for coagulation and flocculation (Diaz et al., 1999).

Another natural coagulant obtained by extraction Moringa Oleifera seeds was used for different surface waters and an average 50% turbidity removal was achieved (Muyibi and Okuofu, 2001). In another study, the effect of extraction technique of Moringa Oleifera on turbidity removal was investigated and it was found that extraction technique changed the efficiency of the coagulant. Same study reported the necessity of divalent cations for coagulation (Okuda et al, 2001). In an advance, the active component of Moringa Oleifera was extracted and coagulation-flocculation experiment was performed with that extracted active component on synthetic and river water. The result was promising in reducing turbidity, where initial turbidity was as low as 9 mg kaolin/L, without an increase in dissolved organic carbon concentration (Okuda et al, 2001).

In addition to the natural polymers discussed above, cactus, chitosan, cationic starches and extracellular polymeric substance derived from Rhodovulum sp. were studied as alternative coagulants and results concluded that they have coagulation and flocculation capacity for turbidity removal (Zhang et al., 2006; Divaharan and Pillai, 2001, 2002; Pal et al., 2005; Watanabe et al., 1999).

The application of biopolymers is not only limited in water treatment but also they are applied in wastewater treatment like COD removal from sewage water, color reduction in textile wastewater, and suspended solid and oil removal from palm oil wastewater (Zhang et al., 2006; Mishra and Bajpai, 2005; Ahmad and Hameed, 2005).

2.7.1 Alginate and its Application in Environmental Field

2.7.1.1 Physicochemical Properties of Alginate

Alginic acid or alginate is a natural polysaccharide obtained from marine brown algae which can also be produced by certain bacterial strains such as Azotobacter Vinelandii and Pseudomonas Aeruginosa. It is formed by two monomeric units: α-L guluronic acid and β-D mannuronic acid residues in varying proportions, order, and molecular weight as shown in Figure 2.11 (Martinsen et al., 1991; Sabra et al., 2001). Alginic acid is the only polysaccharide, which naturally contains carboxyl groups in each constituent residue, and possesses various abilities for functional materials (Ikeda et al., 2000).

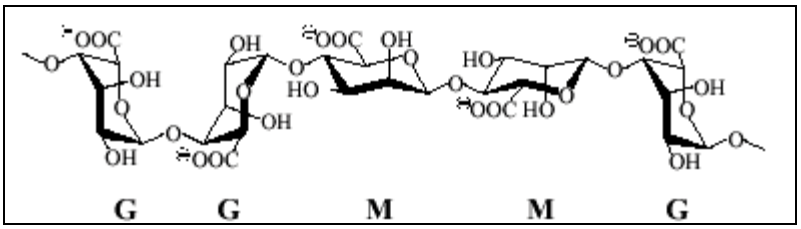

Figure 2.11 Structural composition of alginate (Sabra et al., 2001)

It was indicated that an alginate solution turns into gel in the presence of multivalent cations, usually Ca^{+2}, Ba^{+2} or Sr^{+2}. Bivalent cations,

especially calcium, play an important role in the formation of the gel network, since they establish the junction nodes between neighboring alginate strands. In case of these polysaccharides, gel formation was attributed to the formation of chelate complexes between calcium ions and two or more adjacent mono-G-blocks, commonly referred to as the "egg box" model (Figure 2.12). This formation, egg-box structure, is dependent on ratio of mannuronic and guluronic acid monomers: alginates possessing a high guluronic acid content develop stiffer, more porous gels which maintain their integrity for longer periods of time. During cationic cross-linking, they do not undergo excessive swelling and subsequent shrinking, thus they better maintain their form. Conversely, alginates rich in mannuronic acid residues develop softer, less porous gels that tend to disintegrate with time. Alginates with a high mannuronic acid content are also plagued by a high degree of swelling and shrinking during cationic cross linking (Davis et al., 2000; Simpson et. al, 2004).

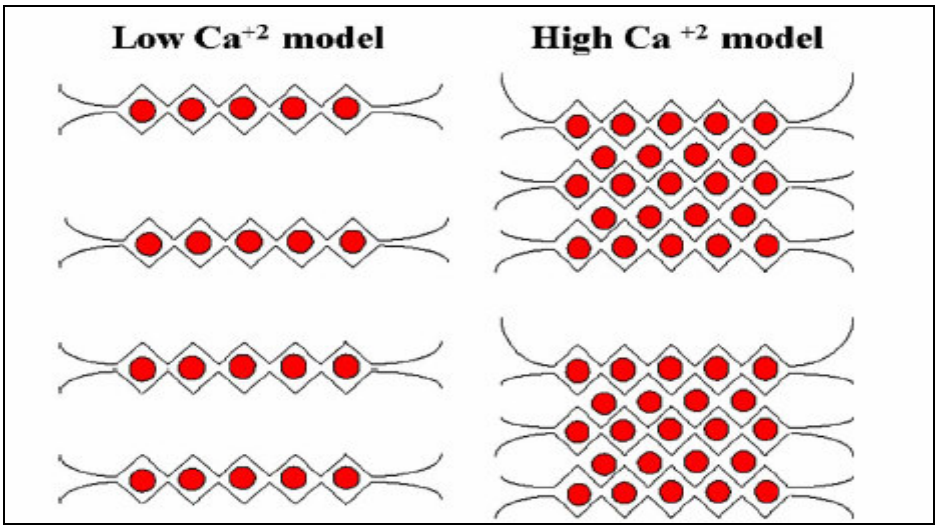

Figure 2.12 Egg-box model of calcium alginate under different calcium concentration (Simpson et. al, 2004)

2.7.1.2 Use of Calcium Alginate in Wastewater Treatment

Hydrogel-based materials were utilized in various biomedical applications including drug or bioactive molecule delivery vehicle, due to their many advantageous features. Recently, hydrogels have been increasingly utilized as cell immobilization matrices to produce various biological products (e.g., vaccines, proteins, and antibodies), and in tissue engineering to recreate tissues intended to replace those damaged or lost. In these applications, hydrogels mechanically support encapsulated cells, and regulate the function of the cells. In general, use of immobilized systems has some advantages like high biomass concentrations in the reactor, preserve viability of cells, better process control, reduced operational cost, prevention of washout of cells and continuous removal of toxic metabolites. In environmental engineering immobilized growing cell studies are carried out to understand and model the behavior of the immobilized organisms in wastewater. In most of the studies, as a hydrogel Ca-alginate are used, because alginate is a biopolymer and not toxic to bacteria and as indicated before it has strong binding capacity with Ca^{+2} ion (Kong et al., 2003). One of the studies regarding to treat azo-dye containing wastewater with immobilized culture was done to assess the degradation rate of both suspended and immobilized cultures under various treatment conditions and found that entrapped cell's degradation rate was faster than that of suspended one (Steffan et al., 2005).

Besides use of calcium alginate in biological system, it is used in heavy metal removal from the solutions. Since traditional methods like chemical precipitation, ion exchange and membrane processes have some disadvantage; they often produce large quantity of sludge or involve high investment and operational costs. In recent years, use of biopolymers as

an absorbent came out as an alternative to these processes (Volesky, 2001). Again, calcium alginate hydrogels or beads are one of the absorbent in the removal of wide variety heavy metal species (e.g. chromium (III), copper, zinc, nickel and cobalt) from the water (Ibanez and Umetsu, 2002).

2.7.1.3 Use of Calcium Alginate in Water Treatment

Before this thesis study, another thesis study with subject of “use of calcium alginate as a coagulant in water treatment” was carried out by Çoruh (2005). The thesis covered the effect of initial calcium and alginate concentration, dosing order, sodium and magnesium ions concentrations on the turbidity removal. To evaluate the effect of initial turbidity, three different initial turbidity values as high (150 NTU), medium (80 NTU) and low (10 NTU) were tried using jar test apparatus employing the mixing regime: a 1 minute rapid mixing at 120 rpm right after the calcium or alginate is dosed, followed by a 1 minute rapid mixing at 120 rpm after the alginate or calcium is dosed, then a 20 minutes slow mixing at 40 rpm and finally 30 minutes of settling.

The calcium concentrations tested varied between 30 and 200 mg/L and alginate concentrations studied varied between 0.008 and 40 mg/L. The results suggest that solely calcium addition gave better turbidity removal efficiencies than solely alginate addition. Also, it is indicated that calcium alginate system did not alter the solution pH.

Figures 2.13 and 2.14 show the final turbidity results obtained with the 150 NTU and 80 NTU initial turbidity water samples. For the sake of showing the region around 0 to 5 NTU, only low turbidity regions of the graphs are presented. For most of the calcium and alginate doses added, the turbidity values fell near 1 NTU Generally, the turbidity

removal efficiencies decreased as the dose of both calcium and alginate decreased. The greatest turbidity removal efficiencies were achieved at calcium concentrations greater than 60 mg/L and for alginate concentrations in the range of 0.2 to 40 mg/L. At low calcium concentrations (below 60 mg/L) calcium alginate gel was not forming properly. Generally, alginate concentrations as low as 1 mg/L was enough to achieve the required turbidity levels. However; for low turbidity (10 NTU) samples, the turbidity removal efficiency decreased remarkably compared to the high turbidity water samples as shown in Figure 2.15. Additionally, TOC measurements showed that alginate did not increase TOC content of synthetic water which reduces the possibility of by products formation during disinfection.

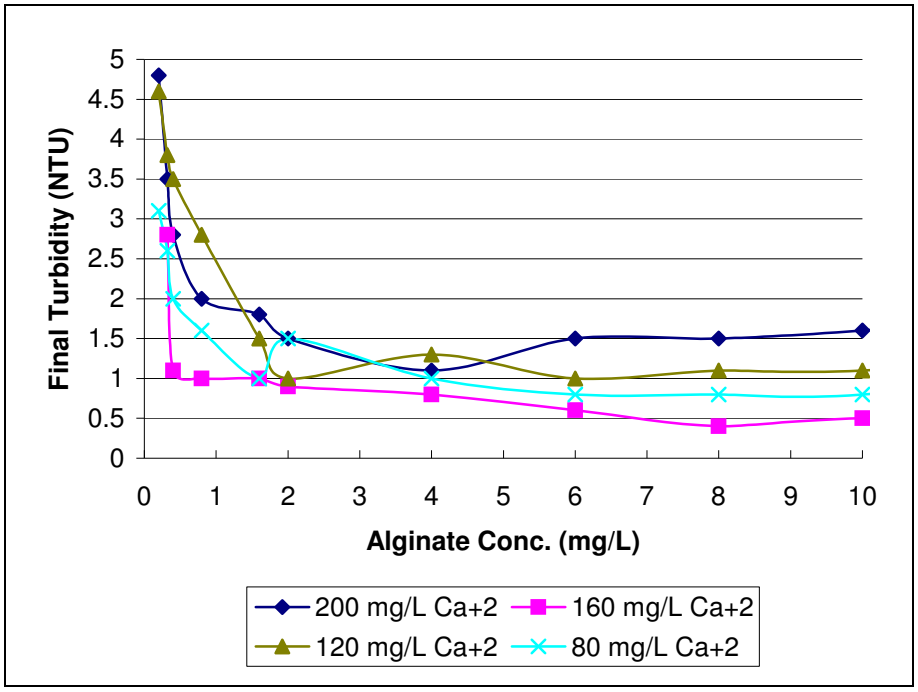

Figure 2.13 Effect of change in calcium concentration on final turbidity (initial turbidity of 150 NTU)

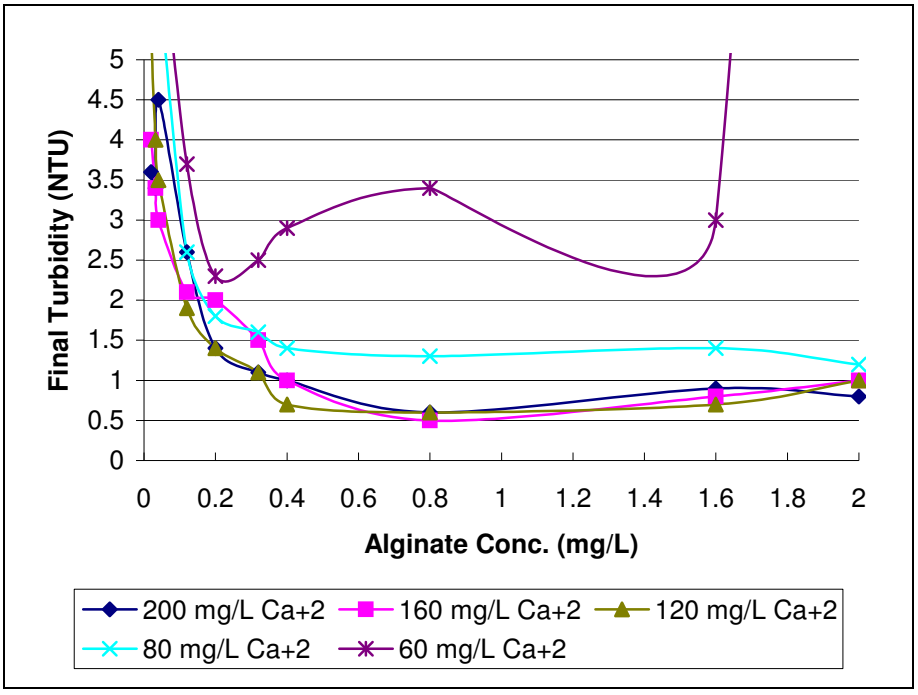

Figure 2.14 Effect of change in calcium concentration on final turbidity (initial turbidity of 80 NTU)

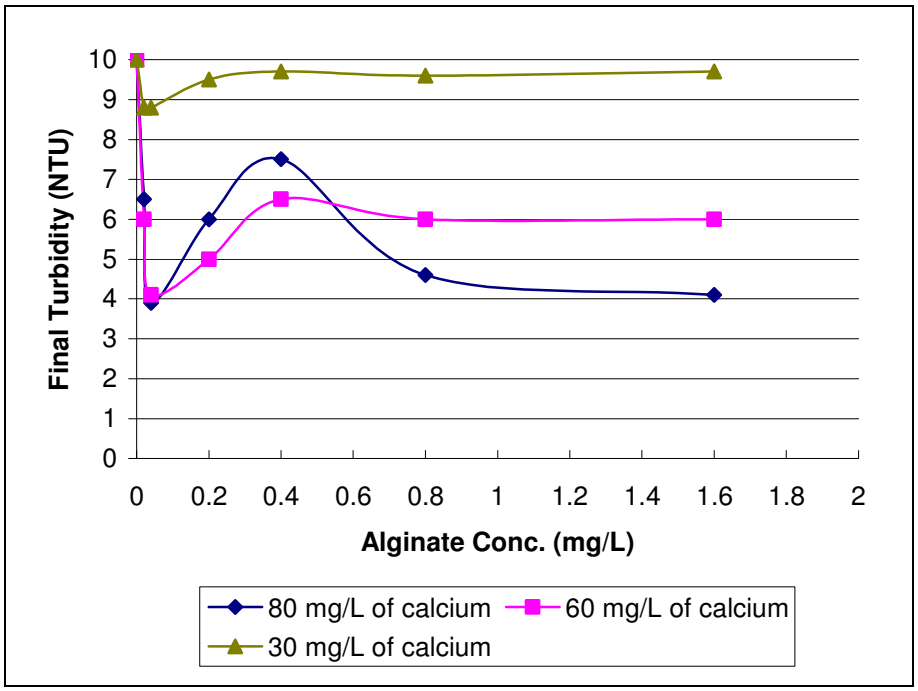

Figure 2.15 Effect of change in calcium concentration on final turbidity (initial turbidity of 10 NTU)

Inefficient turbidity removal for low turbid water raises the necessity to focus on this subject further. So in this thesis study it was tried to improve system performance in terms of turbidity removal. To do that some variables like molecular weight, rapid mixing intensity and duration, pH and alkalinity were investigated on the system performance to solve the system deficiency problem. Sludge properties and unsteady state electrokinetic observation were performed to get a detailed insight into coagulation mechanism. Also a comparison study is conducted between calcium alginate and alum. Finally, in the guidance of results, raw water taken from water treatment plant was tried to purify.

CHAPTER 3

MATERIALS and METHODS

3.1 MATERIALS

3.1.1 Water Samples

3.1.1.1 Synthetic Water

Investigation of coagulant's efficiencies and parameters related to coagulation were conducted with synthetically prepared turbid water. The synthetic water was prepared by adding approximately 0.180 g of clay to 6L distilled water and left mixing by magnetic stirrer for 24 hours to hydration and complete destabilization of clay particles. Prepared synthetic water had an average of 10±0.2 NTU initial turbidity value.

The synthetic water used throughout the experiments had a -22.61mV zeta potential value at pH 6 which was measured in METU central laboratory with Zetasizer Nano ZS90 (Malvern) apparatus and analysis demonstrated that clay particles were mainly composed of smectite (Çoruh, 2005).

3.1.1.2 Raw Water

During the coagulation experiments, raw water was also used to compare how coagulants perform with natural water. Raw water was supplied from Ankara Ivedik Water Treatment Plant (IWTP) in winter season. IWTP supplies its water from Çamlıdere and Kurtboğazi reservoirs. Water coming from Kurtboğazi is aerated with tapered

aeration, located in blending unit, and mixed with water coming from Çamlıdere reservoir. The raw water was taken from where both reservoirs' waters mix with each other and be pumped to coagulation unit. The initial physical and chemical characteristics of raw water before coagulation were as follows: 83 mg/l as $CaCO_3$ alkalinity, 7.7 pH, 1.95 NTU turbidity and 14.3 ^{0}C temperature.

3.1.2 Coagulants and Coagulant Aids

3.1.2.1 Calcium Chloride Solution

As a calcium source $CaCl_2$*$2H_2O$ (Merck) was used by preparing 15,000 mg/L or 16,000 mg/L calcium ions containing stock solutions, which were prepared by dissolving 5.5133 g and 5.8808 g of $CaCl_2$*$2H_2O$ in 100 mL distilled water, respectively. Required amount of 15,000 mg/L and 16,000 mg/L stock solutions were dosed to get 120, 80 and 60 mg/L of initial calcium concentration.

3.1.2.2 Alginate Solution

Sodium alginate salt from marine algae, shortly alginate, was used as coagulant along with calcium or alum by preparing a stock solution at 1000 mg/L concentration by weight. Since alginate does not dissolve in water easily, stock solutions were mixed with magnetic stirrer for one hour. In case of low concentration requirement 40 mg/L stock solution was used by diluting 1000 mg/L stock solution. Two types of alginate possessing different viscosities were used in jar test experiment. Viscosities of two alginates were measured at three different rotation speeds (60, 12 and 6 rpm) at constant alginate concentration of 1000 mg/L. Alginate (Fluka) showed viscosity values of 4.3, 5.05 and 5.3 cP at 60, 12 and 6 rpm respectively. Alginate (Sigma) showed higher viscosity values of 6.18, 5.88 and 6.5 cP at 60, 12 and 6 rpm respectively.

Therefore the former alginate was denoted as low molecular weight alginate and the latter as high molecular weight alginate.

3.1.2.3 Alum Solution

In jar test experiments aluminum was supplied by $Al_2(SO_4)_3*18H_2O$ (Merck). 15.4378 g or 1.2350g of $Al_2(SO_4)_3*18H_2O$ was dissolved in 100 mL distilled water yielding an initial Al(III) concentration of 12,500 mg/L or 1,000 mg/L, respectively. 12,500 mg/L solution was dosed to get lower than 4 mg/L initially Al(III) containing solutions and 1,000 mg/L solution was used for higher than 5 mg/L ones. Also, 5,000 mg/L concentration solution, which were prepared by dissolving 30.8757g of $Al_2(SO_4)_3*18H_2O$ in 500 mL distilled water, was used in jar test experiment conducted with raw water taken from Ivedik Water Treatment Plant.

3.1.2.4 Sodium Carbonate Solution

Alkalinity was supplied in the form of Na_2CO_3 (Merck) to be used in experiments related to alum or calcium-alginate. 7.95, 7.42 or 2.12 grams of Na_2CO_3 was dissolved in 100 mL distilled water to provide stock concentrations as 79.5, 74.2 or 21.2 g/L, respectively.

3.1.2.5 Clay Suspension

Two highly concentrated (10,000 mg/L and 2500 mg/L) clay suspensions were prepared as explained in section 3.1.1.2 to be used as a coagulant aid in increasing turbidity of raw water taken from IWTP's inlet.

3.1.3 Chemicals

3.1.3.1 Hydrochloric Acid Solution

Depending on the buffer capacity of waters, 1 N or 0.1 N hydrochloric acid (HCl) solutions were used in the pH adjustment of samples. 1N HCl acid solution was prepared from 37% pure concentrated hydrochloric acid (Merck) by diluting 41.449 mL in 500 mL distilled water. Similarly, 4.145 mL of concentrated acid was diluted in 500 mL distilled water in preparation of 0.1 N HCl solutions.

3.1.3.2 Sodium Hydroxide Solution

Increasing the pH of waters was carried out with 0.1 N sodium hydroxide (NaOH) solution. Dissolution of 4 g NaOH pellets (Merck) in 1000 mL distilled water yielded a basic solution with normality 0.1.

3.1.3.3 Standard Sulfuric Acid Solution

To measure the alkalinity, 0.02 N standard sulfuric acid (H_2SO_4) solutions were used as a titrant. Diluting 0.139 mL 96% pure concentrated H_2SO_4 (Merck) in 250 mL distilled water provided 0.02 N standard sulfuric acid solution.

3.1.3.4 Standard Calcium Chloride Solution

Three different calcium standards (0.5, 2.5 and 5 mg/L) that were obtained by diluting 1000±10 mg/L calcium standard with deionized water were used in the calibration of atomic absorption spectrometer for the measurement of residual calcium concentration.

3.2 METHODS

Throughout the experiment a series of jar tests were run with VELP Scientifica JLT6 leaching Jar Test apparatus having six mixers each with two flat blades. The jar test experiments were performed with 500 mL water samples. General layout of jar test experiments can be figured out like: rapid mixing after coagulant (calcium or alum) dosing, following that depending on the experiment another rapid mixing period after alginate addition (if any), then slow mixing period for flocculation and finally 30 minutes settling to allow flocs to settle. When settlement period finished, samples were carefully taken from supernatant to measure final turbidity, residual calcium concentration, alkalinity or pH. Total detention time of reaction is kept constant at 52 minutes within all the experiments except related to sludge's ones. Using jar test experiments, effect of initial calcium and alginate concentrations, alginate's molecular weight, mixing schedule, alkalinity and pH as independent variables were investigated in calcium-alginate system for turbidity removal efficiencies. Moreover, comparison of calcium-alginate system to alum on turbidity removals and sludge properties were performed with jar test experiment. In addition to these; electrokinetic pathway of coagulation-flocculation were examined to understand coagulation mechanisms of calcium-alginate and in the sight of the results obtained from experiments done with synthetic water, it was tried to treat raw water taken from IWTP. Jar test experiments conducted in duplicate to ensure results repeatability and the results were presented as average values.

3.2.1 Comparison of the Effect of Alginate's Molecular Weight

Molecular weight of polymers used in coagulation is an important parameter that affects coagulation efficiencies. For this reason, jar test

experiments were run parallel using both low and high molecular weight alginate. In Jar Test experiments, three different initial calcium concentrations of 120, 80 and 60 mg/L and for each calcium concentration, alginate concentrations varied in a wide range of 0, 0.004, 0.008, 0.01, 0.02, 0.04, 0.08, 0.1, 0.2, 0.4, 0.6, 0.8, 1.2, 2 mg/L to find out maximum turbidity removal efficiency. Jar test experiment had such a mixing schedule listed below.

1. 1 minute rapid mixing at 120 rpm after $CaCl_2$ dosing.
2. 1 minute rapid mixing at 120 rpm after alginate dosing.
3. 20 minutes slow mixing at 40 rpm.
4. 30 minutes allowed flocs to settle.

At the end of the experiments, final turbidity values were immediately measured with the samples taken from supernatant. To investigate the role of calcium in coagulation, residual calcium concentrations were also measured.

The alginate molecular weights were not specified by the manufacturer and they were only sold as low molecular weight and high molecular weight alginate. Viscosity measurements (Section 3.1.2.2) as suggested by Mark-Houwink equitation (Section 2.5.2) indicate that the polymer called as high molecular weight has high viscosity and low molecular weight has low viscosity. Unfortunately, it a healthy and consistent molecular weight determination in professional laboratories that analyze the molecular weight of polymers could not be obtained.

3.2.2 Effect of Mixing Time and Intensity

To improve the system performance, mixing schedule of jar test experiment was modified in a way that rapid mixing time was increased

from 2 minutes to a total of 10 minutes while slow mixing time was reduced from 20 minutes to 12 minutes to keep total reaction time constant. Additionally mixing intensity of rapid mixing was varied in the order of 120, 160, 200 rpm. Experiments were conducted with three initial calcium concentrations of 120, 80, 60 mg/L at the high molecular weight alginate concentration varying as 0.004, 0.008, 0.02, 0.04, 0.08, 0.1, 0.2, 0.4, 0.8, 2 mg/L. Mixing schedule of these two jar test experiments were listed below.

1. 5 minute rapid mixing at 120/160/200 rpm after $CaCl_2$ dosing.
2. 5 minute rapid mixing at 120/160/200 rpm after alginate dosing.
3. 12 minutes slow mixing at 40 rpm.
4. 30 minutes allowed flocs to settle.

Similarly, to get an idea for coagulation mechanism, mixing time schedule was modified by changing mixing times after calcium chloride dosing to 8 minutes and that of alginate dosing to 2 minutes.

1. 8 minute rapid mixing at 120/160/200 rpm after $CaCl_2$ dosing.
2. 2 minute rapid mixing at 120/160/200 rpm after alginate dosing.
3. 12 minutes slow mixing at 40 rpm.
4. 30 minutes allowed flocs to settle.

By modifying mixing time and intensity, it was aimed to investigate what was happening after dosing of calcium and alginate and the impact of velocity gradient and shear stress applied to the flocs by measuring final turbidity values.

3.2.3 Effect of pH

Natural waters vary in terms of pH depending of their sources. In coagulation-flocculation experiments, pH is a key parameter affecting the process. For this reason; turbidity removal efficiencies of coagulants should be checked for water with different pH values. To do that three different pH values, acidic (pH=4), neutral (pH=7) and basic (pH=9), were set in Jar Test experiment. pH adjustments were done with 1000 mL synthetic water by slowly adding from a 0.1 N HCl solution for pH reduction and 0.1 N NaOH for pH raise while mixing with magnetic stirrer. After adjusting pH, water sample were separated into 500 mL volumes and used for coagulation experiment done with calcium-alginate. The effect of pH on the process was studied at a calcium concentration of 120, 80 and 60 mg/L and an alginate concentration of 0.2 mg/L. Jar test was conducted as listed below.

1. 5 minute rapid mixing at 120 rpm after $CaCl_2$ dosing.
2. 5 minute rapid mixing at 120 rpm after alginate dosing.
3. 12 minutes slow mixing at 40 rpm.
4. 30 minutes allowed flocs to settle.

At the end of experiment, following final turbidity readings, final pH values were measured.

3.2.4 Effect of Alkalinity

One of the constituents that occur in natural waters is alkalinity. In this part of the study, it was examined how calcium alginate system reacts with alkalinity. So, alkalinity of synthetic waters were adjusted to 75, 150, 300 mg/L as $CaCO_3$ by adding Na_2CO_3 solution. Since addition Na_2CO_3 increased pH to levels of 10, pH of synthetic water was dropped to pH 8 by addition of 1 N HCl acid to convert all carbonate ions to bicarbonate

ions. In the experiments three different initial calcium concentrations of 120, 80, 60 mg/L with 0.2 mg/L alginate concentration were tested. After adjusting the alkalinity of synthetic water, jar tests were performed as;

1. 5 minute rapid mixing at 120 rpm after $CaCl_2$ dosing.
2. 5 minute rapid mixing at 120 rpm after alginate dosing.
3. 12 minutes slow mixing at 40 rpm.
4. 30 minutes allowed flocs to settle.

At the end of experiment, final turbidities and then alkalinity of supernatant were measured.

3.2.5 Flow Chart of Calcium Alginate Experiments with Synthetic Water

For a better visualization the flow chart of this study till this part is drawn in Figure 3.1. It would be worthwhile to remember that the experiments were performed with three different calcium concentrations of 60, 80 and 120 mg/L.

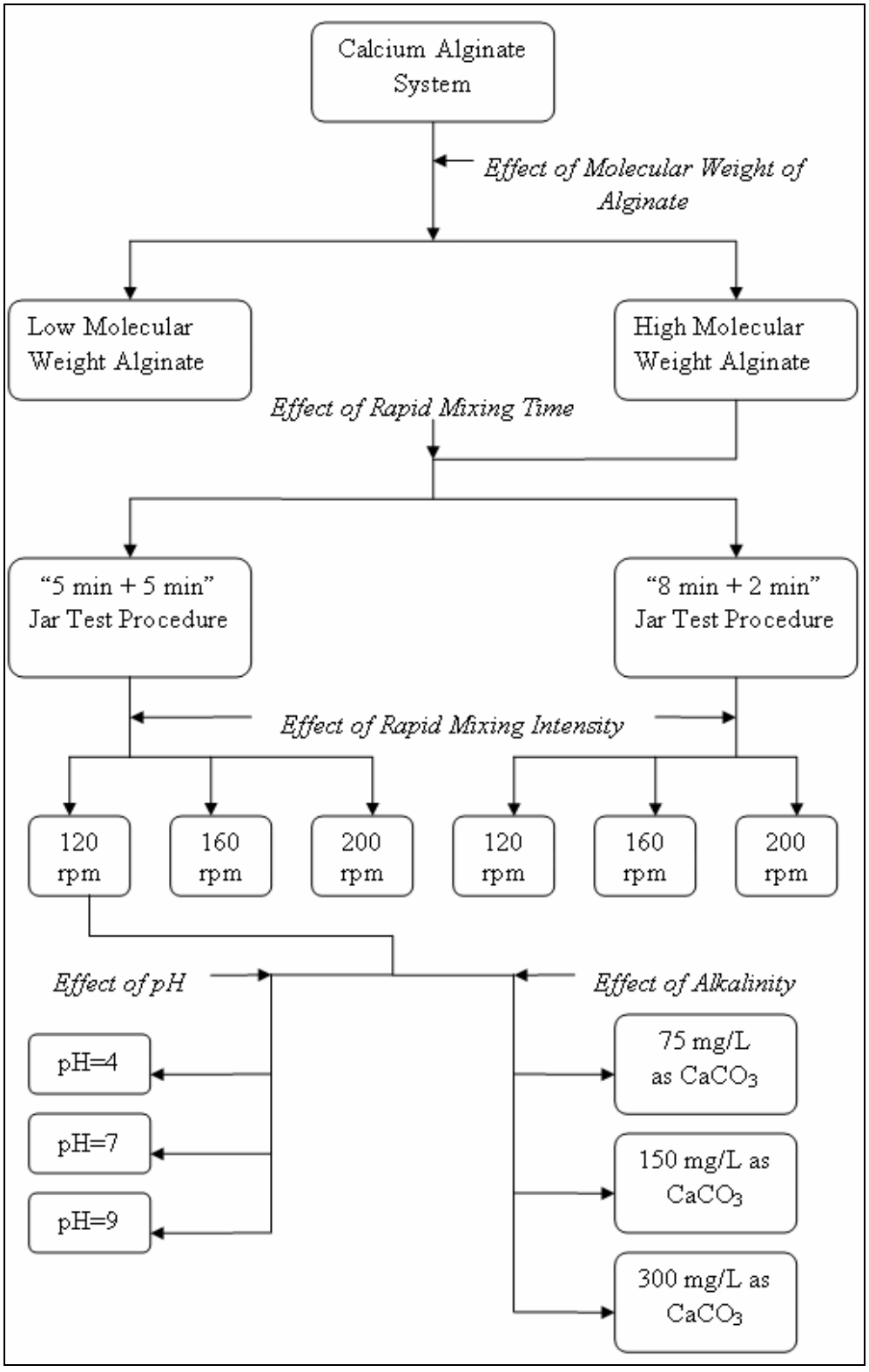

Figure 3.1 Experimental flow chart of calcium alginate system conducted with synthetic turbid water

3.2.6 Comparison with Alum Coagulant

Alum is one of the widely used coagulants in water treatment. Despite its drawbacks like requirement for alkalinity, proper pH control in operation, or large amount of sludge production etc. Alum is still used in water treatment plants. So it would worth to compare studies conducted with calcium alginate to that of alum. Consequently, a series of jar test were applied to evaluate performance of alum on synthetic water with independent variables of pH and alkalinity. Effect of mixing schedule when alum was used in combination with alginate were also investigated under varying alginate concentration between 0.004 and 2 mg/L.

3.2.6.1 pH

When alum is dosed into water, it reduces pH immediately by producing metal hydroxides. For coagulation processes done with alum, initial and final pH values should always be checked because of solubility of aluminum species like $Al(OH)_4^-$, $AlOH^{+2}$ or Al^{+3}. Appropriate water for alum coagulation needs to be alkaline meaning that they usually have pH value above 7. So in jar test experiment three different initial pH values of 7, 8, 9 were set with an initial alkalinity concentration at 35 mg/L as $CaCO_3$. After arranging alkalinity and pH of the synthetic water, a mixing schedule was applied for jar test as listed below.

1. 1 minute rapid mixing at 120 rpm after alum dosing.
2. 21 minutes slow mixing at 40 rpm.
3. 30 minutes allowed flocs to settle.

At the end of experiment, performance of alum on synthetic water was evaluated by measuring final turbidity, alkalinity and pH values.

3.2.6.2 Alkalinity

Since alum reduces pH of water, alkalinity becomes a crucial chemical to make alum work properly. Hence, in jar test alkalinity was supplied in two ways: Required amount according to stoichometry based on complete conversion of aluminum ions to aluminum hydroxide. Secondly, 150 mg/L as $CaCO_3$, constant alkalinity. Jar test conducted at pH 8 with following mixing schedule.

1. 1 minute rapid mixing at 120 rpm after alum dosing.
2. 21 minutes slow mixing at 40 rpm.
3. 30 minutes allowed flocs to settle.

By measuring final turbidity, alkalinity and pH values, one was able to compare alum to calcium-alginate in terms of performance.

3.2.6.3 Mixing Time

The effect of rapid mixing time on alum-alginate system was investigated in a similar way explained in sections 3.2.1 and 3.2.2. Instead of calcium, alum was dosed as a coagulant. Experiment was conducted with three different rapid mixing schedules: One minute or five minutes at 120 rpm after each one of the alum or alginate solution addition or 8 minutes at 120 rpm after alum and 2 minutes at 120 rpm after alginate dosing, mixing regimes were applied. For total rapid mixing times equals to 10 minutes and that of equals to 2 minutes, slow mixing times was set to 12 and 20 minutes at 40 rpm. Sedimentation period was same for all three of experiment as 30 minutes. In this experiment 0.5 mg/L aluminum ions concentration at an initial pH 8 was provided with varying alginate concentration in the range of 0-2 mg/L.

3.2.7 Investigation of Electrokinetic Pathway of Coagulation

In colloidal system surfaces charges play a major role indicating the stability of colloidal particles. Measuring surface charges at different stages of jar test might be useful to understand the mechanism of coagulation and flocculation. Surface charges were measured with Electrokinetic Charge Analyzer (ECA 200P) output of which is streaming current value (SCV). Samples for SCV measurements were taken at 1^{st}, 5^{th}, 8^{th} and 22^{nd} minutes of jar test. Jar test's mixing schedule was same as in section 3.2.1 and 3.2.2. Additionally, jar test was performed with alum at constant alkalinity of 150 mg/L as $CaCO_3$ (section 3.2.6.2) was included in the SCV measuring. Alginate and alum concentrations were chosen for their optimum point in jar test having performed before.

3.2.8 Sludge Properties

In water treatment sludge handling is of major concern in terms of operational and financial aspect. Water treatment operation and processes mainly coagulation and flocculation produces high amount of sludge that are not easy to treat. Therefore, calcium alginate and alum system were studied by measuring and comparing with each other the parameters of sludge's total and suspended solids concentration, capillary suction time and moisture content to determine sludge's quantities and dewaterabilities. For calcium-alginate system, the effect of rapid mixing schedule on sludge properties were studied by conducting jar tests which mixing schedule were like in section 3.2.1 and 3.2.2 but only rapid mixing intensity at 120 rpm were studied. For alum system at constant alkalinity of 150 mg/L as $CaCO_3$, jar test procedure were applied as in section 3.2.6.2. Instead of 30 minutes sedimentation time, 60 minutes sedimentation time were chosen for a better sludge

accumulation. Because of inadequate amount of sludge accumulation in one beaker, experiments were done parallel in six beakers. At the end of sedimentation period, water inside the beakers where siphoned till 25 mL sludge remaining and all the sludges in these six beakers were mixed in one beaker slowly avoiding any floc destruction due to transfer.

3.2.9 Experiments on Raw Water

Raw water taken from IWTP were tried to treat with calcium-alginate system. To do that best mixing schedule were chosen relying on afore done experiments with synthetic water. Since raw water's initial turbidity was very low, it was also investigated the performance of calcium-alginate system at different higher initial turbidities e.g. 5, 10, 20 and 80 NTU. Initial turbidities of raw water were increased by adding clay suspension and mixing at 120 rpm for one minute. After that, three samples' initial turbidities from six jars were recorded as an average initial turbidity. Mixing schedule for calcium- alginate system was as following;

1. 8 minute rapid mixing at 120 rpm after $CaCl_2$ dosing.
2. 2 minute rapid mixing at 120 rpm after alginate dosing.
3. 12 minutes slow mixing at 40 rpm.
4. 30 minutes allowed flocs to settle.

Also Jar Test with alum coagulant were tried to manipulate how alum performs with raw water. Besides final turbidity values, final pH and alkalinity values were measured for experiments with alum. Applied mixing schedule for that Jar Test was like as follows;

1. 1 minute rapid mixing at 120 rpm after alum dosing.
2. 21 minutes slow mixing at 40 rpm.

3. 30 minutes allowed flocs to settle.

It was thought that alginate could also be used with alum instead of calcium as a coagulant aid. For this reason, another Jar Test was done in conjunction with alginate and its mixing schedule was listed below;

1. 1 minute rapid mixing at 120 rpm after alum dosing.
2. 1 minute rapid mixing at 120 rpm after alginate dosing.
3. 20 minutes slow mixing at 40 rpm.
4. 30 minutes allowed flocs to settle.

3.3 ANALYTICAL MEASURMENTS

3.3.1 Turbidity Measurement

Turbidity measurement was done using nephelometric method in accordance with Standard Methods No. 2130 (Standard Methods, 2005). Hach 2100N Model Turbidity meter were calibrated or checked its calibration with equipment specific standards of <.01, 20, 200, 1000 and 4000 NTU. Calibration or calibration control were done daily for proper measurements.

3.3.2 Residual Calcium Measurements

Since calcium was used as coagulant, it was required to measure residual calcium concentration at the end of jar test. So approximately 50 mL samples were taken from jars and centrifuged at 3500 rpm for 5 minutes to remove particles that were not able to settle within 30 minutes. After centrifugation, samples were taken from upside of the centrifuged water and diluted by a ratio of 1/40 or 1/20. The pH of diluted sample were dropped below 2 with concentrate nitric acid (HNO_3) and measured with Perkin Elmer 110 B Atomic Absorption Spectrometer.

Atomic Absorption Spectrometer was calibrated before measurements with calcium chloride standards having prepared as described in section 3.1.3.4.

3.3.3 Alkalinity Measurement

Alkalinity of water was measured according to Standard Methods No 2320 (Standard Methods, 2005). Only total alkalinity was measured by titration of alkaline water with 0.02 N H_2SO_4 till the pH 4.5-4.3 (end point of methyl orange) and total alkalinity was calculated with the modified formula for including the cases of high volume of standard acid consumption as below.

$$Total\ Alkalinity\,(mg/L\,as\,CaCO_3) = \frac{V_{mo} * N_{H2SO4} * 50{,}000}{(mLsample + V_{mo})}$$

Where;

V_{mo}: Volume of H_2SO_4 used till pH of 4.5 [ml]

N_{H2SO4}: Normality of standard H_2SO_4 solution [eq/L]

Because of another measurement method requirement for alkalinities lower than 20 mg/L as $CaCO_3$, it was preferred to report these values as <20 mg/L.

3.3.4 Total Suspended Solids Measurement

Total suspended solid of sludge measurements were performed with 0.45 µm pore size filter paper (Milipore). Filter papers were dried before filtration at 105°C for one hours and left in desiccator for 24 hours to cool down. Following weighing filter paper's tare, 10 mL sludge samples were filtered through prepared filter papers. Filter papers were dried again at 105°C for one hour and left in desiccator for 24 hours and reweighed. Triplicate analyses were performed to account for any deviation in determination. Total suspended solids were calculated as following;

$$TSS = \frac{(W_{Fil+Sld} - W_{Fil}) * 1000}{V_{Samp}}$$

TSS: Total Suspended Solids [mg/L]

$W_{Fil+Sld}$: weight of filter paper and dried residue [mg]

W_{Fil}: Weight of dried filter paper [mg]

V_{Samp}: Volume of filtered sample [mL]

3.3.5 Total Solid and Moisture Content Measurement

Total solid (TS) and moisture content (MC) were measured by pouring 20 mL sludge sample into dried and weighed crucible. Crucible filled with sludge sample were weighed again and dried at 105^{o}C for 24 hours. Following kept in desiccator for 24 hours, it weighed again. Total solid and moisture content calculations are as follows;

$$TS = (W_{Cru+Sld} - W_{cru}) * 50$$

$$MC = \frac{(W_{Cru+Sld+Wat} - W_{Cru+Sld})}{(W_{Cru+Sld+Wat} - W_{cru})} * 100$$

Where;

TS: Total Solid [mg/L]

MC: Moisture Content [%]

$W_{Cru+Sld+Wat}$: Wet weight of crucible filled with sludge [mg]

$W_{Cru+Sld}$: Dried weight of crucible including sludge in it [mg]

W_{Cru}: Tare of empty crucible [mg]

3.3.6 Capillary Suction Time

Capillary Suction Time (CST) was measured in accordance with Standard Methods No 2710.G (Standard Methods, 2005) with CST meter (Trition Electronics Ltd. Type 304M) by using the fabricated special CST papers 7x9 cm in dimensions to determine sludge's dewaterability. Approximately 10 mL sludge samples were poured inside the ring of the

device and output were read in units of seconds. Either triplicate or five determinations per sample were repeated depending on the deviation in measurements to have statistically reliable data.

CHAPTER 4

RESULTS and DISCUSSION

4.1 Comparison of the Effect of Alginate's Molecular Weight

The effect of molecular weight of alginate were investigated at 60, 80 and 120 mg/L calcium concentrations using low and high molecular weight alginate in varying concentrations between 0.004 and 2 mg/L. Figure 4.1 and 4.2 shows optimum region of the final turbidity values at different calcium and alginate doses for 10 NTU sample when low and high molecular weight alginate were used, respectively. The optimum points were also tabulated in Table 4.1 to easily compare the effect of molecular weight under different initial calcium concentrations.

In the experiments, two different molecular weight alginates were used and comparison of Figures 4.1 and 4.2 verified that HMW alginate works better in turbidity removal in a major part of the tried alginate doses for the same initial calcium concentrations. However, one of the minor points in which LMW alginate reveal better turbidity removal coincides with the optimum point at 60 mg/L calcium concentration. The difference between final turbidities was as low as 0.25 NTU so that it can be neglected by assuming that experimental error might be experienced. The reason why HMW alginate is more effective in turbidity removal might be possessing HMW alginate longer chain structure than LMW one so that bridging, which is main mechanism in flocculation, between particles can easily take place by extending of polymer chains from one particle's surface to another particle.

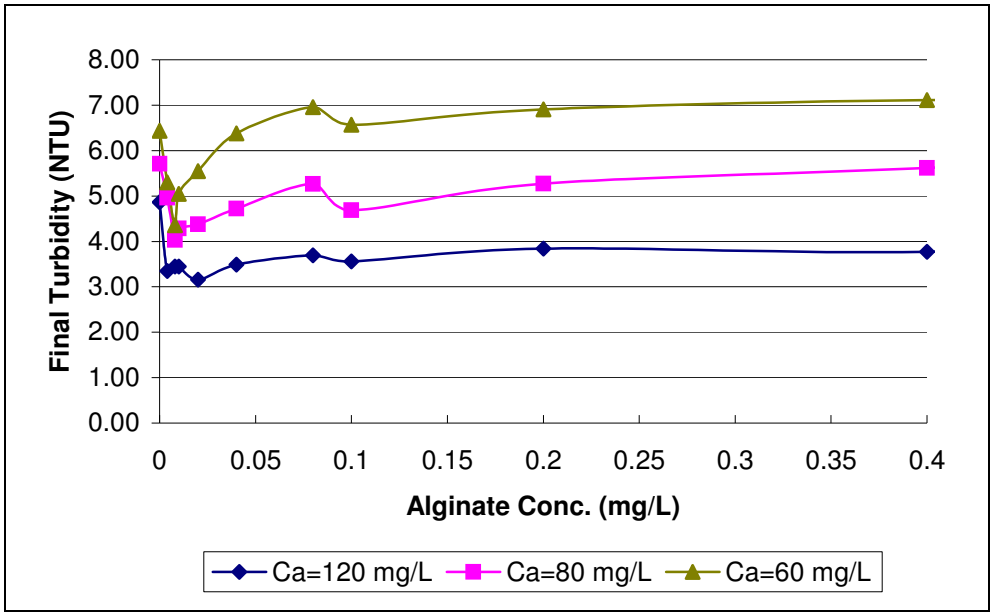

Figure 4.1 Effect of initial calcium concentrations when low molecular weight alginate was used

As can be seen from both Figure 4.1 and 4.2, initial calcium concentration had dramatic effects on coagulation and flocculation: the more calcium ions present in solution, the better turbidity removal efficiency were observed. Studies proposed three ways in which calcium may affect anionic polymer-clay systems.

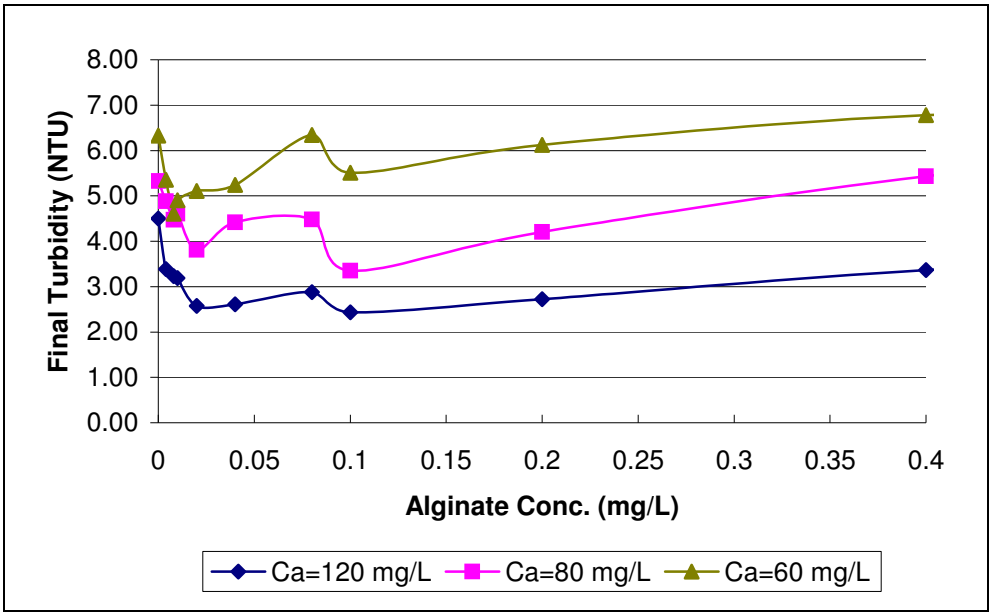

Figure 4.2 Effect of initial calcium concentrations when high molecular weight alginate was used

First, Ca^{+2} ions may compress the diffuse layer surrounding the clay particles or be adsorbed and thereby reduce the repulsive forces between particles (Black et al., 1965); For the calcium concentrations increasing from 60 to 120 mg/L, approximately 15% addition improvement in turbidity removal efficiencies were observed in the absence of alginate because of increasing the degree of charge neutralization and double layer compression improved at higher calcium concentrations. In that situation it could be expected a reduction in the residual calcium concentrations of supernatant: Residual calcium concentration measurements demonstrated 2-3 mg/L of calcium removal, on the other hand some part of measurements resulted higher calcium concentrations than the initial calcium concentrations. These results leaded to perform an uncertainty analysis to determine the limits how much sensitive the system was in calcium measurements. The analysis indicated ±10% (Appendix A) deviation in measured values. As a result it could not directly be concluded whether calcium is adsorbed or

not because all the measurements stayed in the undetectable limits. Nonetheless, previous study conducted by Çoruh (2005) demonstrated that calcium were removed in the range between 15% and 80% from the system having an initial turbidity of 150 and 80 NTU with an initial calcium concentrations of 60, 80 and 120 mg/L. In sight of these data, it could be accepted calcium adsorption took also place for 10 NTU turbidity waters but since the concentration of clay particles were very low, removal percent could not directly be detected.

Table 4.1: Optimum alginate concentrations and residual turbidities at these points

Calcium concentration (mg/L)	LMW alginate concentration (mg/L)	Residual Turbidity (NTU)
60	0.008	4.36
80	0.008	4.03
120	0.02	3.16
Calcium concentration (mg/L)	HMW alginate concentration (mg/L)	Residual Turbidity (NTU)
60	0.008	4.61
80	0.1	3.35
120	0.1	2.44

Second, for a successive coagulation by interparticle bridging, polymer molecules should be initially adsorbed on the particles and then polymer adsorbed particles should form bridges with other polymer adsorbed clay particles. Repulsive forces exist in both interactions between two polymer adsorbed particles or polymer and clay particles due to carrying similar charges. Addition of calcium ions reduces the range of the repulsive interaction and assists interparticle bridging consequently

(Neyens et al., 2004). This theory is suited well with the calcium-alginate system.

Referring to Table 4.1 , while the optimum LMW alginate concentrations were 0.008 mg/L for 60 and 80 mg/L calcium concentration, the optimum point shifted up to 0.02 mg/L alginate concentration for 120 mg/L calcium concentration. Similarly, a shift from 0.008 mg/L to 0.1 mg/L at the optimum HMW alginate concentration was observed while increasing calcium concentration from 60 mg/L to 80 or 120 mg/L. The observation indicated increasing calcium concentration resulted in a better repulsive force reduction and cause more alginate molecules involved in the coagulation mechanism. Higher alginate concentrations than optimum concentration resulted in residual turbidity increase meaning that domination of calcium ions on the repulsive forces was overcome by excessive anionic alginate molecules and colloids were restabilized or not able to agglomerate any further by rise of the non-adsorbed potion of polymer molecules in the bulk solution .

Third, some anionic polymers consist of carboxyl groups which have affinity to divalent cations. These functional groups are known to contribute to the flocculation of clays (Zajic and Knetting, 1971). Calcium ions can form complexes with carboxyl groups on the polymer and on the clay particle surface. That property makes them form chemical complexes at the particle-solution interface where the concentration of divalent cations is high (Sommerauer et al., 1968). Complex formation provides a better attachment of polymer on the particle surface and thereby allows strong floc formation. Being flocs stronger make them to less susceptible to floc breakage which allows forming larger flocs. Alginate is one of polymers contains carboxyl groups and form gel structure when interacts with calcium ions.

Briefly, calcium ions involved in the reduction of repulsive forces existing between each one of clay-polymer-polymer adsorbed clay and also react with the polymer near the particle surface leading calcium concentration became a key parameter in calcium-alginate system. Therefore, for the same alginate concentration, the system performed a better turbidity removal as calcium concentration increased in the order of 60, 80 and 120 mg/L.

Even though calcium had an important role, it could not decrease the turbidity to the limit values required in drinking water standards all by itself. The strong interaction between alginate and calcium ions improved the turbidity removal and caused the achievement of low final turbidity values in such a way that following the calcium dosing, subsequent addition of alginate adsorbed on to the destabilized clay particles and formed bridges between these particles. In the bridge formation the length of the polymer chain is another important parameter affecting the flocculation ability.

From the result obtained in this part, it can be seen that although HMW alginate improved the system performance, the residual turbidity values were still not enough to meet required standards. The reason for this low removal efficiency was believed to be the absence of enough particles to constitute condensation nuclei for the flocs to form. Visual observations confirmed the floc formation, however, the flocs were not heavy enough to settle and separate out of the solution. Çoruh (2005) investigated the settling rate of flocs by tracking residual turbidity values over an extended settling period of 60, 90 and 120 minutes. The results indicated that turbidity reduction continues even at the 120 minutes. With these observations of inefficient floc formation at low turbidity values, the study concentrated on the improvement of performance for low turbidity water samples. In the next section high molecular weight alginate and different

mixing regimes were tested on 10 NTU water samples to improve usability of calcium alginate as a coagulant.

4.2 Effect of Mixing Time and Intensity

Since the HMW alginate showed better turbidity removal efficiency, further studies during which the effect of mixing regime was investigated, were carried out with HMW alginate. The effect of mixing time was investigated by increasing rapid mixing times from 1 minute to 5 minutes following the dosing of both calcium and alginate (shown shortly as “5min+5min at 120 rpm” in Figures). Similarly, another series of jar testes were also carried out mixing schedule of which was 8 minutes and 2 minutes rapid mixing after calcium and alginate addition, respectively (shown shortly as “8min+2min at 120 rpm” in Figures). Again all the jar tests performed at 60, 80 and 120 mg/L calcium, separately. Results of the experiments and their comparisons to previous experiment with HMW alginate were shown in Figures 4.3-4.5 below.

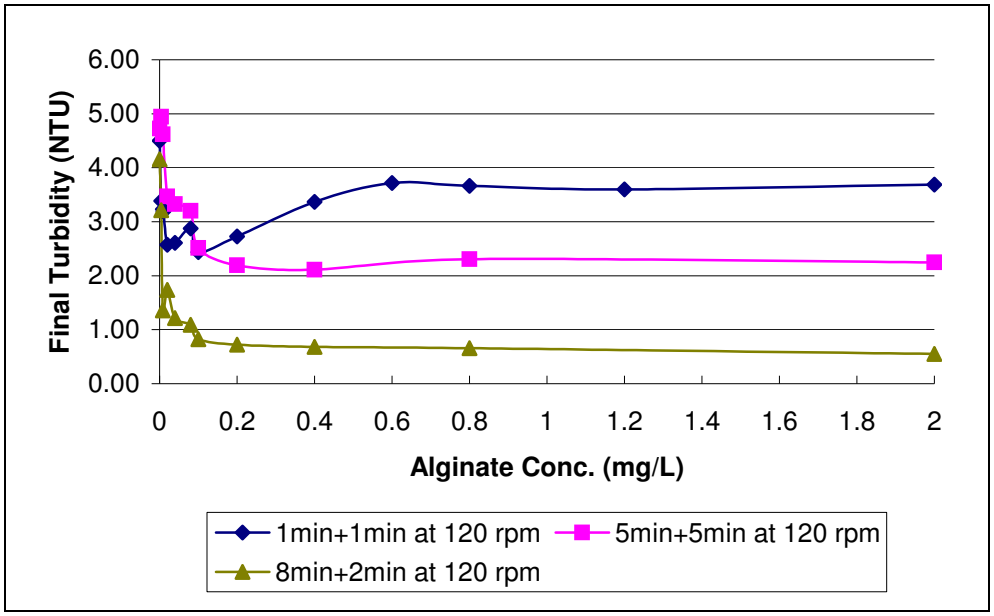

Figure 4.3 Effect of mixing schedule on residual turbidities at 120 mg/L calcium concentration

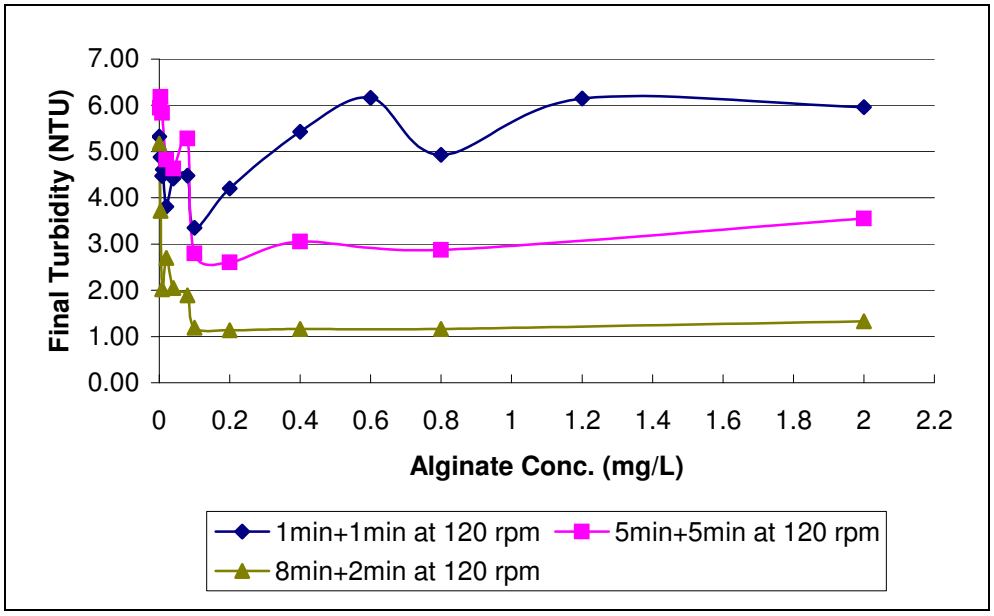

Figure 4.4 Effect of mixing schedule on residual turbidities at 80 mg/L calcium concentration

Prolonged rapid mixing during which 5 minutes of rapid mixing were applied at 120 rpm after each one of calcium and alginate dosing ("5min+5min at 120 rpm") yielded lower final turbidities of 3.52, 2.60, and 2.11 NTU with optimum doses 0.1, 0.2, 0.4 mg/L of alginate for initial calcium concentration of 60, 80, 120 mg/L, respectively. In the next set of tests, 10 minutes rapid mixing times separated into 8 and 2 minutes after calcium and alginate addition ("8min+2min at 120 rpm"), respectively, improved system performance 1-1.5 NTU further by yielding lowest final turbidities of 2.05, 1.14, and 0.55 NTU with optimum doses 0.2, 0.2, 0.1 mg/L of alginate for initial calcium concentration of 60, 80, 120 mg/L, among all other applied mixing schedule so far.

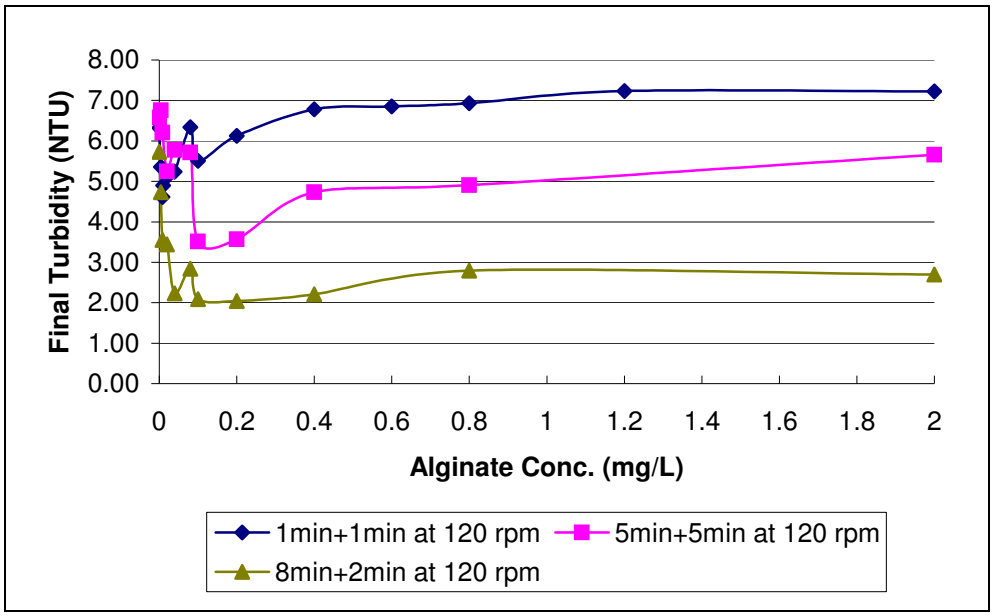

Figure 4.5 Effect of mixing schedule on residual turbidities at 60 mg/L calcium concentration

Increasing total rapid mixing time from 2 minutes to 10 minutes altered the effect of some mechanism in coagulation and flocculation. These can be grouped in two categories: Physical and chemical effects. In terms of

physical effects, increased mixing time might cause to increase number of successive collision leading to attachment by allowing destabilized clay particles either by calcium or alginate to form flocs. In case of an extended period of rapid mixing time, besides coagulation, flocculation also took place because formation of small flocs or microflocs was visually observed before alginate addition. Occurrence of flocculation at rapid mixing period had the advantage to form more compact and dense microflocs. Studies revealed that flocs formed at higher velocity gradients (in this study flocculation was allowed to start at 120 rpm rather than 40 rpm) produces more compacted flocs than those of produced at lower mixing intensities (Tambo, 1991). To start flocculation with compacted and dense microflocs instead of destabilized colloidal particles results in more easily settleable flocs. In chemical aspect, starting with the assumption that adsorption and double layer compression by calcium ions were unsteady state processes, calcium ions enhance the degree of destabilization in a longer period of rapid mixing time by itself. This suggestion can be proved by comparing the improvement in residual turbidities between the jar test process of “5min+5min at 120 rpm” and “8min+2min at 120 rpm”. As more time was allowed for calcium ions before alginate dosing, final turbidities tends to decrease. Another evidence strengthing the suggestion was that the optimum alginate concentration shifted up, when the rapid mixing time after calcium and before alginate dosing increased gradually from 1 minute to 5 minutes and then to 8 minutes: Especially, a gradual increase in the order of 0.008, 0.1, 0.2 and 0.1, 0.4, 0.2 mg/L of alginate concentration was observed at the initial calcium concentration of 60 and 120 mg/L. This might be due to allowing more time for Ca^{+2} ions to compress double layer so that polymers could easily adsorb on the clay particles. On the other hand, for the jar test procedure “5min + 5min at 120 rpm” and “8min + 2min at 120 rpm” decreasing rapid mixing time from 5 minutes to 2 minutes for alginate agitation seemed not to cause any deficiency in

the turbidity removal. Hogh (1999) stated that polymer adsorption occurs rapidly within a time scale of seconds or less. Basing on the study of Hogh (1999) and this study, one can conclude that the important parameter for better flocculation efficiency in calcium-alginate system was allocating more time for only calcium at rapid mixing stage rather than subsequent alginate dosing.

Studies on the effect of rapid mixing times showed that increasing rapid mixing times improved the turbidity removal efficiencies. Especially, applied “8min+2minat 120 rpm” jar test procedure yielded good results meeting the required standards, which was set for this study as 1 NTU, for the calcium concentrations of 120 and 80 mg/L. For 80 mg/L calcium dose, even though final turbidity value was above 1 NTU, namely 1.14 NTU, it could be accepted well enough for just coagulation and flocculation processes because like in most of the water treatment processes effluents from sedimentation tanks is filtered through sand filters and that little excess turbidity values would be decreased below to 1 NTU without any extra loading on the filtration process. However, for the studies performed with 60 mg/L calcium, the results are far away from the required standards. To recover this deficiency and get a better insight on mixing parameters, new jar tests were done at different rapid mixing intensities.

As already told, two parameters affects calcium-alginate system efficiency when rapid mixing times were increased, number of successive collision and degree of destabilization by calcium ions. When the total rapid mixing time increased from 2 minutes to 10 minutes at 120 rpm, the applied shear rate on the particles were not changed but rather duration of exposing to high shear rates increased resulting in increase in the fraction of successive collisions leading to attachment. In an

analogous way, the velocity gradient was not altered but the product of G*t was increased.

In this following part of the study, velocity gradient was altered and duration of rapid mixing time was held constant at a total 10 minutes. The aim of this study was to investigate the relative impact of physical parameters over the chemical and time related parameters. To do that mixing intensity of the jar test procedures of “5min+5min at 120 rpm” and “8min+2min at 120 rpm” was increased to 160 and 200 rpm abbreviated shortly as “5min+5min at 160 rpm” and alike for other procedures.

Figures 4.6-4.8 show the effect of mixing intensities on the turbidity removal rates at “5min+5min at 120/160/200 rpm” jar test procedure at three different calcium concentrations of 60, 80, 120 mg/L (The data used for 120 rpm mixing speeds were quoted from previous section).

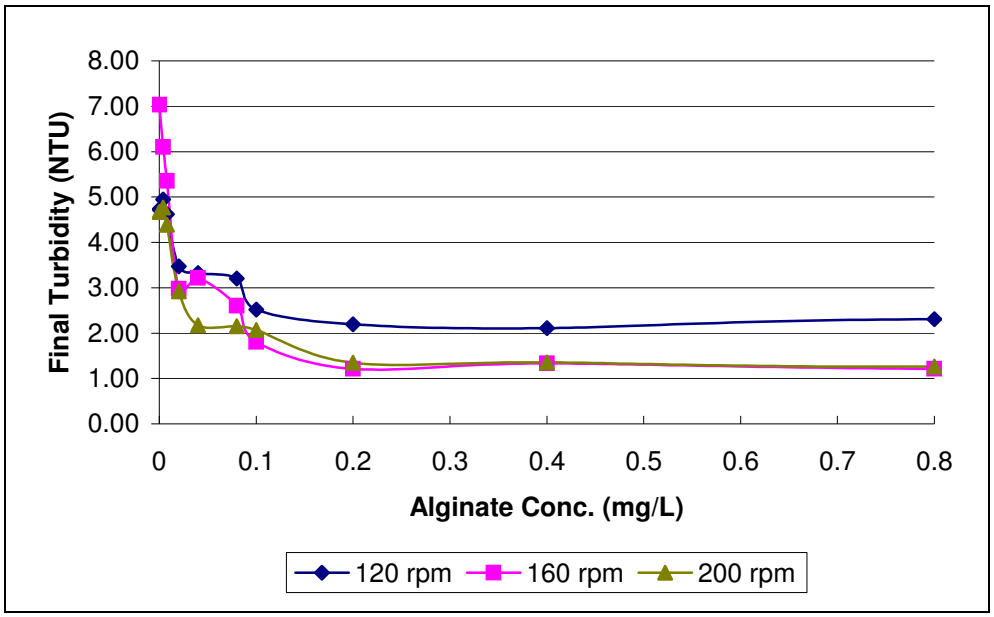

Figure 4.6 Effect of mixing intensity on residual turbidities at 120 mg/L calcium concentration (“5min+5min” jar test procedure)

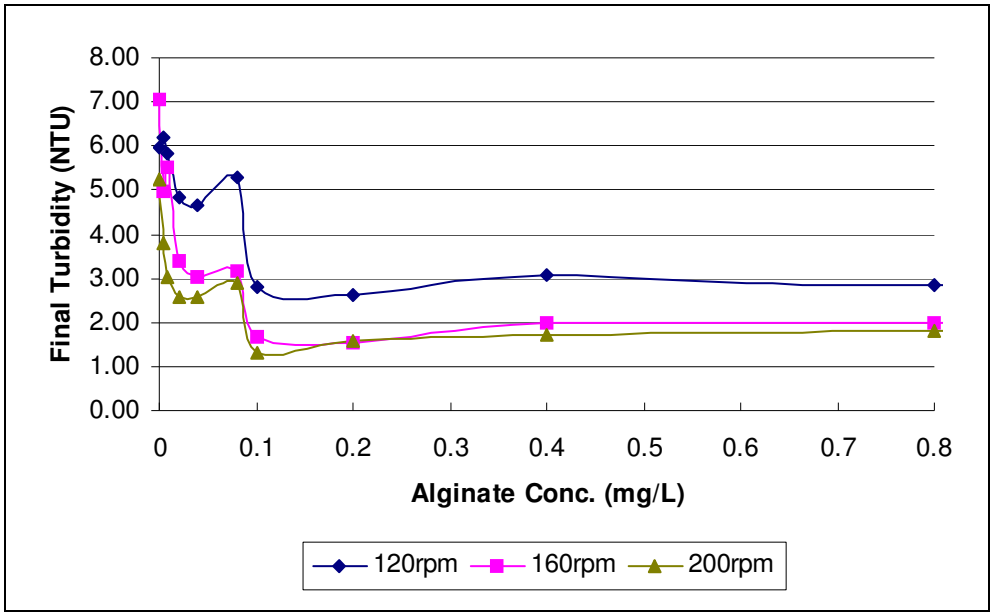

Figure 4.7 Effect of mixing intensity on residual turbidities at 80 mg/L calcium concentration ("5min+5min" jar test procedure)

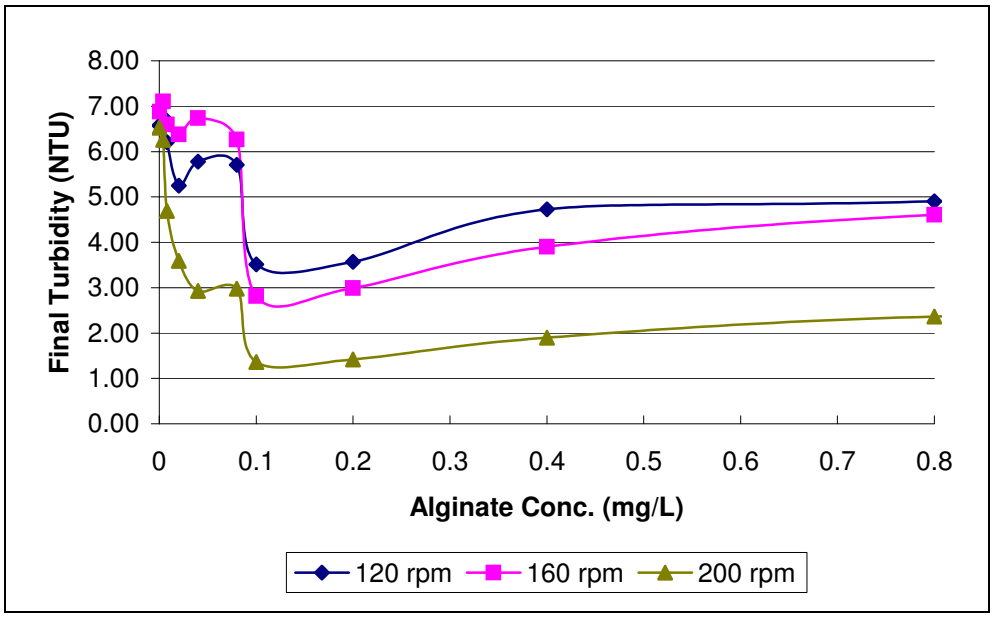

Figure 4.8 Effect of mixing intensity on residual turbidities at 60 mg/L calcium concentration ("5min+5min" jar test procedure)

In case of increasing rapid mixing speeds to 160 and 200 rpm improved turbidity removal efficiencies approximately by 10-30% by increasing fraction of successive collisions. However, there were little differences between mixing the system at 160 rpm or 200 rpm especially for the initial calcium concentrations of 120 and 80 mg/L. The phenomena can be explained by the fact that the coagulation capacity of alginate or equilibrium between flocculation and deflocculation is reached. On the other hand, the mixing intensity affected turbidity removal for initial calcium concentration of 60 mg/L as given in Figure 4.8. As calcium concentration is decreased in water, the compression of double layer is decreased resulting in more energy requirement for interparticular bridging. To overcome the energy barrier increasing mixing intensity from 120 rpm to 160 rpm or to 200 rpm affects turbidity removal significantly.

In a similar manner series of jar test were performed with jar test procedure of “8min +2min at 120/160/200 rpm” (Figures 4.9-4.11). (The data used for 120 rpm mixing speeds were quoted from previous section). For the calcium concentration of 60 mg/L, there were no significant differences between mixing the system at 160 rpm or 200 rpm. However; increasing mixing speed from 120 rpm to 160 or 200 rpm resulted an approximately 7% improvement in turbidity removal rates. At 80 and 120 mg/L calcium dose, that additional improvement of mixing intensity on turbidity removal was not there. The reason might be due to well enough destabilization brought by only calcium ions within 8 minutes so that increased mixing intensity could not improve the system any further.

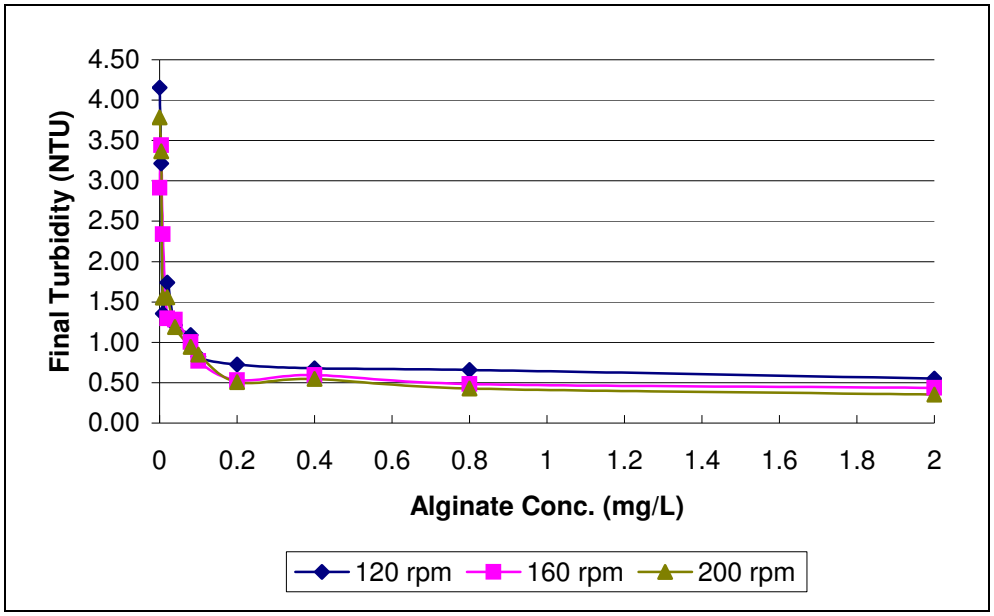

Figure 4.9 Effect of mixing intensity on residual turbidities at 120 mg/L calcium concentration ("8min+2min" jar test procedure)

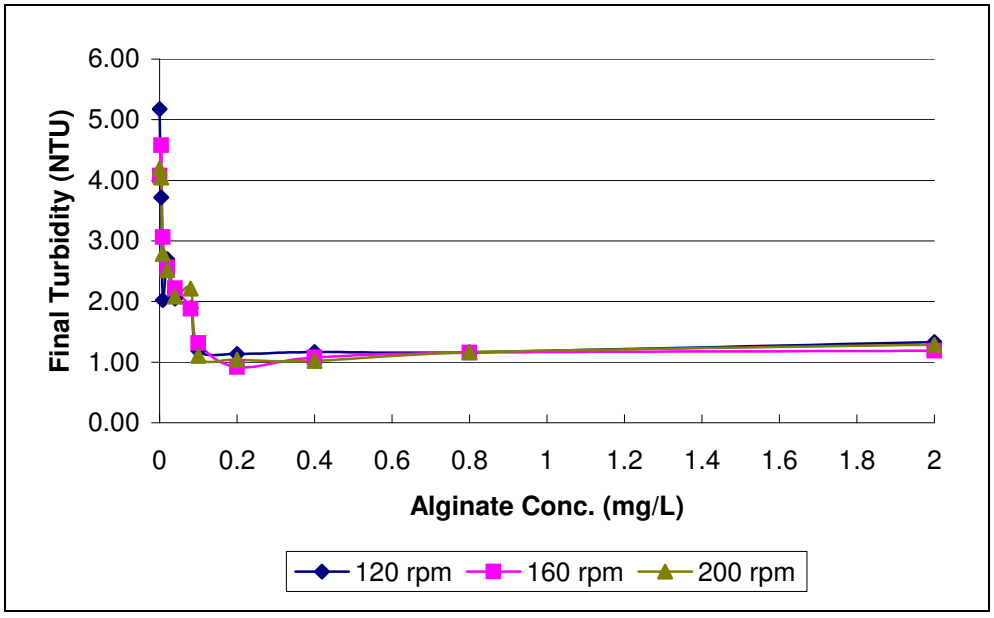

Figure 4.10 Effect of mixing intensity on residual turbidities at 80 mg/L calcium concentration ("8min+2min" jar test procedure)

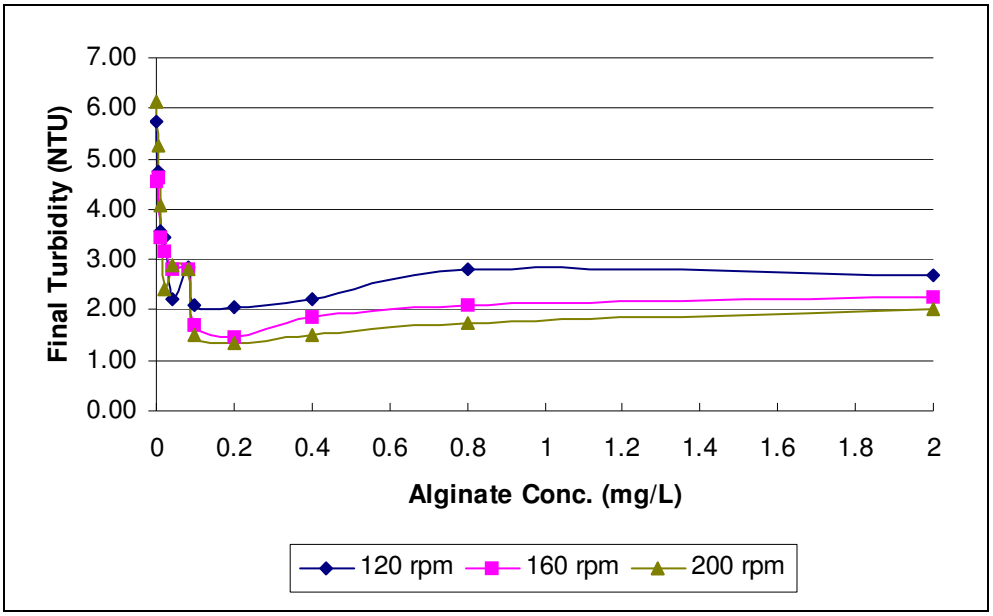

Figure 4.11 Effect of mixing intensity on residual turbidities at 60 mg/L calcium concentration ("8min+2min" jar test procedure)

The relative impact of mixing intensity and so collision rates with respect to destabilization achieved by calcium ions were investigated by increasing mixing velocity and tracking the final turbidity values. For the "5min+ 5min at 120/160/200 rpm", collision related parameters kept their importance about coagulation and flocculation as physical parameters, especially, the impact become more obvious for the low calcium doses. Nonetheless, when the mixing schedule was turned into 8min+2min at 120/160/200 rpm", chemical processes (charge neutralization or double layer compression) dominate over physical parameters (collision rates). For high calcium concentration, there were almost no differences on the final turbidity values ultimately. In another words, chemical parameters become the determining parameter in the calcium-alginate system. Exceptionally, for 60 mg/L calcium concentration none of the parameter discussed above become main parameter, because being charge neutralization lower than other tried calcium concentration made the system more sensitive to be affected by other parameters.

Consequently, it seems more advantageous to apply mixing schedule of “8min+2min at 120 rpm” rather than “5min+5min at 120/160/200” in terms of concerning financial and operational aspects. Since as the mixing speed is increased, the power consumption increases also causing an extra load on treatment expenditures.

4.3 Effect of pH

pH of the solution has some characteristic influences on the polymers and colloidal particles. Initially, it changes the conformation of the polymer in the solution or in adsorbed state. Secondly, pH might react with specific sites on the polymers resulting in alteration on polymer capacity and lastly, hydrogen ions might be adsorbed by the colloidal particles and the net surface charges could change. All of the above listed circumstances make pH a crucial parameter that should be tracked carefully. In this section three different pH values were tested by applying “5min+5min at 120 rpm” jar test procedure. The reason to choose this procedure was that this application yielded intermediate results, neither best nor worst, so that the changes in residual turbidities could clearly be observed whether improving or deteriorating direction. Before conducting the experiments, pH of the solution was fixed to 4, 7 and 9 as representative of acidic, neutral and alkali ranges. To discard any positive or adverse effects arising from alginate concentration, all the alginate concentration was fixed to 0.2 mg/L which was the optimum or close to optimum alginate concentration at calcium doses of 60, 80 and 120 mg/L.

Figure 4.12 shows the residual turbidity values jar test obtained following jar tests performed at different pH values. At 80 and 120 mg/L calcium concentrations the system do not seem to be affected by the pH values 4 and 7 but at pH 9 the system efficiency improved approximately 0.7

NTU. This improvement can theoretically be speculated by the conformation of the alginate polymer in the solution at different pH values: Alginate molecules possess carboxyl groups and termed as an anionic polymer. As pH of the bulk solution increase, the polymer chain starts to expand from coiled structure to a more straight structure by repulsion of OH- ions in the solution. This expansion increases the distances between the two ends of the molecule. A stretched polymer structure can easily extend from particle surface to other particle surface rather than in a coiled form that makes agglomeration of the particles via bridging easier and improve flocculation capacity ultimately. Besides structural conformation of alginate polymer, at low pH values, the carboxyl groups could be protonated by hydrogen ions making it less reactive with calcium ions. Carboxylic acid dissociation constants of Mannuranate and Guluranate subunits of alginate have been determined as pK_a = 3.38 and pK_a= 3.65, respectively (Davis, 2003). Referring acid dissociation constant it can be said that almost half of the subunits of alginate were occupied by hydrogen ions at pH 4.

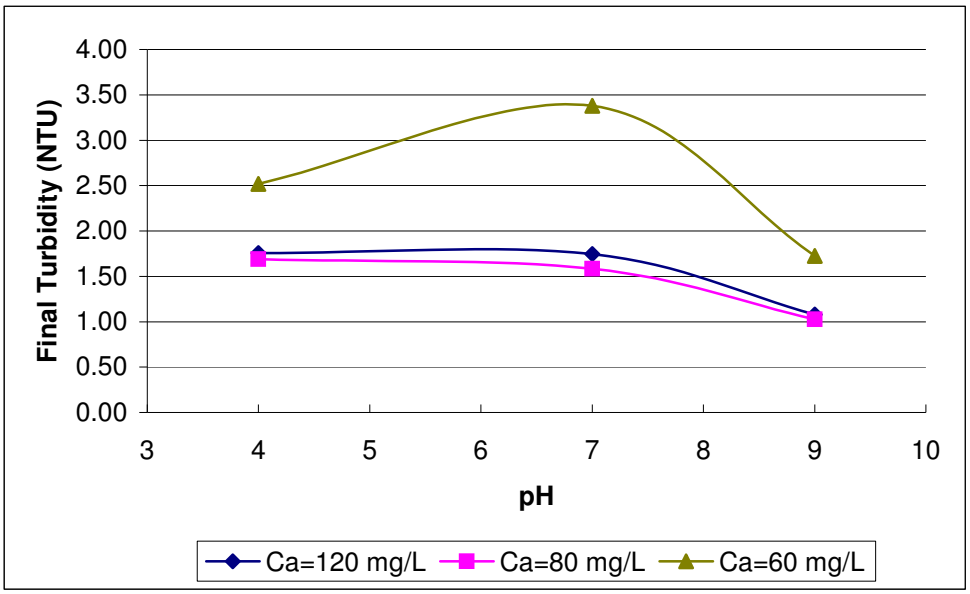

Figure 4.12 Effect of pH on residual turbidities at 0.2 mg/L alginate concentration

Like in the previous sections, experiments conducted with 60 mg/L calcium concentration were more sensitive to other parameters involved in the coagulation and flocculation. Unlike the experiment done with 80 mg and 120 mg/L, a peak was observed at pH 7 when 60 mg/L calcium dose were used. In this situation, the effect of pH on the particle surface charge and on polymer properties might take place: As pH of solution was dropped off from basic to acidic levels, the surface charges of the clay starts to turn more positive in nature and vice versa. Additionally, at pH 4 almost half of the polymer ionizable groups were protonated, even though its capacity for flocculation was hindered, alginate charge density decrease at the same time by which repulsion forces between alginate and clay were decreased favoring the approach and adsorption of alginate onto the clay particles. As the pH was increased to pH 7, both alginate's monomers get deprotonated and so its charge density increase and in addition to that surface charge of the clay particles increased resulting an increase in residual turbidity. Stretching of

alginate polymers at pH 7 could not compensate the negative impacts of other factor aforementioned. However when the pH of the solution was increased to alkali level (pH 9) continuing stretching of alginate polymer could assist in bridging flocculation and yielded the lowest turbidity results within the tried pH ranges. Within this context, the reason why no significant changes were observed for the 80 and 120 mg/L calcium concentration between pH 4 and pH 7 could be speculated that destabilization of clay particles would be enough by that amount of calcium concentrations preventing from further improvement consequently.

Finally, it was found that there were no significant pH changes during the experiments. The measured initial and final pH values were listed in Table 4.2 below. This finding highlights an advantage of calcium-alginate coagulant system over inorganic coagulants such as alum, which cause significant changes during coagulation.

Table 4.2: Initial and final pH values of jar tests

			Initial pH		
	Ca.(mg/L)	Alg.(mg/L)	4	7	9
Adjusted initial pH	120	0.2	4.09	7.06	9.14
Final pH			4.47	6.68	9.35
Adjusted initial pH	80	0.2	4.05	6.97	8.87
Final pH			4.44	6.82	8.82
Adjusted initial pH	60	0.2	4.10	7.32	9.20
Final pH			4.60	6.36	9.21

4.4 Effect of Alkalinity

Since most of natural waters contain alkalinity, in this chapter it was investigated the effect of alkalinity on turbidity removal efficiencies. To do that alkalinity values was adjusted to adjust 75, 150, 300 mg/L as $CaCO_3$

by dosing sodium carbonate. Addition of alkalinity in the form of carbonate increased the pH of the synthetic water to levels around 10. It was thought that pH 10 would not be widely encountered operational parameter so pH of the synthetic water was then reduced to pH 8. As a consequence, synthetic water contained an alkalinity which was composed of 98% bicarbonate ions. Inevitable dilution has to be conducted during alkalinity and pH adjustment. To check this dilution ratios, alkalinities of the synthetic water was measured before jar tests and found as 78, 144, 254 mg/L as $CaCO_3$ instead of 75, 150, 300 mg/L as $CaCO_3$. Highest deviation was observed at the desired alkalinity level of 300 mg/L as $CaCO_3$ due to higher dilution ratios than the other alkalinity levels as expected. Therefore; it was preferred to discuss the measured alkalinity values as initial alkalinity instead of theoretically calculated ones. Even though the fraction of carbonate ions in the solution were 0.5% of the bicarbonate ions, solubility limits of $CaCO_3$ was exceeded due to presence of high calcium concentration. However, carbonate ions being very low in concentration a significant precipitation of the calcium ions was not possible.

In tried alkalinity ranges (Figure 4.13), the system performed a better turbidity removal than zero alkalinity level. The reason might be due to the formation of small amounts of $CaCO_3$ precipitates. The precipitate formation was most likely to occur at the clay particle surface where calcium concentration was high so it brought in the advantage of a denser nuclei formation and producing flocs of higher settling rate. Additionally, since alkalinity was added in the form of Na_2CO_3, Na^+ ions may compress the double layer, which can clearly be seen in Section 4.6.4 where SC of suspension decreased from -9.95 to -5.0 after alkalinity adjustment. Reduction in double layer thickness may be resulted in better turbidity removal.

For 254 mg/L as $CaCO_3$ alkalinity the system performance deteriorated a little bit. The little increase might be due to the presence of bicarbonate ions in rather higher concentration which might constitute an obstacle in polymer/polymer and clay/polymer interaction since they all were carrying same charges. Also, the effect of different Na^+ concentrations on the turbidity removal efficiency of calcium alginate system were studied in detail by Çoruh (2005) and it was found that Na^+ ions did not improve system efficiency but also for some concentrations it worsened the turbidity removal than when there were no Na^+ ions. The negative impact of Na^+ ions on the system might be due to reaction of Na^+ ions with alginate polymers which might inhibit gel formation of alginate with calcium ions. Table 4.3 shows alkalinity and pH values of the synthetic water before and after the jar test. The system did not show any significant pH changes and a minor amount of alkalinity were removed possibly with calcium precipitation.

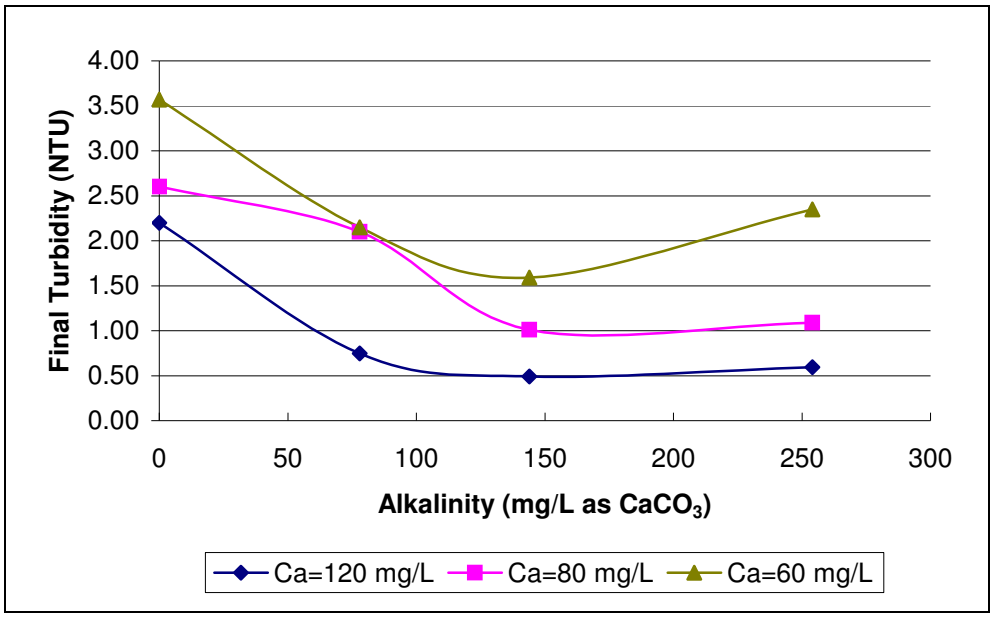

Figure 4.13 Effect of alkalinity on residual turbidities at 0.2 mg/L alginate concentration

Table 4.3: Initial and residual alkalinity and pH values of alkalinity experiment

Adjusted initial alkalinity as $CaCO_3$	78	144	254
Initial pH	8.00	8.00	8.00
Residual alkalinity (Ca=120 mg/L)	69	126	223
Residual alkalinity (Ca=80 mg/L)	77	139	250
Residual alkalinity (Ca=60 mg/L)	70	127	222
Final pH (Ca=120 mg/L)	7.96	8.00	8.02
Final pH (Ca=80 mg/L)	8.02	8.12	8.20
Final pH (Ca=60 mg/L)	7.98	8.13	8.19

4.5 Investigation of Electrokinetic Pathway of Coagulation

Changing mixing schedule profoundly affected the turbidity removal efficiency of calcium-alginate and inclusively the way that interaction between calcium/alginate and clay particles as discussed previously: Briefly, increasing total rapid mixing times from 2 to 10 minutes improved the turbidity removal efficiency and especially “8min+2min at 120 rpm” jar test procedure yielded additional turbidity removal. Even though total mixing time was fixed to 22 minutes, different responses were observed at different mixing schedules leading to assume that adsorption and double layer compression by calcium ions were unsteady state processes and calcium ions enhance the degree of destabilization in a longer period of rapid mixing time by itself. Therefore, it was decided to investigate the changes of particle charges over time during coagulation to get a better understanding of the mechanism of coagulation by calcium alginate.

As aforementioned, there is a theoretical proportionality between electrophoretic mobility and streaming current (SC); however, an offset from the origin was observed in the regression analysis for SC and

electrophoretic mobility in practical application. In the analysis study, deionized filtered water's SC was found to be negative due to surface characteristics of SCD's annulus (Dentel et al., 1989). Accordingly, it was decided to adjust SC of deionized water to -9.50 instead of zero to check the proper functioning of SCD, SC at time zero(-9.95) was not sketched for a better visualization in figures and suggested to interpret data acquired from SCD on relative basis. Additionally, residual turbidity value with its alginate concentrations were quoted from previously done similar experiments related to turbidity reduction and indicated in figures as a reminder.

Effect of different calcium concentration on particle charges measured as streaming current value for different jar test procedures were demonstrated through the Figures 4.14-4.16. The pathway of destabilization of particles generally followed the parallel ways independent from calcium concentration. Especially, for first two minutes a very rapid increase in SC was observed from -9.95 to around -1.20, -1.40, then destabilization rate started to slow down and experiments usually finished between the SC range of 0.20 and -0.40. Regardless of which jar test procedure was applied, the clay particles got more destabilized as calcium concentration in the bulk solution was increased and resulted in better turbidity removal as well. Degree of destabilization achieved by different calcium concentration could more clearly be seen in Figure 4.16 because of elimination possible deviations in negative direction originating from different alginate concentration usage. As expected, the higher the calcium concentration, the lower the surface charges. At high calcium concentrations, the adsorption and double layer compression was higher resulting in better turbidity removal efficiency.

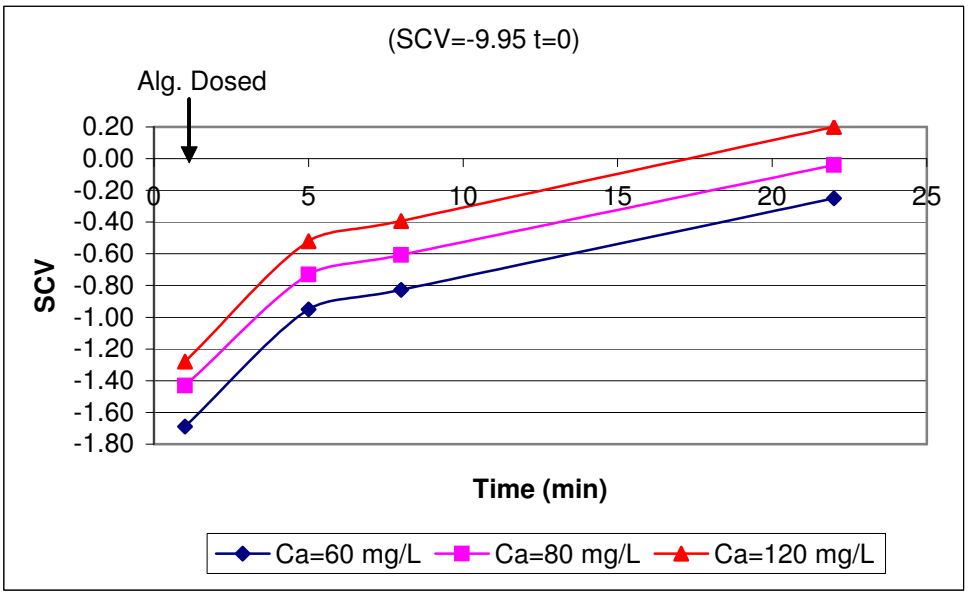

Figure 4.14 Changes of streaming current value over time for jar test procedure "1min+1min at 120 rpm"

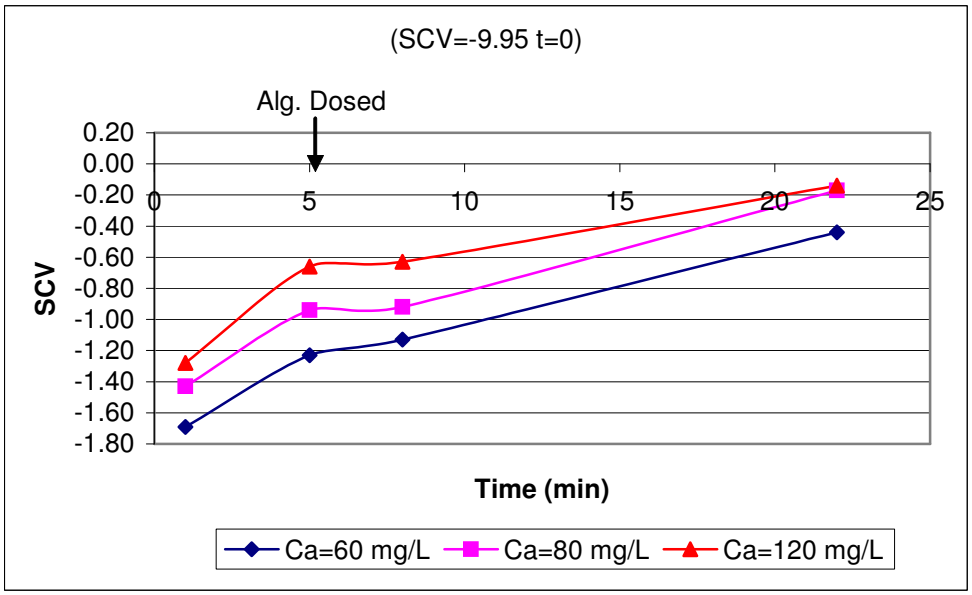

Figure 4.15 Changes of streaming current value over time for jar test procedure "5min+5min at 120 rpm"

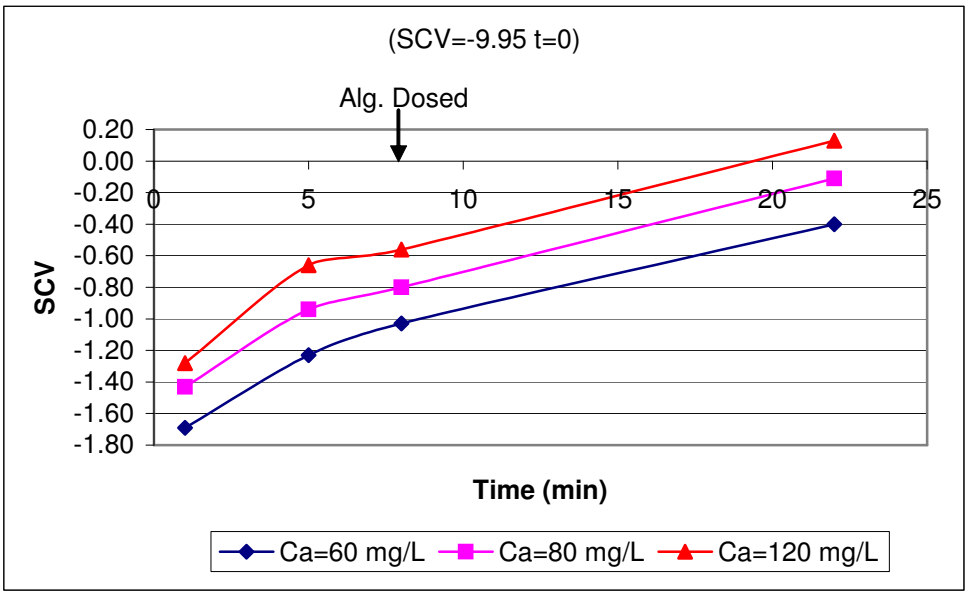

Figure 4.16 Changes of streaming current value over time for jar test procedure "8min+2min at 120 rpm"

Different mixing schedules and their effects on particle's charges can be seen for calcium concentration of 60, 80 and 120 mg/L in Figure 4.16. In previous section it was indicated that allocating more time after calcium and before alginate addition improved turbidity removal efficiency significantly due to allowing more time for calcium ions to reduce negative charges of clay particles. This suggestion was proven by measuring and comparing SC values at the points before alginate dosing for the jar test procedures of "1min+1min at 120 rpm", "5min+5min at 120 rpm" and "8min+2min at 120 rpm" (alginate addition times corresponds to 1, 5 and 8 minutes, respectively). E.g.: for the mentioned jar test procedures SC values increased in the order of -1.69, -1.23, -1.03 at the minutes 1, 5 and 8 for 60 mg/L of calcium concentration resulted in residual turbidities 4.61, 3.52 and 2.05 NTU respectively. (Similar results were also obtained for 80 and 120 mg/L of calcium concentration). It can equally be pronounced the net effect of calcium over time at 120 rpm. Briefly, prolonging mixing time after calcium and before alginate addition

gave the calcium ions a better chance to neutralize clay particles and following alginate addition, alginate aggregated particles being in a less negative charge state resulting better turbidity removal.

Through the Figures 4.17-4.19, the effect different mixing intensity at initial calcium concentrations of 120, 80 and 60 mg/L was seen on the SC value. Results showed that the mixing intensity had minor impact on the surface charge explaining improvement in turbidity removal at higher mixing intensity was due to collision efficiency rather than electrokinetic effect.

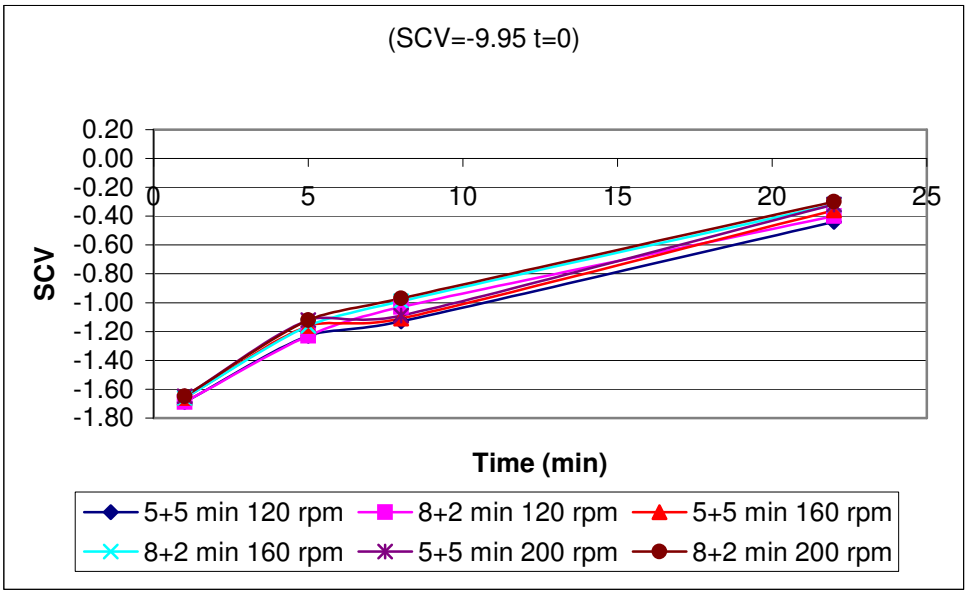

Figure 4.17 Effect of mixing intensity at different mixing schedule on surface charge at Ca=60 mg/L

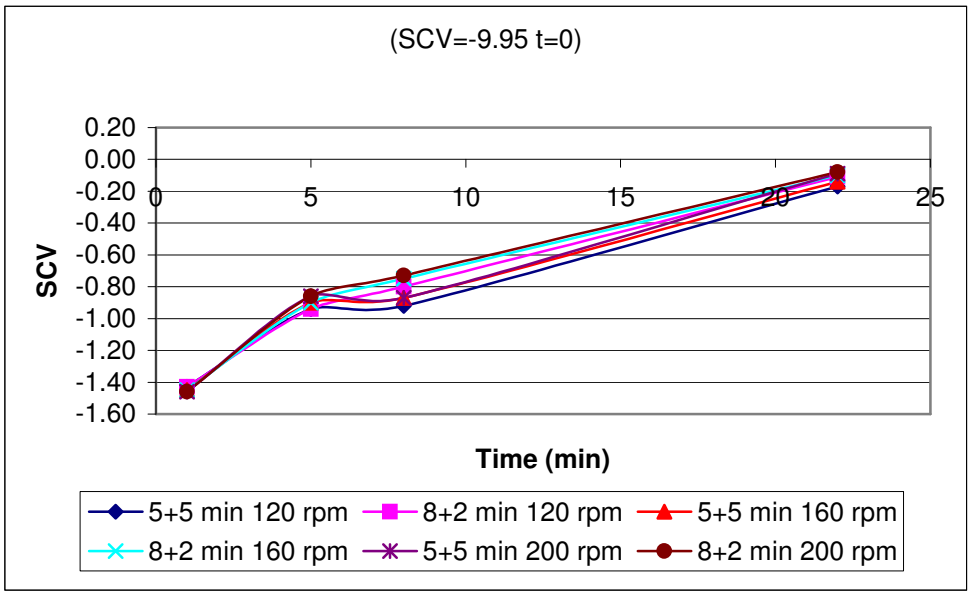

Figure 4.18 Effect of mixing intensity at different mixing schedule on surface charge at Ca=80 mg/L

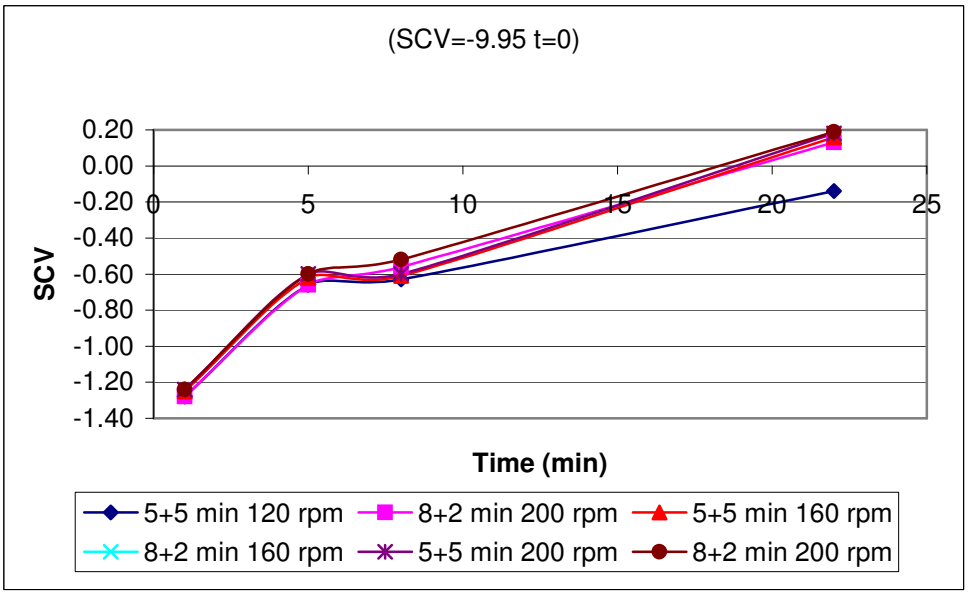

Figure 4.19 Effect of mixing intensity at different mixing schedule on surface charge at Ca=120 mg/L

4.6 Comparison with Alum as a Coagulant

4.6.1 Effect of Alum Dose and Alkalinity

Alkalinity of the solution plays an important role in coagulation experiments with hydrolyzing metal salts. It buffers the acid production coming from hydrolysis of metal salts. To investigate the effect of alkalinity and alum concentration on coagulation, synthetic water's alkalinities were prepared basing on two different fashions. In the first way, alkalinity of the solution was adjusted to slightly higher value than that of required to convert all Al ions to $Al(OH)_3$ precipitate. In this phase, it was aimed to keep pH of the solution constant around neutral by varying alkalinity in the ranges between 6 and 343 mg/L as $CaCO_3$ according to dosed aluminum concentration changing between 0.1 and 60 mg/L. This first phase was named as "varying alkalinity" in the figure presentations and during the rest of the discussion. At the second phase (named as "constant alkalinity"), suspension's initial alkalinity was fixed at a concentration of 150 mg/L as $CaCO_3$ and the aluminum concentrations were varied over the range 0.1 to 60 mg/L aiming to simulate low turbidity waters with high alkalinity.

The residual turbidities of jar test conducted with varying and constant initial alkalinities were shown in Figure 4.20. Varying alkalinity experiments resulted in two optimum points at the Al concentrations of 0.5 and 5 mg/L with residual turbidities of 0.66 and 0.92 NTU. Occurrence of two optimum points drew the borders where adsorption and charge neutralization or sweep flocculation was the operative mechanism. Till reaching the first optimum point (0.5 mg/L Al), aluminum ion concentrations were not enough to complete destabilization of the clay particles. After 0.5 mg/l aluminum dose, the residual turbidities started to increase due to restabilization of clay particles with excess

amount of aluminum species. However, around the 5 and 10 mg/l of aluminum concentration another decrease in final turbidities were observed indicating sweep flocculation mechanism operated. Stumm and O'Melia (1968) suggested that there should be a stoichiometric relationship between the particle concentration and coagulant dosage in case of being charge neutralization predominant mechanism. Duan and Gregory (2003) commented additionally that at low particle concentration, coagulant dose should be lower and stay in a quite narrow range. The comments fitted well to experiments with varying alkalinity: While sharp turbidity increases were observed around the optimum point of 0.5 mg/L of Al (Even 0.3 mg/L Al concentration variation exerted great differences in final turbidities), on the other hand, effective sweep flocculation concentrations expanded to rather wider range like 5-10 mg/L of Al and smoother residual turbidity changes were observed around these Al concentrations. Residual aluminum concentration was another concern in coagulation with alum and it was determined by the solubility of the hydroxide precipitate which is strongly pH-dependent (Iriarte-Velasco et al., 2007). In the "varying alkalinity" experiments the average final pH values were 6.8±0.2. Kabsch-Korbutowicz (2005) stated that residual aluminum concentration was the lowest at pH units of 6-7. Accordingly, one can conclude that keeping pH in the suggested ranges and being sweep flocculation more preferable than charge neutralization in operational aspects makes 5 mg/L Al(III) concentration the optimum point.

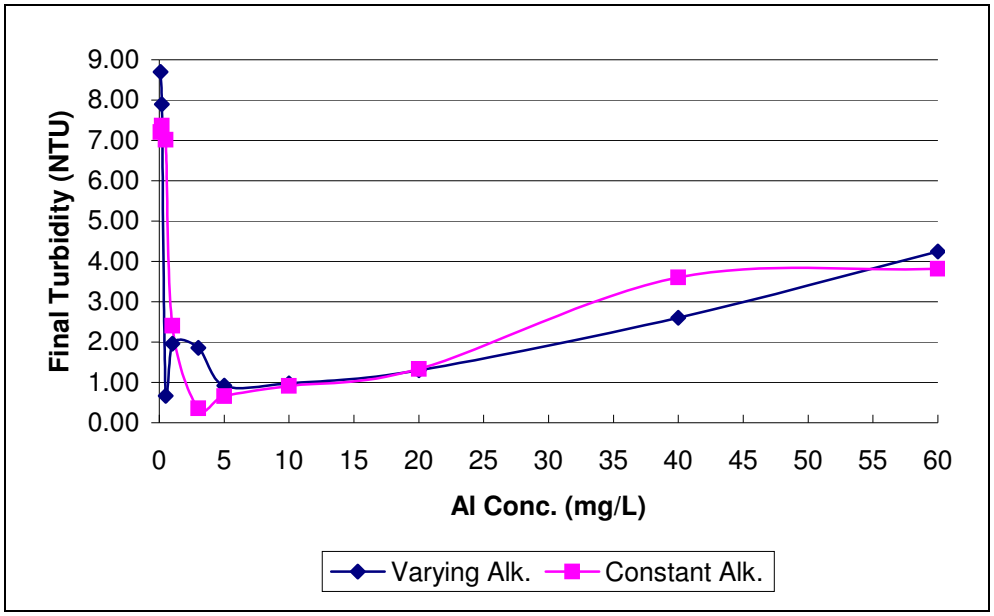

Figure 4.20 Effect of varying and constant alkalinity on residual turbidities

When the initial alkalinity was fixed to 150 mg/L as $CaCO_3$ for all the tried aluminum concentrations, only one optimum point was observed at Al(III) concentration of 3 mg/L with 0.36 NTU residual turbidity. In addition to that, 5 and 10 mg/L Al(III) concentrations were able to reduce the residual turbidity below 1 NTU. Comparison final pH values or operational pH values showed that while varying alkalinity experiments were conducted at around pH 6.8, those of "constant alkalinity" were conducted at pH 8, especially for the Al(III) concentrations below than 20 mg/L. Alkalinity of solution in conjunction with pH seemed to affect the coagulation mechanism of alum by changing surface charges and precipitate formation rate. Ye et al. (2007) stated that sweep flocculation was more efficient under high alkalinity because of formation hydroxide precipitate less and slower under low alkalinity than under high alkalinity. Similarly, "Constant Alkalinity" experiments resulted in slightly better turbidity removal than "varying alkalinity" experiments around the sweep flocculation region.

Alum has been shown to reduce the turbidities to really low values of less than 1NTU without much effort. It can be concluded that it is a higher efficiency coagulant than calcium-alginate system.

4.6.2 Effect of pH

It was aimed in this chapter to determine optimum initial pH value when alum was used as a coagulant. Neutral and alkali ranges of pH were chosen because coagulation with alum requires alkaline waters to function properly. Same amount of Na_2CO_3 were added to synthetic water and pH of the waters then reduced to 7, 8 and 9 assuming that the variation in alkalinity owing to conversion bicarbonate ions to carbonate and carbon dioxide was negligible.

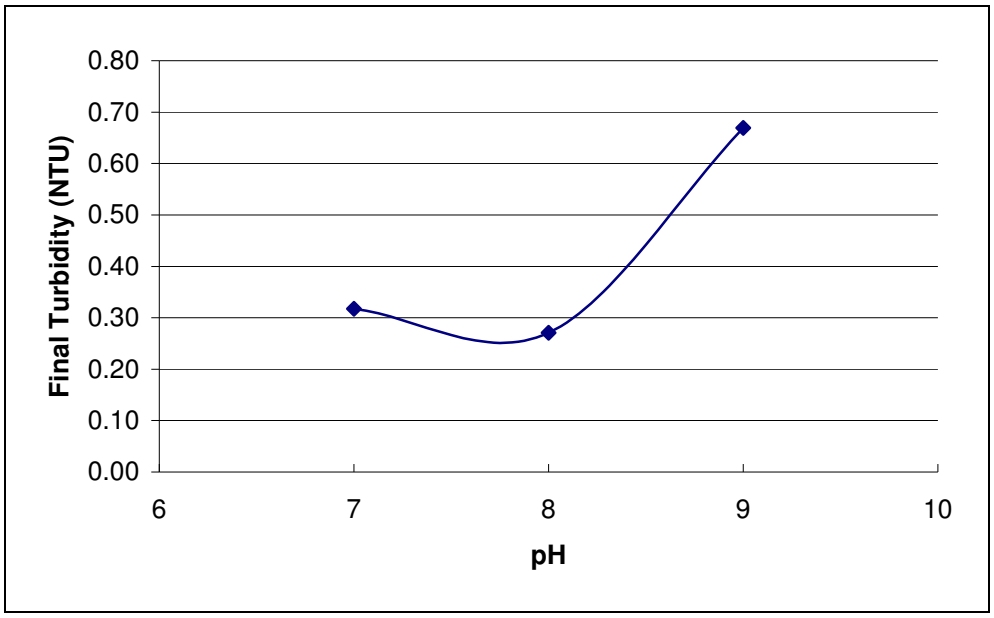

Figure 4.21 Effect of pH on residual turbidities at 5 mg/L aluminum concentration

Among three different pH values (Figure 4.21), pH 8 yielded the best turbidity removal at a constant Al and alkalinity concentrations of 5 mg/L and 35 mg/L as $CaCO_3$ respectively. Since pH 8 was found as optimum initial pH, the rest of the study related to alum was performed at that pH value.

4.6.3 Alginate as a Coagulant Aid with Alum and Effect of Mixing Time

Alginate is known to cause gel structure in the presence of calcium ions. However, it is thought that it can also work as a coagulant aid with alum. Some of the researchers tried to use alginate in conjunction with alum and were successful in some improvements on turbidity removal consequently (Kawamura, 1973, 1991; Jun et al., 2001). In this part of the study, it was tried to improve turbidity removal efficiency of alum using alginate. During the experiments the lowest and nearest to optimum alum concentration, which did not result in a desired level of turbidity removal, was chosen as 0.5 mg/L Al(III) by referring the results of the previous section experiments with “constant alkalinity”. Under the initial alkalinity of 150 mg/L as $CaCO_3$, alum was dosed first and alginate was dosed subsequently. Similar mixing schedules were tested like in calcium-alginate experiments (“1min+1min at 120 rpm”, “5min+5min at 120 rpm”, “8min+2min at 120 rpm”) aiming also to investigate the effect of mixing schedule. The results of the experiments are shown in Figure 4.22.

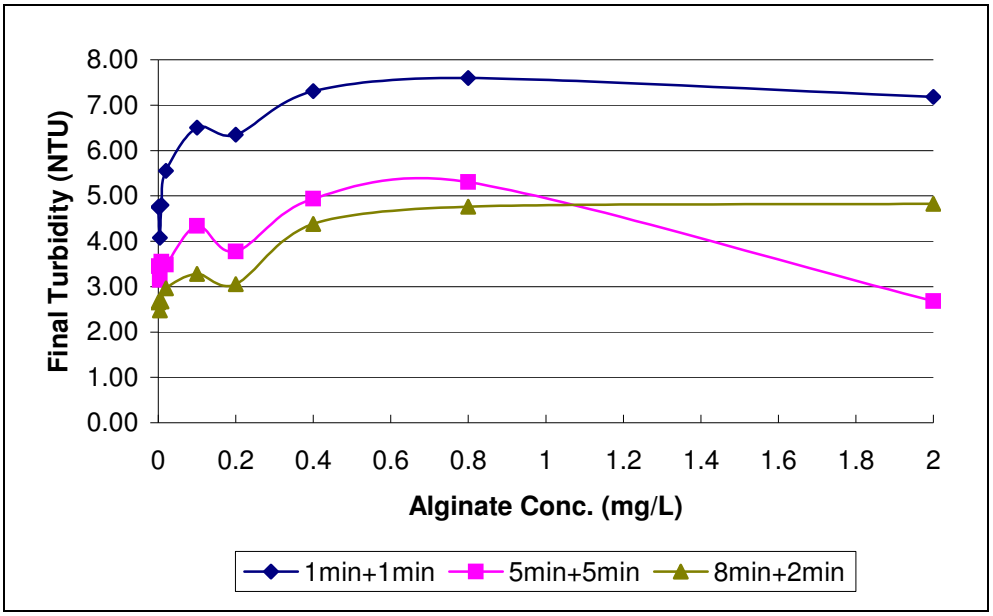

Figure 4.22 Effect of mixing time on residual turbidities when alum used with alginate

Like in calcium-alginate experiments, as the allocated time after alum addition were increased, the turbidity removal efficiency improved regardless of alginate concentrations and differently from those of calcium-alginate, presence of alginate worsened the turbidity removal efficiency achieved by alum itself (except at 2 mg/L alginate concentration in "5min+5min at 120 rpm" procedure). The reason was that alginate reduces the interaction between destabilized particles by their negative charges so that resulted in higher residual turbidity values. Additionally, Al(III) concentrations were so low that alginate could not easily interact with aluminum; in comparison with previous studies Al(III) concentration used in the experiment were far below than those of used in other studies (Kawamura, 1991; Jun et al., 2001). Observing similar effects of changing mixing schedule on the turbidity removal efficiency as in calcium-alginate system indicated that allocating more time following cation addition and before polymer addition improves the turbidity removal efficiency regardless of whether divalent or trivalent cations

were used and it promises for other cation-anionic polymer coagulation-flocculation experiments applicability of changing mixing schedule in similar way. Also, the importance of calcium's ability of gelling the alginate is a very critical mechanism of calcium-alginate coagulant system which was not valid in the case of aluminum working with alginate.

4.6.4 Streaming Current Experiment with Alum

Once all the experiments were conducted with calcium-alginate coagulant system, a brief set of experiment was done to with alum as coagulant compare with calcium alginate system. In this section, an extensive dose determination of alum was not done; but this part was kept rather simple just to differentiate between the working mechanisms of two coagulant systems.

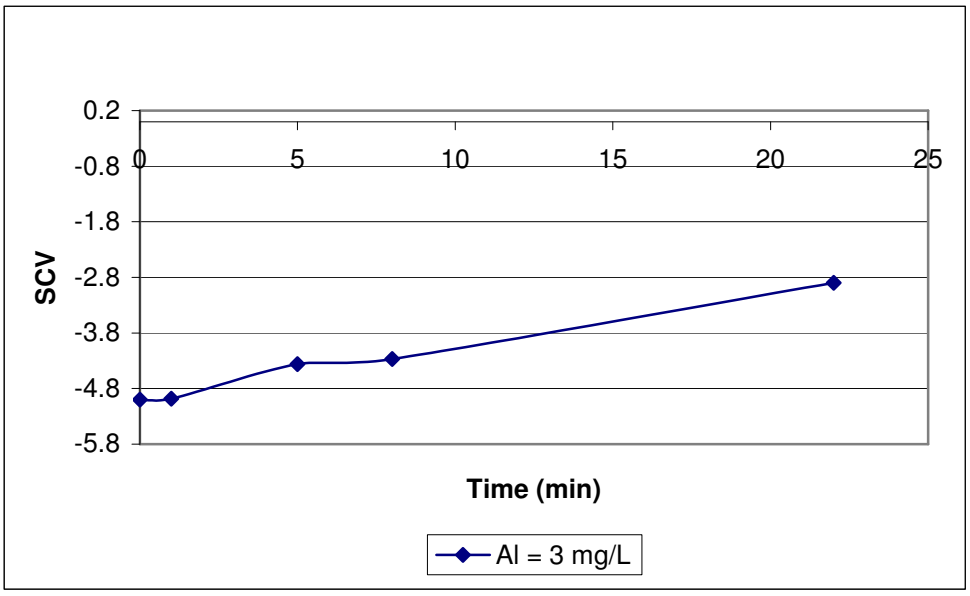

Figure 4.23 Electrokinetic pathway of alum experiment

When SC measurement was carried out for alum experiments, it was encountered that lower SC values than those for calcium would be enough for coagulation with alum. As shown in Figure 4.23, SC of clay suspension modified with alkalinity had different SC from the original clay suspensions: Due to presence of sodium ions in alkalinity modified synthetic water, surface charges of the solution were reduced by double layer compression. The SC of the jar test started with -5.0 and finalized at -2.9. Dentel et al. (1989) realized some transitions in SC when alum solubility was exceeded. Since the experiment covered the sweep flocculation region, it would be wrong comparing alum result with calcium-alginate experiments in terms of relative value. . Even if a direct comparison is not suitable, the electrokinetic pathway of coagulation with alum shows some differences from calcium alginate like destabilization achieved in a shorter period of time than calcium alginate did.

4.7 Produced Sludge Properties

Sludge handling issues are other important concerns in water and wastewater treatment processes due to their financial aspects. Besides turbidity removal efficiencies, sludge produced from different coagulants should be characterized in terms of their behavior such as their dewaterabilities. Characterization of sludge produced from calcium alginate under three different jar test procedures at 120 rpm and initial calcium concentration are tabulated and compared to alum sludge produced from “constant alkalinity” experiment Table 4.4 and 4.5, respectively. The optimum concentrations of alginate and aluminum were chosen by referring optimum points of the same previously performed jar tests in which turbidity removal efficiencies had been investigated.

Table 4.4: Sludge properties produced from calcium-alginate system

Ca^{+2}			Standard Deviation (±)	Standard Deviation (%)	CST/SS (sec/g/L)	Jar Test Procedure
120	TS (mg/L)	877	43	5	14.3	1min+1min 120rpm, 20min 40rpm,
	Moisture Content (%)	99.91	0.00	0		
	SS (mg/L)	307	25	8		
	CST(sec)	4.4	0.6	14		
	TS (mg/L)	890	5	1	14.3	5min+5min 120rpm, 12min 40rpm,
	Moisture Content (%)	99.91	0.00	0		
	SS (mg/L)	367	21	6		
	CST(sec)	5.2	0.2	3		
	TS (mg/L)	938	16	2	11.7	8min+2min 120rpm, 12min 40rpm,
	Moisture Content (%)	99.91	0.00	0		
	SS (mg/L)	470	36	8		
	CST(sec)	5.5	0.1	2		
80	TS(mg/L)	737	19	3	13.6	1min+1min 120rpm, 20min 40rpm,
	Moisture Content (%)	99.93	0.00	0		
	SS (mg/L)	367	21	6		
	CST(sec)	5.0	0.5	10		
	TS (mg/L)	782	31	4	13.3	5min+5min 120rpm, 12min 40rpm,
	Moisture Content (%)	99.92	0.00	0		
	SS(mg/L)	400	26	7		
	CST(sec)	5.3	0.6	11		
	TS (mg/L)	733	25	3	10.4	8min+2min 120rpm, 12min 40rpm,
	Moisture Content (%)	99.93	0.00	0		
	SS (mg/L)	503	15	3		
	CST(sec)	5.2	0.8	16		

Table 4.4(cont'd)

Ca^{+2}			Standard Deviation (±)	Standard Deviation (%)	CST/SS (sec/g/L)	Jar Test Procedure
60	TS(mg/L)	592	77	13	19.9	1min+1min 120rpm, 20min 40rpm,
	Moisture Content (%)	99.94	0.01	0		
	SS(mg/L)	247	31	12		
	CST(sec)	4.9	0.6	13		
	TS (mg/L)	638	36	6	11.9	5min+5min 120rpm, 12min 40rpm,
	Moisture Content (%)	99.94	0.00	0		
	SS(mg/L)	410	0	0		
	CST(sec)	4.9	0.7	15		
	TS (mg/L)	627	28	4	10.4	8min+2min 120rpm, 12min 40rpm,
	Moisture Content (%)	99.94	0.00	0		
	SS(mg/L)	447	15	3		
	CST(sec)	4.6	0.4	8		

Table 4.5: Sludge properties produced from alum

Al			Standard Deviation (±)	Standard Deviation (%)	CST/SS (sec/g/L)	Jar Test Procedure
3	TS(mg/L)	900	9	1	11.5	1min 120rpm, 21min 40rpm,
	Moisture Content (%)	99.91	0.00	0		
	SS(mg/L)	607	21	3		
	CST(sec)	7.0	0.4	5		

Regardless of which rapid mixing schedule was applied, total solids (TS) concentration of calcium alginate sludge increased with increasing calcium concentrations which was basically due to two reasons: First, calcium concentration was contributed to TS concentration as dissolved solid concentration. Second, based on observations of better turbidity removal at higher calcium concentrations, accumulation of more suspended solids (SS) in sludge was reasonable and might increase TS

values subsequently. The effect of second reason can be proved by comparing the alteration of TS with respect to calcium increases; as calcium concentration increase in the order of 60, 80 and 120 mg/L, TS concentrations did not increase in the same order or at least no proportional increase were observed over change in calcium concentration.

From SS point of view, it was not possible to find a particular relationship between calcium dose and SS concentrations. However, mixing schedule had an apparent effect on SS values: as the mixing time after calcium addition and before alginate addition was increased, SS concentration also increased like, the similar relationship which had already been observed between the effects of mixing schedule on turbidity removal efficiency. So it could be commented on that in such a way that the increase in SS concentration resulted due to better turbidity removal efficiency or participation more suspended particles in flocs accordingly.

Capillary suction time (CST) is an easy tool to measure sludge dewaterability. Nonetheless; Wu et al., (1997) stated that only CST might be misleading parameter if suspended solids concentration in sludge is ignored; same CST values could be obtained at different sludge concentrations. So, the CST must be normalized to include the suspended solids concentration in it. For normalized CST values, i.e. CST/SS, the lower the value, the easier the sludge can be dewatered. As shown in Figure 4.24 (time corresponds to the point at which alginate was dosed for different mixing schedules, namely ,each point in the graph represent one of the mixing schedules' results of "1min + 1min at 120" rpm", "5min + 5min at 120" rpm", "8min + 2min at 120" rpm"), almost identical dewaterability results were observed for the sludge produced with 80 and 120 mg/L initial calcium concentrations. However, sludge

produced at 60 mg/L calcium exhibited rather more variation to change in rapid mixing schedules. Generally, as the time allocated after calcium dosing was increased the dewaterability of sludge improved as well. The reason of that can be associated to previous statement in section "Investigation the Effect of Mixing Time and Intensity": Occurrence of flocculation at rapid mixing period had the advantage to form more compact and dense microflocs. In addition to that, Turchiuli and Fargues (2004) stated compact flocs were easily dewaterable than those having loose structure. Accordingly, one can ultimately come to a conclusion that more compact flocs were produced by increasing rapid mixing time during only calcium rapid mixing period.

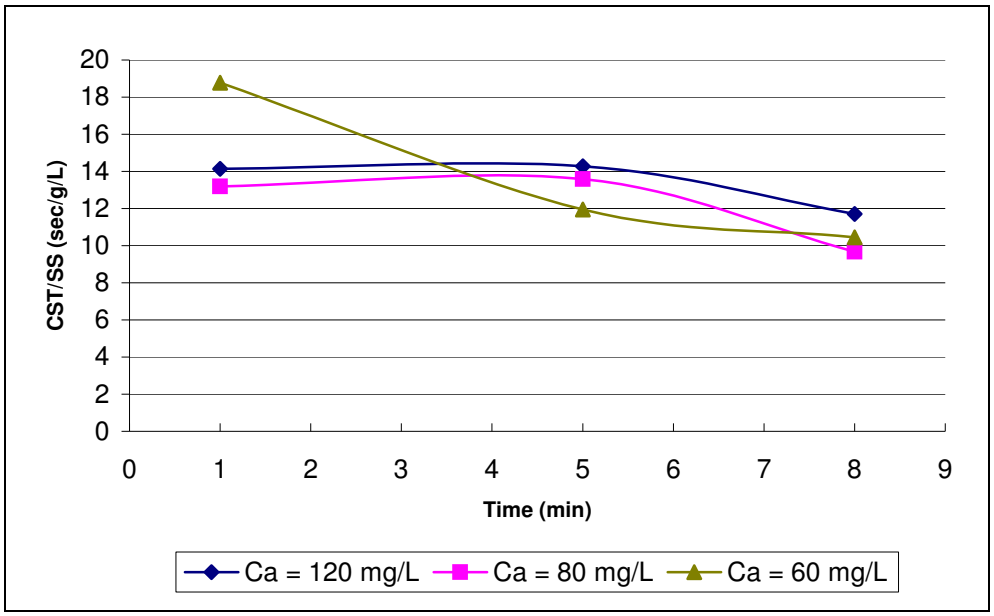

Figure 4.24 Effect of mixing schedule on the sludge properties

Comparison of calcium alginate sludge with alum sludge indicates that TS concentration of alum sludge was near to calcium alginate sludge produced at 120 mg/L calcium dosage. However, SS concentration of alum sludge was higher than calcium alginate sludge. The reason was in

the coagulation mechanism of alum, hydroxide precipitates were formed, and they contribute to SS concentrations. One thing obvious from these results is that use of alum would cause much higher quantities of sludge needing to be disposed of. This highlights a significant advantage of calcium alginate system. On the other hand, calcium-alginate coagulant system causes slightly more dissolved solids in the liquid phase and led up producing higher harnesses. It seemed there were no great differences between dewaterability of alum and calcium-alginate sludge. Generally, for short mixing times alum sludge seems to dewater slightly better; whereas in longer mixing times calcium-alginate sludge seems to dewater slightly better.

Average moisture content of all sludge was calculated around 99.9%; being moisture content such a high value, however, might cause some over or under estimation of sludge properties. Fortunately, being moisture contents near to each other did not avoid comparing of sludge properties with each other. Containing synthetic water low amount of SS and subsequent production of very low amount of sludge was the main reason of poorly thickened sludge. This problem could be solved by scaling up the volumes working with them.

4.8 Experiments on Raw Water

Finally experiments were conducted on natural water samples. Raw water supplied from IWTP inlet had very low initial turbidity value (1.95 NTU), especially comparing to this study. Treatment of raw water with alum (Figure 4.25) resulted in turbidity levels meeting the standard requirement's residual turbidities of 0.26 NTU was obtained at 5 mg/L Al concentrations between tried ranges of 1 and 20 mg/L Al. Since alkalinity of raw water was high enough to buffer pH depression, final pH value were also remained in desirable level of pH 7.1 with residual alkalinity of

60 mg/L as $CaCO_3$. This experiment showed that this raw water can easily be treated with alum.

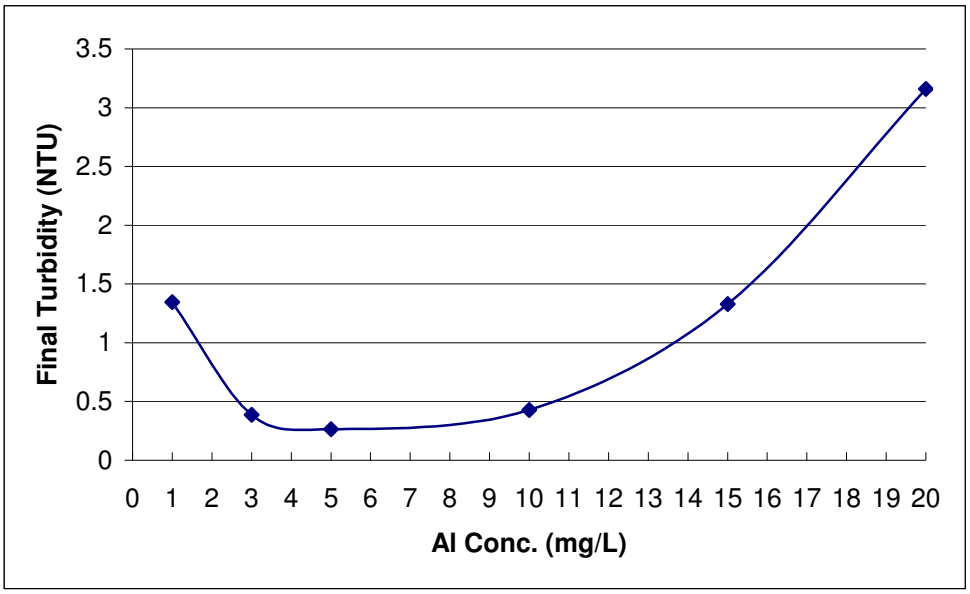

Figure 4.25 Jar test result of alum with natural raw water

The mixing procedure of "8min+2 min at 120 rpm" was chosen for jar test conducted to evaluate the usability of calcium alginate as a coagulant in the highlight of obtained best results from the earlier tests. As shown in Figure 4.26 , alginate concentration was varied over the range of 0.02-0.8 mg/L, however, the system failed to remove turbidity into desired levels (lower than 1 NTU) and it seems that the addition of alginate worsened the turbidity removal efficiency than when calcium used alone. Since obtaining non-promising results with calcium alginate at 120 mg/L of calcium, it was decided to evaluate lower calcium concentrations were not worth to try. Instead of that, it was tried to use alginate as a flocculant aid in combination with alum. The lowest Al(III) concentrations which did not yield desired residual turbidity was chosen (1 mg/L Al(III)) to investigate the additional effect of alginate on turbidity removal. When

aluminum was replaced with calcium, insignificant improvements were observed in residual turbidities; however, they were not well enough to meet the requirements of standards as shown in Figure 4.26.

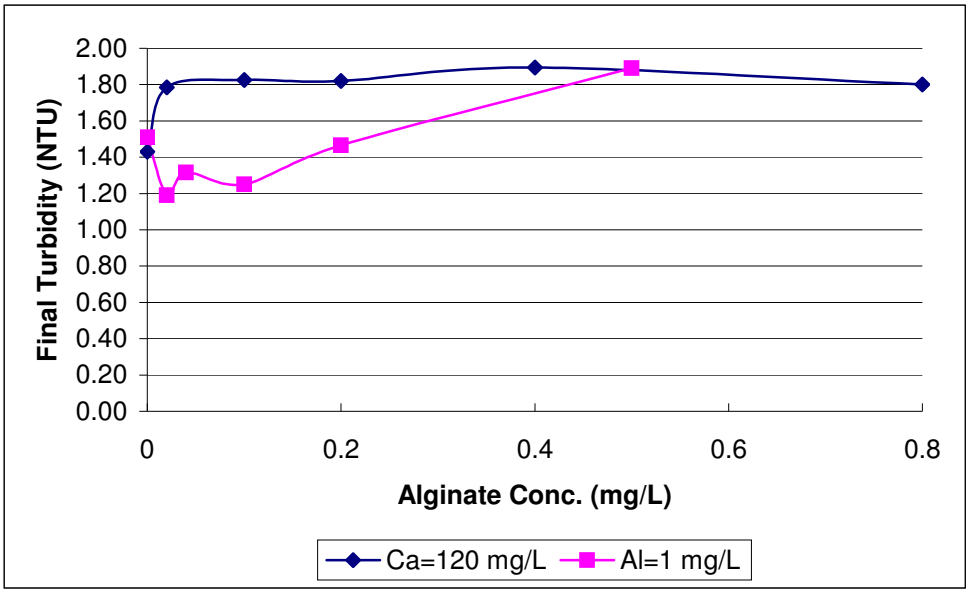

Figure 4.26 Jar test result of alum and calcium with alginate on raw water

Then it was thought that for the waters in which there is not enough particles present for proper coagulation, turbidity addition could be an alternative solution to improve coagulation efficiency. Within this context, it was tried to raise the initial turbidity of raw water to higher values like 5, 10, 20 and 80 NTU. Results of the experiments are shown in Figures 4.27-4.28 for initial calcium concentration of 120 and 80 mg/L, respectively (RWC: Clay added raw water).

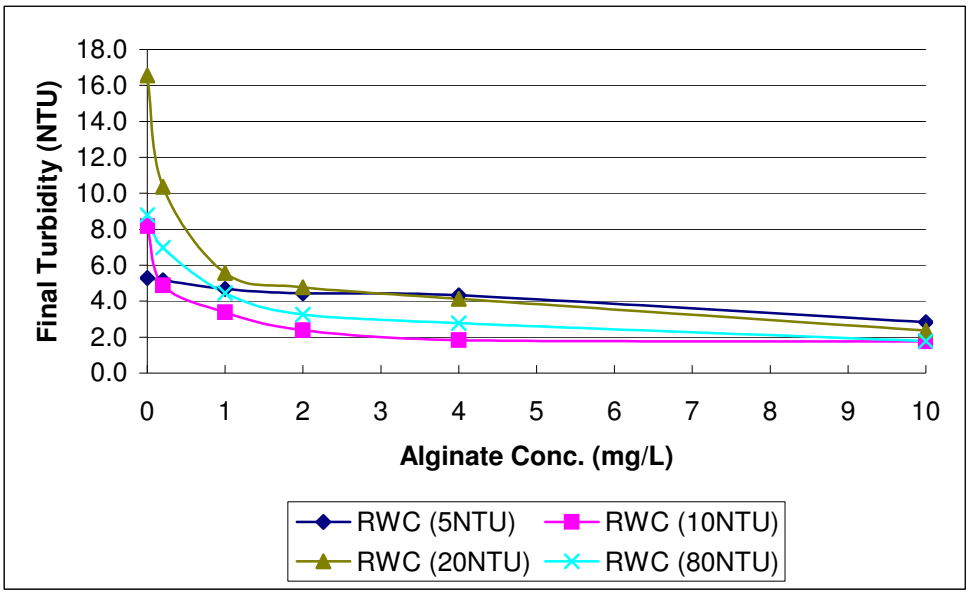

Figure 4.27 Residual turbidities of calcium-alginate system at 120 mg/L calcium concentration at "8min+2min at 120 rpm"

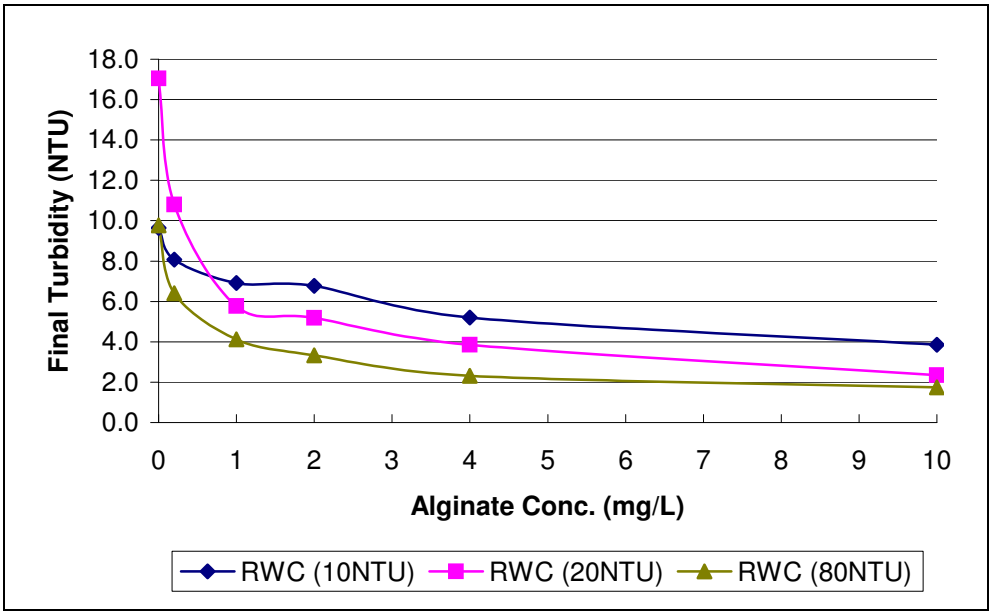

Figure 4.28 Residual turbidities of calcium-alginate system at 80 mg/L calcium concentration at "8min+2min at 120 rpm"

Even though initial turbidity values were raised as high as 80NTU, calcium alginate was not able to reduce final turbidity below 1 NTU for the alginate concentrations between 0-10 mg/L and it was also observed that effective alginate concentrations shifted from around 0.2 to 10 mg/L in comparison with synthetic water experiments. Regardless of initial turbidity of modified raw water, residual turbidity values converged to around 2 NTU especially for 120 mg/L initial calcium concentrations. The limit value of achievable turbidity removal corresponded to the initial turbidity of raw water itself indicating that turbidity of raw water mainly consist of organic matters rather than suspended materials. Website of (Ankara Water Sewage Authority) also reports that SS concentration as 5.6 mg/L and TOC as 8.94 mg/L for the inlet water with an initial turbidity of 5.0 NTU. Since the water samples were collected in drought season, the residual turbidity decreased to values 1.92 NTU and having had a relatively dry winter season is thought to alter the composition of raw water in a way like decreasing SS concentration further due to extended period of sedimentation and increasing TOC due to biological activities. The reason of increasing the effective concentration of alginate and decreasing the turbidity removal efficiency can be explained by the difference of composition between raw water and synthetically prepared water and the presence of organic matter in natural raw water which does not exist in synthetic water. It is known that organic matter hinders the efficiency of coagulation by interacting with coagulants. As a result, the needs of further research come up about interaction of alginate with organic matters.

CHAPTER 5

CONCLUSION

The potential use of calcium-alginate as a coagulant in low turbidity waters was achieved in several steps. Calcium concentration of solution was the key parameter, it acts as reducing the repulsion forces between forces of clay/clay, polymer/clay and polymer/polymer. It also reacts with alginate from gels which produces stronger flocs. First, the effect of molecular weight was investigated and found that higher molecular weight alginate showed a better performance. Then, rapid mixing time was increased from a total of 2 minutes to a total 10 minutes and was separated into two parts: 5 or 8 minutes after calcium addition and 5 or 2 minutes after alginate addition, respectively. The result demonstrated that prolonged rapid mixing improved the system efficiency and additionally allocating more time after calcium addition resulted in better turbidity removal efficiency. Also, increasing mixing intensity improves system efficiency in minor amount for 120 and 80 mg/L calcium concentration. However, it was found that the system was highly affected by mixing intensity at 60 mg/L calcium concentration which was proven by streaming current measurements.

pH of the suspension was another parameter affecting the turbidity removal efficiency. As the pH values increased from acidic levels to basic levels, the residual turbidities decreased gradually. The reason was thought to be alginate forming an expanded structure at higher pH values.

Alkalinity of the synthetic water produced slightly better turbidity removal efficiency. It was observed same improved in turbidity removal independent from tried alkalinity values.

Jar test conducted to determine the alum efficiency showed that alum can also be used as coagulant for low turbidity waters. However, there should be alkalinity addition to water and initial alkalinity of the synthetic water affects the efficiency of alum.

Alginate was used as coagulant aid in combination with alum; however results were not promising for its use for low alum concentrations like 1 mg/L.

Sludge properties of calcium alginate and alum were compared and noticed that calcium-alginate produces low amount of sludge than alum, however there were no differences in dewaterability.

Since raw water taken from IWTP had very low initial turbidity as 1.98 NTU, calcium-alginate could not perform properly while alum worked sufficiently. Obtaining inefficient results even in turbidity increase of raw water showed that organic matter of the water affecting the efficiency of calcium-alginate.

As a summary, the results showed that calcium alginate system had some advantages and disadvantages over alum coagulant as listed below;

Advantages of calcium alginate system over alum:

- There is not any risk of remaining heavy metal ions, presence of which in treated water may cause some health problems.

- Presence of residual monomers from manufacturing process and formation of disinfection by products in case of synthetic polymers usage is avoided by using alginate biopolymer.
- Calcium alginate system is almost able to work independent from pH and alkalinity of the medium meaning that easier to operate than alum.
- The system produces less amount of sludge than that of alum produced.

Disadvantages of calcium alginate system:

- The system contributes additional hardness to water which might be problematic in water distribution.
- There are some indications that organic matters present in water inhibits calcium alginate system efficiency.

As a result, calcium alginate system could be used for waters with 10 NTU or higher turbidity values provided that turbidity of water is mainly composed of inorganic suspended materials. However; calcium alginate system still includes some uncertain parameters needing to be investigated for its efficient usage in water treatment plants which were discussed in the next chapter.

CHAPTER 6

RECOMMENDATIONS for FUTURE STUDIES

In this study, calcium ions were supplied in the form of $CaCl_2$, since $CaCl_2$ is an expensive chemical, it could be replaced with different calcium sources like $CaCO_3$ or $CaSO_4$. Meanwhile, the effect of different anions on the system would also be investigated by changing the source of calcium.

Rapid mixing time and intensity had dramatic effects on the calcium alginate system. Additionally, it could be studied the effect slow mixing time and intensity on the system efficiency.

There is still insufficient information about the reactions of calcium alginate with natural organic matter present in water. Jar tests could be conducted to investigate the effect of natural organic matters on calcium alginate system.

Alginate was tried to be used as coagulant aid in conjunction with alum, however, alum concentrations were not varied over a wide range. Alum and alginate concentrations and produced sludge properties from this system could be studied in more detail.

REFERENCES

Abu-Orf, M. M., Walkerb, C. A., and Dentel, S. K. (2003). “Centrate viscosity for continuous monitoring of polymer feed in dewatering applications” *Advances in Environmental Research*, 7, 687–694

Abu-Orf, M.M. and Dentel, S.K. (1997). "Polymer dose assessment using the streaming current detector" *Water Environment Research*, 69, 1075-1085

Abu-Orf, M.M. and Dentel, S.K. (1998). "Automatic control of polymer dose using the streaming current detector" *Water Environment Research*, 70, 1005-1018

Ahmad, A. L., Sumathi, S., Hameed, and B. H. (2006). “Coagulation of residue oil and suspended solid in palm oil mill effluent by chitosan, alum and PAC” *Chemical Engineering Journal*, 118, 99–105

Amirtharajah, A. and Mills, P. (1982). “Rapid mix design for mechanism of alum coagulation” *Journal of AWWA*, April, 210-216

Bernazau, F., Pierrone, P., and Duguet, J. P. (1992). “Interest in using a streamline current detector for automatic coagulant dose control” *Water Supply*, 10(4), 87-96

Besra, L., Sengupta, D. K., and Ay, P. (2002). “Polymer adsorption: its correlation with flocculation and dewatering of kaolin suspension in the presence and absence of surfactant” *Journal of Mineral Processing*, 66, 183-202

Besra, L., Sengupta, D. K., Roy, S.K., and Ay, P. (2004). “Influence of polymer adsorption and conformation on flocculation and dewatering of kaolin suspension” *Separation and Purification Technology*, 37, 231–246

Black, A. P., Birkner, F. B., and Morgan J. J. (1965). “Destabilization of dilute clay suspensions with labeled polymers” *Journal AWWA*, 57, 1547-1560

Bolto, B., and Gregory, J. (2007). “Organic polyelectrolytes in water treatment” *Water Research*, 41, 2301-2324

Bolto, B., Dixon, D., Eldridge, R., and King, S. (2002). “Removal of THM precursors by coagulation or ion exchange” *Water Research*, 36, 5066-5073

Bouyer, D., Coufort, C., Liné, A., and Do-Quang, Z. (2005). “Experimental analysis of floc size distributions in a 1-L jar under different hydrodynamics and physicochemical conditions” *Journal of Colloid and Interface Science*, 292, 413–428

Bratby, J. (1980). *Coagulation and flocculation: with an emphasis on water and wastewater treatment*, Croydon, Eng, Uplands Press

Chakraborti, R. K., Gardnerb, K. H., Atkinsona, J. F., and Van Benschotena, J. E. (2003). “Changes in fractal dimension during aggregation” *Water Research*, 37, 873–883

Ching, H. W., Elimelech, M., and Hering, J. G. (1994). “Dynamics of coagulation of clay particles with aluminum sulfate” *Journal of Environmental Engineering*, 120(1), 169-189

Cohen, J. M., and Hannah, S. A (1971). *In: Water and Quality and Treatment,* 3rd Ed., McGraw Hill, New York, 66-122

Coufort, C., Dumas, C., Bouyer, D., and Liné, A. (2007). "Analysis of floc size distributions in a mixing tank" *Chemical Engineering and Processing* (Article in Press)

Csempesz, F. (2000). "Enhanced flocculation of colloidal dispersions by polymer mixtures" *Chemical Engineering Journal*, 80, 43–49

Çoruh, H. A. (2005). "Use of calcium alginate as a coagulant in water treatment" *Ms. Thesis*, Middle East Technical University

Davis, T. A., Volesky, B., and Muccib, A. (2003) "A review of the biochemistry of heavy metal biosorption by brown algae" *Water Research*, 37, 4311–4330

Dentel, S. K. (1988). "Application of the Precipitation-Charge Neutralization Model of Coagulation" *Environ. Sci. Technol.*, 22, 825-832

Dentel, S. K., Thomas, A. V., and Kingery, K. M. (1989). "Evaluation of the streaming current detector – I. Use in jar test" *Water Research*, 23(4), 413-421

Dentel, S.K., Abu-Orf M. M.,, and Walker, C. A. (2000). "Optimization of slurry flocculation and dewatering based on electrokinetic and rheological phenomena" *Chemical Engineering Journal*, 80, 65-72

Diaz, A., Rincon, N., Escorihuela, A., Fernandez, N., Chacin, E., and Forster, C.F. (1999). “A preliminary evaluation of turbidity removal by natural coagulants indigenous to Venezuela” *Process Biochemistry*, 35, 391–395

Divakaran, R., and Pillai, V. N. S. (2001). “Flocculation of kaolinite suspensions in water by chitosan” *Wat. Res.*, 35(16), 3904–3908

Divakaran, R., and Pillai, V. N. S. (2002). “Flocculation of river silt using chitosan” *Water Research*, 36, 2414–2418

Duan, J., and Gregory, J. (2003). “Coagulation by hydrolyzing metal salts” *Advances in Colloid and Interface Science*, 100 –102, 475–502

Edney, D. (2005). “Introduction to the theory of the streaming current meter” *on website: http://www.accufloc.com/literature.html* (accessed in November 2007)

Ersoy, B. (2005). “Effect of pH and polymer charge density on settling rate and turbidity of natural stone suspensions” *Int. J. Miner. Process.*, 75, 207– 216

Françoise, R. J. (1988). “Growth kinetics of hydroxide flocs” *Journal of AWWA*, June, 92-96

Glover, S. M., Yan, Y., Jameson, and G. J., Biggs, S. (2000). “Bridging flocculation studied by light scattering and settling*” Chemical Engineering Journal*, 80, 3–12

Gray, S. R., and Ritchie, J. B. (2006). “Effect of organic polyelectrolyte characteristics on floc strength” *Colloids and Surfaces A: Physicochem. Eng. Aspects*, 273, 184–188

Gregory, J. (1973). “Rates of flocculation of latex particles by cationic polymers” *Journal of Colloid and Interface Science*, 42(2), 448-456

Gregory, J. (1985). “The use of polymeric flocculants” *Proc. of the Engineering Foundation Conference on Flocculation, Sedimentation and Consolidation*, American Institute of Chemical Engineers, New York, USA, 125–137

Grisafi, F. (1994). “Mass transfer kinetics in solid-liquid stirred system” *Ph. D Thesis, Chemical Engineering Department,* Federico II University, Napoli, Italy.

Guibal, E., and Roussy, J. (2007). “Coagulation and flocculation of dye-containing solutions using a biopolymer (Chitosan)” *Reactive & Functional Polymers*, 67, 33–42

Hogg, R. (1999). “The role of polymer adsorption kinetics in flocculation” *A: Physicochemical and Engineering Aspects*, 146, 253-263

Hou, T., Xu, R., Tiwari, D., and Zhao, A. (2007). “Interaction between electrical double layers of soil colloids and Fe/Al oxides in suspensions” *Journal of Colloid and Interface Science*, 310, 670–674

Huang, C., Chen, S., and Pan J. S. (2000). “Optimal condition for modification of chitosan: a biopolymer for coagulation of colloidal particles” *Wat. Res.*, 34(3), 1057-1062

Hunter, K. A., and Liss, P. S. (1982). “Organic matter and the surface charge of suspended particles in estuarine waters“Limnology *and Oceanography*, 27(2), 322-335

Ibanez, J. P. and Umetsu, Y. (2002). “Potential of protonated alginate beads for heavy metal uptake” *Hydrometallurgy*, 64, 89-99

Ikeda, A., Takemura, A., and Ono, H. (2000). “Preparation of low molecular weight alginic acid by acid hydrolysis” *Carbohydrate Polymers*, 42, 421-425

Iriarte-Velasco, U., A´ lvarez-Uriarte, J. I., and Gonza´lez-Velasco, J. R. (2007). “Enhanced coagulation under changing alkalinity-hardness conditions and its implications on trihalomethane precursors removal and relationship with UV absorbance” *Separation and Purification Technology*, 55, 368-380

Jaussens, J. G. (1992). “Development in coagulation, flocculation and dissolved air floatation” *Water Engineering and Managament*, January, 26-31

Julien, R., and Meakin, P. (1989). “Simple models for restructuring of three-dimensional Ballistic Aggregates” *J. Colloid Interface Sci.*, 127, 265-272

Jun, H. B., Lee, Y. J., Lee, B. D., and Knappe, D. R. U. (2001). “Effectiveness of coagulants and coagulant aids for the removal of filter-clogging Synedra“ *Journal of Water Supply: Research and Technology*, 50(3), 135-148

Kabsch-Korbutowicz, M. (2005) “Effect of Al coagulant type on natural organic matter removal efficiency in coagulation/ultrafiltration process” *Desalination*,185, 327–333

Katchalsky, A. (1953) “Polyelectrolytes”, *Endeavour*, April, 90-94

Kawamura, S. (1973). “Coagulation considerations” *Journal of AWWA*, 65(6), 417-423

Kawamura, S. (1991). “Effectiveness of natural polyelectrolytes in water treatment” *Journal of AWWA*, 83(10), 88-91

Kleimann, J., Gehin-Delval, C., Auweter, H., Borkovec, M. (2005). “Super-stoichiometric charge neutralization in particle-polyelectrolyte systems” *Langmuir*, 21(8), 3688–3698

Kong, H. J., Smith, M. K., and Mooney, D. J. (2003). “Designing alginate hydrogels to maintain viability of immobilized cells” *Biomaterials*, 24, 4023–4029

Kusters, K. A. (1991). “The influence of turbulence on aggregation of small particles in agitated vessels’’ *Ph.D. Thesis*, Eindhoven University of Technology, The Netherlands

Kusters, K. A., Wijens, J. G., and Thoenes, D. (1996). “Aggregation kinetics of small particles in agitated vessels” *Chem. Eng. Sci.*, 52, 107-121

La Mer, V.K. (1966). “Filtration of colloidal dispersions flocculated by anionic and cationic polyelectrolytes” *Disc. Faraday Soc.*, 42, 248–254

Labille, J., Thomas, F., Milas, M., and Vanhaverbeke, C. (2005). "Flocculation of colloidal clay by bacterial polysaccharides: effect of macromolecule charge and structure" *Journal of Colloid and Interface Science*, 284, 149–156

Lee, S. H., Lee, S. O., Jang K. L. and lee T. H. (1995). "Microbial flocculant from Arcuadendron sp. TS-49" *Biotechnol Lett.*, 17, 95-100

Levin, S., and Friesen, W. T. (1987). "Flocculation of particles by water soluble polymer" *Attia YA, editor, Flocculation in biotechnology and separation systems,* Amsterdam Elsevier, 3-20

Li, T., Zhu, Z., Wang, D., Yao, C., and Tang, H. (2006). "Characterization of floc size, strength and structure under various coagulation mechanisms" *Powder Technology*, 168, 104–110

Malvern Inc. (2007). "Zeta Potential an introduction in 30 minutes" *Zetasizer Nano Series Technical Note on website: www.nbtc.cornell.edu/facilities/downloads/Zeta%20potential%20%20An%20introduction%20in%2030%20minutes.pdf (accessed in July 2007)*

Martinsen, A. Skjak-Braek, G., and Smisrod, O. (1991), "Comparison of different methods for determination of molecular weight and molecular weight distribution of alginates" *Carbohydrate Polymers*, 15, 171-193

Maximova, N., and Dahl, O. (2006). "Environmental implications of aggregation phenomena: Current understanding" *Current Opinion in Colloid & Interface Science*, 11, 246–266

McConnachie, G. L., and Lium J. (2000). "Design of baffled hydraulic channels for turbulence-induced flocculation" *Wat. Res.*, 34(6), 1886-1896

McFadyen P. (2004). “Zeta Potential of Macroscopic Surfaces from Streaming Potential Measurements” *on website: www.bic.com/PDFs/ZetaPotentialofMacroscopicSurfaces.pdf* (accessed in July 2007)

Menezes, F. M., Amal, R., and Luketina, D. (1996). “Removal of particles using coagulation and flocculation in a dynamic separator” *Powder Technology*, 88, 27-31

Mishra, A., and Bajpai, M. (2005). “Flocculation behavior of model textile wastewater treated with a food grade polysaccharide” *Journal of Hazardous Materials*, B118, 213–217

Mpofu, P., Addai-Mensah, J., and Ralston, J. (2003). “Investigation of the effect of polymer structure type on flocculation, rheology and dewatering behavior of kaolinite dispersions” *Int. J. Miner. Process.*, 71, 247– 268

Muyibi, S. A., and Okuofu, C. A. (1995). “Coagulation of low turbidity surface waters with Moringa Oleifera seeds” *Int. J. Envin. Study*, (48(3-4), 263-273

Neyens, E., Baeyens, J., Dewil, R., and De Heyder, B. (2004). “Advanced sludge treatment affects extracellular polymeric substances to improve activated sludge dewatering” *Journal of Hazardous Materials*, 106(B), 83-92

Okuda, T., Baes, A. U., Nishijima, W., and Okada, M. (2001). “Coagulation mechanism of salt solution-extracted active component in moringa oleifera seeds” *Wat. Res.*, 35(3), 830-834

Okuda, T., Baes, A. U., Nishijima, W., and Okada, M. (2001). “Isolation and characterization of coagulant extracted from moringa oleifera seed by salt solution” *Wat. Res.*, 35(2), 405-410

Oles, V. (1992). “Shear induced aggregation and breakup of polystyrene latex particles” *J. Colloid Interface Sci.*, 154, 351-358

Özacar, M., and Sengil, İ. A. (2003). “Evaluation of tannin biopolymer as a coagulant aid for coagulation of colloidal particles” *Colloids and Surfaces A: Physicochem. Eng. Aspects*, 229, 85–96

Pal, S., Mal, D., and Singh, R. P. (2005). “Cationic starch: an effective flocculating agent” *Carbohydrate Polymers*, 59, 417–423

Ravina, L. (2003). “Everthing you want to know about coagulation&flocculation” 4th Ed., Zeta-Meter Inc., Virginia

Reynolds, T. D. (1982). *Unit Operations and Processes in Environmental Engineering*, PWS_KENT Publishing Company, Boston, Massachusetts

Richens, D.T. (1997). *The Chemistry of Aqua Ions: Synthesis, Structure, and Reactivity: A Tour through the Periodic Table of the Elements*, Wiley, New York

Rossini. M., Garrido, J. C., and Galluzzo, M. (1999). “Optimization of the coagulation flocculation treatment: influence of rapid mix parameters” *Wat. Res.*, 33(8), 1817-1826

Sableviciene, D., Klimaviciute, R., Bendoraitiene, J., and Zemaitaitis, A. (2005). “Flocculation properties of high-substituted cationic starches” *Colloids and Surfaces A: Physicochem. Eng. Aspects*, 259, 23–30

Sabra, W., Zeng, A. P., and Deckwer, W. D. (2001). “Bacterial alginate: physiology, product quality and process aspects” *Appl. Microbiol. Biotechno., 56, 315-325*

Salehizadeh, H., and Shojaosadati, S. A. (2001). “Extracellular biopolymeric flocculants Recent trends and biotechnological importance” *Biotechnology Advances*, 19, 371–385

Semerjian, L., and Ayoub, G. M. (2003). “High-pH–magnesium coagulation–flocculation in wastewater Treatment” *Advances in Environmental Research*, 7, 389–403

Shaw, D. J. (1979). *Introduction to Colloid and Surface Chemistry,* Butterworth & Co., London

Simpson, N. E., Stabler, C. L., Simpson, C. P., Sambanis, A. and Constantinidis, I. (2004). “The role of the CaCl2–guluronic acid interaction on alginate encapsulated βTC3 cells” *Biomaterials*, 25, 2603-2610

Singh, R. P., Nayak, B. R., Biswal, D. R., Tripathy, T., and Banik, K. (2003). “Biobased polymeric flocculants for industrial effluent treatment” *Mat. Res. Innovat.*, 7, 331–340

Sommerauer, A., Sussman, D. L., and Stumm, W. (1968) “The role of complex formation in the flocculation of negatively charged sols with anionic polyelectrolytes” *Koll. Z-Z. Polymere*, 225, 147-154

Spicer, P. T. (1997). “Shear-Induced Aggregation-Fragmentation: Mixing and Aggregate Morphology Effects” *Ph. D. Thesis, Chemical Engineering Department*, University of Cincinnati, USA

Spicer, P. T., Pratsinis, S. E., Raper, J., Amal, R., Bushell, G., and Meesters G. (1998). “Effect of shear schedule on particle size, density, and structure during flocculation in stirred tanks” *Powder Technology*, 97, 26-34

Standard Methods for the Examination of Water&Wastewater, (2005), 21st Ed., APHA AWWA, WLF

Steffan, S., Bardib, L., and Marzonaa, M. (2005). “Azo dye biodegradation by microbial cultures immobilized in alginate beads” *Environment International*, 31, 201– 205

Stumm, W. and Morgan, J. J. (1962). “Chemical aspects of coagulation” *Jour. AWWA*¸ 54(8), 971-991

Stumm, W. and O'Melia, C.R. (1968). “Stoichiometry of coagulation” *Journal of AWWA*., 60, 514

Tambo, N. (1991). “Basic concepts and innovative turn of coagulation/flocculation” *Water Supply*, 9(1), 1-10

Tchobanoglous, G., Burton, F. L., and Stensel, H. D. (2003). *Wastewater Engineering Treatment and Reuse*, 4th Ed, Metcalf&Eddy Inc

Thomas, D. G. (1964). “Turbulent distribution of flocs in small particle size suspensions” *AlChe J.*, 10 (4), 517-523

Thomas, D. N., Judd, S. J., and Fawcett, N. (1999). “Flocculation modelling: a review” *Wat. Res.*, 33(7), 1579-1592

Tian, B., Ge, X., Pan, G., Fan, B., and Luan Z. (2006). “Adsorption and flocculation behaviors of polydiallyldimethylammonium (PDADMA) salts: Influence of counterion” *Int. J. Miner. Process.*, (Article in Press)

Torres, F. E., Russel, W. B. and Schowalter, W. R. (1991). “Floc structure and growth kinetics for rapid shear coagulation of polystyrene colloids” *J. Colloidal Interface Sci.*, 142, 554-574

Turchiuli, C., and Fargues, C. (2004). “Influence of structural properties of alum and ferric flocs on sludge dewaterability” *Chemical Engineering Journal*, 103, 123-131

Valentin, N., Fotoohi, F., and Denoeux, T. (1999). “Modelling of coagulant dosing in a water treatment plant” *Proc of EANN’99(September)*, Warsaw, 165-170

Verrall, K. E., Warwick, P., and Fairhurst, A. J. (1999). “Application of the Schulze–Hardy rule to haematite and haematite: humate colloid stability” *Colloids and Surfaces A: Physicochemical and Engineering Aspects*, 150, 261–273

Volesky, B. (2001). “Detoxification of metal-bearing effluents: biosorption for the next century” *Hydrometallurgy*, 59, 203–216

Walaszek, W., and Ay, P. (2005). “Pelleting flocculation an alternative technique to optimise sludge conditioning” *Int. J. Miner. Process.* , 76, 173-180

Watanabe, M., Suzuki, Y., Sasakl, K., Nakashimada Y., and Nishio, N. (1999). “Flocculating Property of Extracellular Polymeric Substance Derived from a Marine Photosynthetic Bacterium, Rhodovulum sp.” *Journal of Bioscience and Bioengineering*, 87(5), 625-629

Weber, W. J. (1972). *Physicochemical prccesses for water quality control*, New York, Wiley-Interscience, Chapter 2

Wu, C., Huang, C., and Lee, D. J. (1997). “Effect of polymer dosage on alum sludge dewatering characteristics and physical properties” *A: Physicochemical and Engineering Aspects*, 122, 89-96

Wu, X., Ge, X., Wang, D., and Tang, H. (2007). “Distinct coagulation mechanism and model between alum and high Al13-PACl” *Colloids and Surfaces A: Physicochem. Eng. Aspects*, (Article in Press)

Xia, S., Li, X., Zhang, Q., Xu, B., and Li, G. (2007) “Ultrafiltration of surface water with coagulation pretreatment by streaming current control” *Desalination*, 204, 351-358

Ye, C., Wang, D., Shi, B., Yu, J., Qu, J., Edwards, M., and Tang, H. (2007). “Alkalinity effect of coagulation with polyaluminum chlorides:Role of electrostatic patch” *Colloids and Surfaces A: Physicochem. Eng. Aspects*, 294, 163-173

Zajic, J. E. and Knetting, E. (1971). “Flocculants from paraflinic hydrocarbons” Development in industrial microbiology” *American Institute of Biological Science*, Washington (DC), 87-98

Zetasizer Inc. (2004). “Zeta potential theory” *on website: www.nbtc.cornell.edu/facilities/downloads/Zetasizer%20chapter%2016.pdf* (accessed in July 2007)

Zhang, J., Zhang, F., Luo, Y., and Yang, H. (2006). “A preliminary study on cactus as coagulant in water treatment” *Process Biochemistry*, 41, 730–733

APPENDIX A

The procedures of which uncertainty analysis carried consists of two parts: One is starting from preparation of stock calcium solution and finishing in dilution of the sample which will be measured. Second is the preparation of standard solutions for calcium measurements.

The Procedure of the Calcium Dosing and Dilution of Samples

1. Predetermined amount of $CaCl_2*2H_2O$ is weighted.
2. Weighted $CaCl_2*2H_2O$ is dissolved by distilled water in 100 mL flask.
3. 500 mL of synthetic water in which stock calcium will be dosed is measured via graduated cylinder.
4. Using pipettor predetermined volume of calcium is dosed from stock calcium concentration to 500 mL synthetic water.
5. At the end of experiment, predetermined volume of sample is taken from the treated water via pipettor
6. The sample is diluted by using 10 mL pipette.

The diagram of the first part and the uncertainties that could be involved during measurements are shown below Figure A.1.

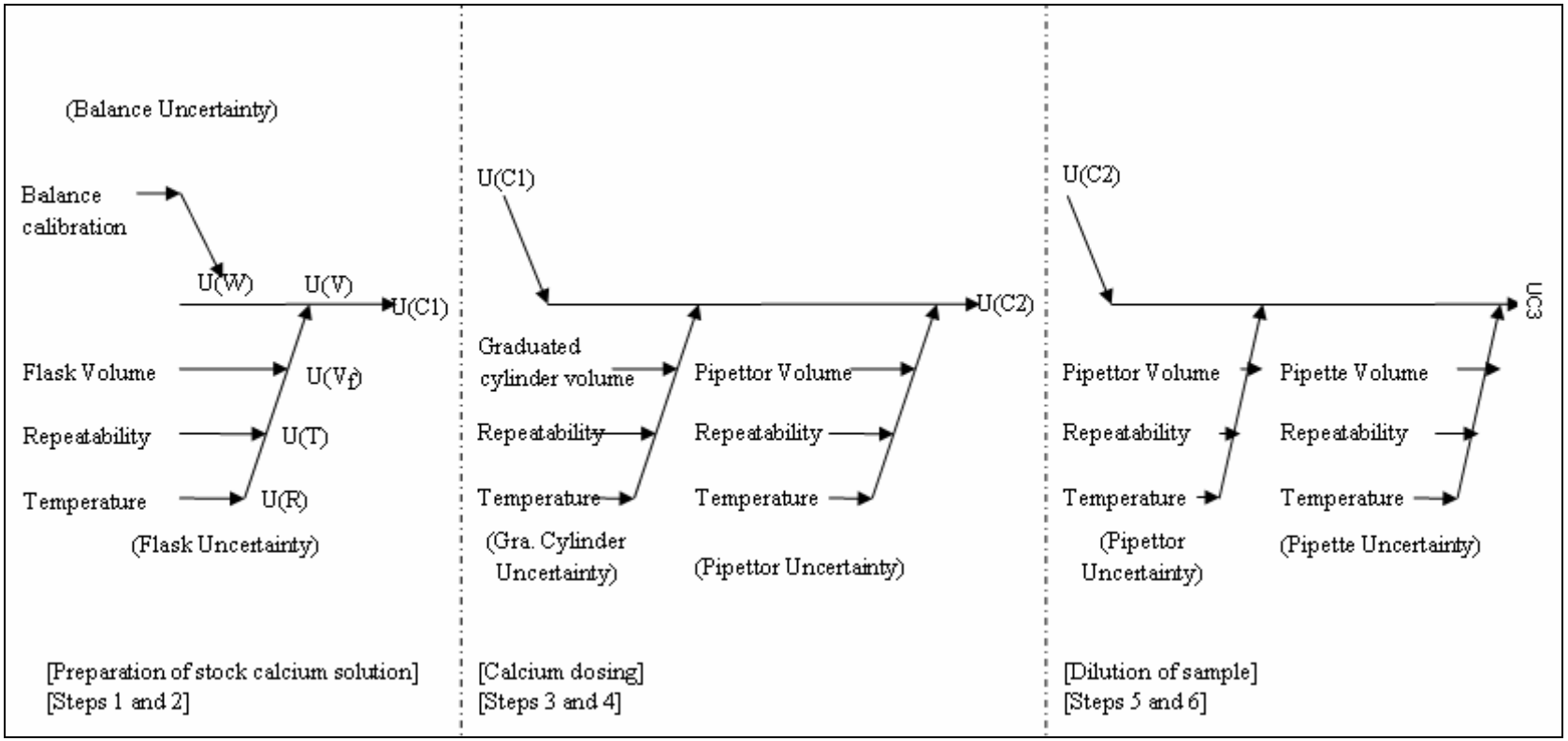

Figure A.1 Diagram of calcium dosing and dilution procedure for uncertainty analysis

During the calcium dosing and sampling some uncertainties are generated related to material and conditions in which the experiments are conducted. Sample calculations of uncertainty analysis for 15000 mg/L stock calcium solution are shown below. (Referring to Figure A.1 would be helpful to analyze the system).

Calibration Uncertainty

To prepare 15000 mg/L Ca^{+2} stock solution 5.5133 g of $CaCl_2*2H_2O$ is weighted. The apparatus has uncertainty function of;

$$U(W) = 0.02235 + 0.000038 * W$$

$$U(W) = 0.02235 + 0.000038 * 5{,}5133 = 0.0226\,g$$

Where;

W: recorded weight from balance [g]

U(W): total weight uncertainty [g]

Flask Volume Uncertainty

The uncertainty of 100 mL flask is reported as ±0.20 mL. Triangular distribution is used in uncertainty analysis.

$$U(V_f) = \frac{0.2}{\sqrt{6}} = 0.0816\,mL$$

Repeatability Uncertainty

After a series of repeating same measurements (5 times), the deviation is found as;

$$U(R) = 0.0790\,mL$$

Temperature Uncertainties

Laboratory temperature is accepted at 20 ±0.2 ^{0}C then uncertainty originating from temperature differences. Rectangular distribution is used in uncertainty analysis of temperature;

$$U(T) = \frac{100\ \text{mL} * 2\ ^{0}\text{C} * 2.1 * 10^{-4}}{\sqrt{3}} = 0.0242\ \text{mL}$$

Total Volumetric Uncertainty

$$U(V) = \sqrt{U(V_f)^2 + U(R)^2 + U(T)^2}$$

$$U(V) = \sqrt{0.0816^2 + 0.0790^2 + 0.0242^2} = 0.1162\text{mL}$$

Total Standard Uncertainty

Total standard uncertainty of stock calcium concentration (U(C1)) is calculated by using the formula below where C1 is the stock solution concentration;

$$U(C1) = C1 * \sqrt{\left(\frac{U(W)}{W}\right)^2 + \left(\frac{U(V)}{V}\right)^2}$$

$$U(Cl) = 15000 * \sqrt{\left(\frac{0.0226}{5.5133}\right)^2 + \left(\frac{0.1162}{100}\right)^2}$$

$$= 63.8034\ \text{mg/L}$$

Summary of calculations for uncertainties of preparation of stock solution are tabulated in Table A.1. Other procedures for 60 mg/L of calcium were calculated basing on Figure A.1and summarized in Table A.1.

Table A.1: Total standard uncertainty calculation tables for 60 mg/L calcium concentration

Preparation of Stock Calcium Solution		
Uncertainty Originating From Balance		
Recorded Value (W):	5.5133	g
Balance Calibration:	0.0226	
Total Weight Uncertainty U(W):	0.0226	g
Uncertainty Originating from Flask		
Flask Volume	100	mL
Flask Volume Uncertainty U(Vf):	0.0816	
Repeatability Uncertainty U(R):	0.0790	
Temperature Uncertainty U(T):	0.0242	
Total Volumetric Uncertainty U(V):	0.1162	mL
Prepared stock calcium concentration (C1)	15000	mg/L
Total Standard Uncertainty U(C1)	63.8034	mg/L
Calcium Dosing		
*Uncertainty Originating from G.C**		
G.C Volume	500	mL
G.C Volume Uncertainty U(Vgc):	2.0412	
Repeatability Uncertainty U(R):	0.6998	
Temperature Uncertainty U(T):	0.1212	
Total Volumetric Uncertainty U(V):	2.1613	mL
Uncertainty Originating from Pipettor		
Pipettor Volume	1	mL
Pipettor Volume Uncertainty U(Vpp):	0.0008	
Repeatability Uncertainty U(R):	0.0049	
Temperature Uncertainty U(T):	0.0002	
Total Volumetric Uncertainty U(V):	0.0049 (x2)**	mL
Dosed calcium concentration (C2)	60	mg/L
Total Standard Uncertainty U(C2)	0.5554	mg/L
*G.C: Graduated Cylinder		
** Uncertainty from pipettor is repeated twice but not shown for better tabulation (include in calculation)		

Table A.1 (cont'd)

Dilution of Sample		
Uncertainty Originating from Pipette		
Pipette Volume	19	mL
Pipette Volume Uncertainty U(Vp):	0.0408	
Repeatability Uncertainty U(R):	0.0445	
Temperature Uncertainty U(T):	0.0046	
Total Volumetric Uncertainty U(V):	0.0606	mL
Uncertainty Originating from Pipettor		
Pipettor Volume	1	mL
Pipettor Volume Uncertainty U(Vpp):	0.0008	
Repeatability Uncertainty U(R):	0.0049	
Temperature Uncertainty U(T):	0.0002	
Total Volumetric Uncertainty U(V):	0.0049	mL
Diluted calcium concentration (C3)	3	mg/L
Total Standard Uncertainty U(C3)	0.0329	mg/L

Like preparing 60 mg/L initially calcium containing synthetic water and its 1/20 dilution to 3 mg/L, same procedure is applied with some differences in dosing volume and initial stock calcium concentration for 80 mg/L. The factors contributed to uncertainty are listed in Table A.2 in details covering from preparation of stock calcium solution to dilution of the samples to 4 mg/L.

Table A.2: Total standard uncertainty calculation tables for 80 mg/L calcium concentration

Preparation of Stock Calcium Solution		
Uncertainty Originating From Balance		
Recorded Value (W):	5.8808	g
Balance Calibration:	0.0226	
Total Weight Uncertainty U(W):	0.0226	g
Uncertainty Originating from Flask		
Flask Volume	100	mL
Flask Volume Uncertainty U(Vf):	0.0816	
Repeatability Uncertainty U(R):	0.0790	
Temperature Uncertainty U(T):	0.0242	
Total Volumetric Uncertainty U(V):	0.1162	mL
Prepared stock calcium concentration (C1)	16000	mg/L
Total Standard Uncertainty U(C1)	64.1674	mg/L
Calcium Dosing		
*Uncertainty Originating from G.C**		
G.C Volume	500	mL
G.C Volume Uncertainty U(Vgc):	2.0412	
Repeatability Uncertainty U(R):	0.6998	
Temperature Uncertainty U(T):	0.1212	
Total Volumetric Uncertainty U(V):	2.1613	mL
Uncertainty Originating from Pipettor		
Pipettor Volume	0.5	mL
Pipettor Volume Uncertainty U(Vpp):	0.0008	
Repeatability Uncertainty U(R):	0.0049	
Temperature Uncertainty U(T):	0.0001	
Total Volumetric Uncertainty U(V):	0.0049	mL
Uncertainty Originating from Pipettor		
Pipettor Volume	1	mL
Pipettor Volume Uncertainty U(Vpp):	0.0008	
Repeatability Uncertainty U(R):	0.0049	
Temperature Uncertainty U(T):	0.0002	
Total Volumetric Uncertainty U(V):	0.0049 (x2)**	mL
Dosed calcium concentration (C2)	80	mg/L
Total Standard Uncertainty U(C2)	1.0772	mg/L
*G.C: Graduated Cylinder		
** Uncertainty from pipettor is repeated twice but not for better tabulation (include in calculations)		

Table A.2 (cont'd)

Dilution of Sample		
Uncertainty Originating from Pipette		
Pipette Volume	19	mL
Pipette Volume Uncertainty U(Vp):	0.0408	
Repeatability Uncertainty U(R):	0.0445	
Temperature Uncertainty U(T):	0.0046	
Total Volumetric Uncertainty U(V):	0.0606	mL
Uncertainty Originating from Pipettor		
Pipettor Volume	1	mL
Pipettor Volume Uncertainty U(Vpp):	0.0008	
Repeatability Uncertainty U(R):	0.0049	
Temperature Uncertainty U(T):	0.0002	
Total Volumetric Uncertainty U(V):	0.0049	mL
Diluted calcium concentration (C)	4	mg/L
Total Standard Uncertainty U(C3)	0.0588	mg/L

Like uncertainty analysis of 60 mg/L initially calcium containing synthetic water, 120 mg/L one is prepared in similar way. Only dosing volume of stock calcium and dilution ratio of samples is changed and tabulated in Table A.3.

Table A.3: Total standard uncertainty calculation tables for 120 mg/L calcium concentration

Preparation of Stock Calcium Solution		
Uncertainty Originating From Balance		
Recorded Value (W):	5.5133	g
Balance Calibration:	0.0226	
Total Weight Uncertainty U(W):	0.0226	g
Uncertainty Originating from Flask		
Flask Volume	100	mL
Flask Volume Uncertainty U(Vf):	0.0816	
Repeatability Uncertainty U(R):	0.0790	
Temperature Uncertainty U(T):	0.0242	
Total Volumetric Uncertainty U(V):	0.1162	mL
Prepared stock calcium concentration (C1)	15000	mg/L
Total Standard Uncertainty U(C1)	63.8034	mg/L
Calcium Dosing		
*Uncertainty Originating from G.C**		
G.C Volume	500	mL
G.C Volume Uncertainty U(Vgc):	2.0412	
Repeatability Uncertainty U(R):	0.6998	
Temperature Uncertainty U(T):	0.1212	
Total Volumetric Uncertainty U(V):	2.1613	mL
Uncertainty Originating from Pipettor		
Pipettor Volume	1	mL
Pipettor Volume Uncertainty U(Vpp):	0.0008	
Repeatability Uncertainty U(R):	0.0049	
Temperature Uncertainty U(T):	0.0002	
Total Volumetric Uncertainty U(V):	0.0049 (x4)**	mL
Dosed calcium concentration (C2)	120	mg/L
Total Standard Uncertainty U(C2)	1.3921	mg/L
*G.C: Graduated Cylinder		
** Uncertainty from pipettor is repeated four times but not for better tabulation (include in calculations)		

Table A.3 (cont'd)

Dilution of Sample		
Uncertainty Originating from Pipette		
Pipette Volume	19	mL
Pipette Volume Uncertainty U(Vp):	0.0408	
Repeatability Uncertainty U(R):	0.0445	
Temperature Uncertainty U(T):	0.0046	
Total Volumetric Uncertainty U(V):	0.0606	mL
Uncertainty Originating from Pipettor		
Pipettor Volume	0.5	mL
Pipettor Volume Uncertainty U(Vpp):	0.0008	
Repeatability Uncertainty U(R):	0.0049	
Temperature Uncertainty U(T):	0.0001	
Total Volumetric Uncertainty U(V):	0.0049 (x2)***	mL
Diluted calcium concentration (C3)	3	mg/L
Total Standard Uncertainty U(C3)	0.0553	mg/L
** Uncertainty from pipettor is repeated four times but not shown for better tabulation (include in calculations)		

The Procedure of Calcium Standards Preparation

The procedure consists of dilution standard stock calcium solution of which uncertainty is reported as ±2 mg/L to concentrations of 0.5, 2.5 and 5 ppm in 100 mL flask. Possible uncertainties involved during dilution are sketched in Figure A.2.

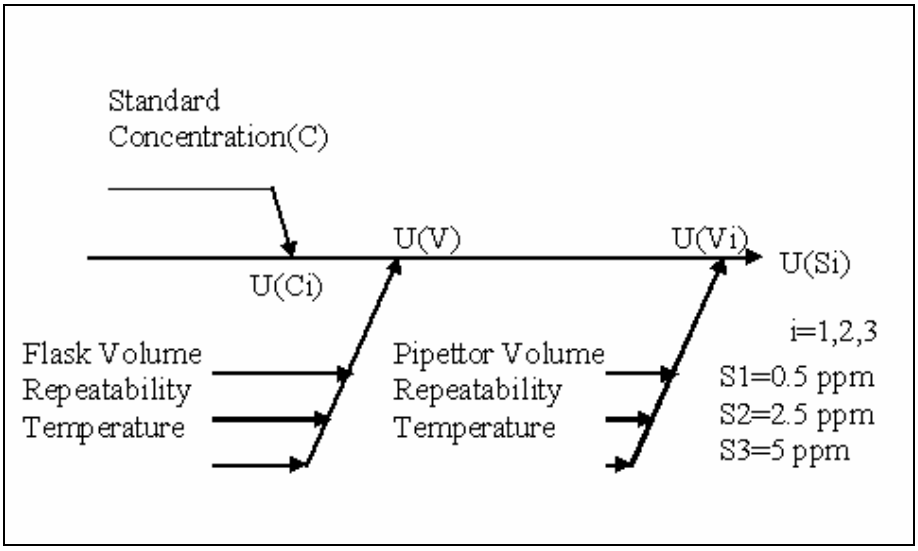

Figure A.2 Diagram of calcium standard preparation procedure for uncertainty analysis

The deviations during standard preparations are summarized and tabulated in Table A.4

Table A.4: Total standard uncertainty calculation tables for standard preparations

Preparation of Standard Solution (0.5 ppm)		
Uncertainty Originating From Stock Standard		
Concentration of Stock Standard Cal. (C)	1000	mg/L
Stock Standard Calibration:	1.1547	
Total Stock Standard Uncertainty U(C):	1.1547	mg/L
Uncertainty Originating from Flask		
Flask Volume	100	mL
Flask Volume Uncertainty U(Vf):	0.0816	
Repeatability Uncertainty U(R):	0.1000	
Temperature Uncertainty U(T):	0.0242	
Total Volumetric Uncertainty U(V):	0.1314	mL
Uncertainty Originating from Pipettor		
Pipettor Volume	0.05	mL
Pipettor Volume Uncertainty U(Vpp):	0.0008	
Repeatability Uncertainty U(R):	0.0020	
Temperature Uncertainty U(T):	0.0000	
Total Volumetric Uncertainty U(V):	0.0021	mL
Prepared stock calcium concentration (S1)	0.5	mg/L
Total Standard Uncertainty U(S1)	0.0214	mg/L
Preparation of Standard Solution (2.5 ppm)		
Uncertainty Originating From Stock Standard		
Concentration of Stock Standard Cal. (C)	1000	mg/L
Stock Standard Calibration:	1.1547	
Total Stock Standard Uncertainty U(C):	1.1547	mg/L
Uncertainty Originating from Flask		
Flask Volume	100	mL
Flask Volume Uncertainty U(Vf):	0.0816	
Repeatability Uncertainty U(R):	0.0582	
Temperature Uncertainty U(T):	0.0242	
Total Volumetric Uncertainty U(V):	0.1032	mL
Uncertainty Originating from Pipettor		
Pipettor Volume	0.25	mL
Pipettor Volume Uncertainty U(Vpp):	0.0008	
Repeatability Uncertainty U(R):	0.0020	
Temperature Uncertainty U(T):	0.0001	
Total Volumetric Uncertainty U(V):	0.0021	mL
Prepared stock calcium concentration (S2)	2.5	mg/L
Total Standard Uncertainty U(S2)	0.0218	mg/L

Table A.4 (cont'd)

Preparation of Standard Solution (5 ppm)		
Uncertainty Originating From Stock Standard		
Concentration of Stock Standard Cal. (C)	1000	mg/L
Stock Standard Calibration:	1.1547	
Total Stock Standard Uncertainty U(C):	1.1547	mg/L
Uncertainty Originating from Flask		
Flask Volume	100	mL
Flask Volume Uncertainty U(Vf):	0.0816	
Repeatability Uncertainty U(R):	0.0558	
Temperature Uncertainty U(T):	0.0242	
Total Volumetric Uncertainty U(V):	0.1018	mL
Uncertainty Originating from Pipettor		
Pipettor Volume	0.5	mL
Pipettor Volume Uncertainty U(Vpp):	0.0008	
Repeatability Uncertainty U(R):	0.0020	
Temperature Uncertainty U(T):	0.0001	
Total Volumetric Uncertainty U(V):	0.0021	mL
Prepared stock calcium concentration (S2)	5	mg/L
Total Standard Uncertainty U(S2)	0.0228	mg/L

Total Uncertainty Budget

Budget covers all the uncertainties from starting of stock calcium solution preparation to deviation during measurement by atomic absorption. In addition to previous tables' data, measurement of known sample deviation is added in the budget which is performed by measuring a known concentration of calcium solution ten times and the deviation is calculated subsequently. Total standard uncertainty is calculated as in Section A.1.6.

Table A.5: Total uncertainty budget for different calcium concentrations

	Unit	Arranged Conc.(C)	Standard Uncertainty U(C)
60 mg/L Calcium Concentration			
Preparation of Stock Calcium Solution	mg/L	15000	63.8034
Calcium Dosing	mg/L	60	0.5554
Dilution of Sample	mg/L	3	0.0329
Preparation of Standard Solution S1	mg/L	0.5	0.0214
Preparation of Standard Solution S2	mg/L	2.5	0.0218
Preparation of Standard Solution S3	mg/L	5	0.0228
Measurement of a known sample	mg/L	3	0.0428
Total Standard Uncertainty U(C)/C			0.0486
Expanded Standard Uncertainty			**0.0972**
80 mg/L Calcium Concentration			
Preparation of Stock Calcium Solution	mg/L	16000	64.1674
Calcium Dosing	mg/L	80	1.0772
Dilution of Sample	mg/L	4	0.0588
Preparation of Standard Solution S1	mg/L	0.5	0.0214
Preparation of Standard Solution S2	mg/L	2.5	0.0218
Preparation of Standard Solution S3	mg/L	5	0.0228
Measurement of a known sample	mg/L	3	0.0428
Total Standard Uncertainty U(C)/C			0.0505
Expanded Standard Uncertainty			**0.1010**
120 mg/L Calcium Concentration			
Preparation of Stock Calcium Solution	mg/L	15000	63.8034
Calcium Dosing	mg/L	120	1.3921
Dilution of Sample	mg/L	3	0.0553
Preparation of Standard Solution S1	mg/L	0.5	0.0214
Preparation of Standard Solution S2	mg/L	2.5	0.0218
Preparation of Standard Solution S3	mg/L	5	0.0228
Measurement of a known sample	mg/L	3	0.0428
Total Standard Uncertainty U(C)/C			0.0513
Expanded Standard Uncertainty			**0.1026**

As separately indicated in Table A.5, total standard uncertainties are 0.0486, 0.0505 and 0.0513 for calcium concentrations of 60, 80 and 120 mg/L, respectively. The expanded total uncertainty of these calcium

concentrations are twice times of total standard uncertainty values: The results shows that around 10% deviation is occurring during the jar test experiment and following calcium concentration measurements.